FINITE ELEMENT ANALYSIS OF A MICRO SATELLITE STRUCTURE UNDER VIBRATION INDUCED LOADS DURING LAUNCH

A THESIS SUBMITTED TO
THE GRADUATE SCHOOL OF NATURAL AND APPLIED SCIENCES
OF
MIDDLE EAST TECHNICAL UNIVERSITY

BY

SUAT ONTAÇ

IN PARTIAL FULFILLMENT OF THE REQUIREMENTS
FOR
THE DEGREE OF MASTER OF SCIENCE
IN
MECHANICAL ENGINEERING

MAY 2008

Approval of the thesis:

FINITE ELEMENT ANALYSIS OF A MICRO SATELLITE STRUCTURE UNDER VIBRATION INDUCED LOADS DURING LAUNCH

submitted by **SUAT ONTAÇ** in partial fulfillment of the requirements for the degree of **Master of Science in Mechanical Engineering Department, Middle East Technical University** by,

Prof. Dr. Canan Özgen _____
Dean, Graduate School of **Natural and Applied Sciences**

Prof. Dr. Kemal İder _____
Head of Department, **Mechanical Engineering**

Assoc. Prof. Serkan Dağ
Supervisor, **Mechanical Engineering Dept., METU** _____

Prof. Dr. Mustafa İlhan Gökler
Co-Supervisor, **Mechanical Engineering Dept., METU** _____

Examining Committee Members:

Assist. Prof. Dr. Merve Erdal _____
Mechanical Engineering Dept., METU

Assoc. Prof. Dr. Serkan Dağ _____
Mechanical Engineering Dept., METU

Prof. Dr. Mustafa İlhan Gökler _____
Mechanical Engineering Dept., METU

Assist. Prof. Dr. Yiğit Yazıcıoğlu _____
Mechanical Engineering Dept., METU

Assoc. Prof. Dr. Altan KAYRAN _____
Aeronautical Engineering Dept., METU

Date: 08 – 05 – 2008

I hereby declare that all information in this document has been obtained and presented in accordance with academic rules and ethical conduct. I also declare that, as required by these rules and conduct, I have fully cited and referenced all material and results that are not original to this work.

Name, Last name: Suat, Ontaç

Signature :

ABSTRACT

FINITE ELEMENT ANALYSIS OF A MICRO SATELLITE STRUCTURE UNDER VIBRATION INDUCED LOADS DURING LAUNCH

Ontaç, Suat

M.S., Department of Mechanical Engineering

Supervisor: Assoc. Prof. Serkan Dağ

Co-Supervisor: Prof. Dr. Mustafa İlhan Gökler

May 2008, 101 pages

This study mainly covers the finite element analysis of a micro satellite structure by considering the vibration effects at the time interval from the launching to the Earth's orbit landing.

Micro-satellites have a great importance in the satellite industry and several developing countries deal with micro-satellite design and production. Turkey is one of these countries by conducting new satellite projects. RASAT project is one the continuing micro-satellite project, which has being developed by TÜBİTAK Space Technologies Research Institute. In this thesis, the RASAT satellite is taken as the model for the study. On this model, many mechanical design studies which are performed according to the specified requirements and constraints are verified by finite element analyses. These analyses cover all the essential vibration loads during launching. In the study, firstly, a finite element model of RASAT is prepared. Then, the essential analyses are performed according to the specifications required by the launchers. In the analyses, commercially available finite element software is used.

Finally all the results obtained from the finite element analyses are compared with the predefined requirements and constraints. The results show that the structural design verification regarding the reliability of the structure for the desired mission has been successfully completed.

Keywords: Micro Satellite, Vibration, Finite Element Analysis, RASAT

ÖZ

FIRLATMA SIRASINDAKİ TİTREŞİM KAYNAKLI YÜKLERE MARUZ KALAN BİR MİKRO UYDU YAPISININ SONLU ELEMANLAR ANALİZİ

Ontaç, Suat

Yüksek Lisans, Makina Mühendisliği Bölümü

Tez Yöneticisi: Doç Dr. Serkan Dağ

Yardımcı Tez Yöneticisi: Prof. Dr. Mustafa İlhan Gökler

Mayıs 2008, 101 sayfa

Bu çalışma, temel olarak, bir mikro uydu yapısının, fırlatma başladığı andan dünya yörüngesine oturtulmasına kadar olan zaman diliminde, titreşim etkilerini gözönüne alınarak sonlu eleman analizini içermektedir.

Mikro uyduların, uydu endüstrisinde önemli bir yeri vardır ve gelişmekte olan birçok ülke, mikro uydu tasarımı ve üretimiyle ilgilenmektedir. Türkiye de yeni uydu projeleri sürdürürek bu ülkeler arasına girmiştir. TÜBİTAK Uzay Teknolojileri Araştırma Enstitüsü'nün geliştirmekte olduğu RASAT uydu projesi de bu projelerden biridir. Bu tezde, RASAT uydusu yapılan çalışmaya model olarak alınmıştır. Bu modelde, verilen kısıtlara ve isterlere uygun olan yapılan birçok mekanik tasarım çalışmaları sonlu eleman analizleriyle doğrulanmıştır. Bu analizler, fırlatma esnasındaki tüm titreşim yüklerini kapsar. Çalışmada, öncelikle RASAT'ın bir sonlu eleman modeli hazırlanmıştır. Daha sonra, fırlatıcılar istenen belirtimlere gore gerekli tüm analizler yapılmıştır. Analizlerde, ticari olarak bulunabilen bir sonlu eleman yazılımı kullanılmıştır.

Son olarak sonlu eleman analizlerinden elde edilen sonuçlar daha önceden belirlenen isterler ve kısıtlamalarla karşılaştırılmıştır. Sonuçlar göstermiştir ki yapısal tasarım doğrulaması, uydu yapısının istenen görevini başarılı bir şekilde yerine getirebilecek kadar güvenli olup olmadığı konusu göz önüne alınarak başarılı bir şekilde tamamlanmıştır.

Anahtar Kelimeler: Mikro Uydu, Titreşim, Sonlu Eleman Analizi, RASAT

To my mother, my sisters, my brother, my colleagues and my friends who supported me through all the good times and the bad times.

ACKNOWLEDGMENTS

First of all, I would like to express my deepest gratitude to my supervisor Assoc. Prof. Dr. Serkan Dağ and my co-supervisor Prof. Dr. Mustafa İlhan Gökler for their guidance, advice, criticism, encouragements and insight throughout the research.

I would like also to thank to TÜBİTAK Uzay Teknolojileri Araştırma Enstitüsü (TÜBİTAK Space Technologies Research Institute), where I had been working as a researcher, for their support and kind approach.

My sincere thanks go to colleagues at TÜBİTAK UZAY for their co-operations and their new suggestions for my study.

Finally; I wish to express my sincere thanks to my family for their infinite support and to my friends who encouraged and assured me continuously along this study.

TABLE OF CONTENTS

LIST OF TABLES

TABLES

LIST OF FIGURES

LIST OF SYMBOLS

a	albedo
c	damping coefficient
f_n	natural frequency
g	gravity
G_s	Solar Flux
m	mass
q_i	earth infrared
Q	transmissibility at resonance
Q_a	aerodynamic load
R	sweep rate
t	time
w	weight
W	power spectral density
$\overline{x}$	mean of x
Ø	diameter
Δf	bandwidth
σ	stress

CHAPTER 1

INTRODUCTION

1.1 History of Satellites and RASAT Micro-satellite Project

After the second half of the 20th Century, investigators have started developing unmanned spacecrafts which are sent to outer atmosphere. Then the manned spacecrafts have been developed. In the earlier times the aim was to see and know the outside of the earth. But, by the time there have been different purposes for making spacecrafts. Today, making satellites and landing them onto the orbit of the earth is one of the main aims of many countries. As a result, the number of the satellites on the orbit of the earth is increasing day by day. Approximately 150-200 satellites are landed onto the orbit of the earth every year. Most of them are being developed by U.S.A. and Russia. Now, many countries are capable of making satellites and their numbers are increasing day by day.

Turkey has not yet developed a satellite which is landed onto orbit. For this reason, in 2001, a scientific satellite development project had been started by TÜBİTAK and SSTL of U.K. Its name was BİLSAT. The project was being carried on by the personnel of TÜBİTAK BİLTEN (present name is TÜBİTAK UZAY) and the personnel of SSTL, in SSTL in U.K. In 2003, the project was completed and BİLSAT was successfully launched to space in September, 2003. This may be assumed to be as the starting point of developing an own satellite for Turkey. By the current time, many official and private associations, such as institutions, universities and private companies have started developing satellites.

Currently, in TÜBİTAK UZAY, there is a satellite project named RASAT. It is the second remote-sensing satellite after the launch of BİLSAT. RASAT, having a high-resolution (panchromatic camera of 7.5 m resolution and multi-spectral image camera of 15 m resolution) optical imaging system and new modules developed by

Turkish engineers, will be the first Earth-observation satellite to be designed and manufactured in Turkey. RASAT is going to be deployed in a polar sun synchronous low earth orbit within the locus extending the Earth's surface up to an altitude of about 685 km. It is planned to be in a module-stack structure having a mass of about 105 kg.

The goals of RASAT project are to improve know-how from design phase to in-orbit commissioning phase of a satellite project gained from BİLSAT project; to develop space qualified systems using current technologies and to gain flight heritage by succeeding in operating these systems in space; to meet the requirements of Turkey in the sense of remote sensing as much as possible; to investigate the current capabilities of Turkey for space technologies; to increase number of qualified man power in the field of satellite technologies; and to meet the requirements of national satellites which are to be designed and built in Turkey. RASAT project is being realized in a teamwork environment. Structural design and analysis are the parts of this teamwork environment.

In this thesis, all the studies, analyses and evaluations are going to be based on RASAT satellite. Working on a real example will make the studies more realistic and after the environmental phases, the analysis results will be correlated with the test results. This will provide us seeing whether the analyses and results are logical or not.

1.2 Scope of the Study

This study covers the structural analysis of a micro satellite on which several types of vibration loads are going to be applied from the beginning of the launching action until the beginning of the first launch separation during the orbit landing operation.

In the second chapter, an introduction to satellites, satellite structures, constraints, requirements on structural design of micro satellites, types of loads induced on satellite structures are given with literature survey.

Then, the third chapter is about structural analysis information for micro satellite structures. It starts with the stiffness and frequency based analyses such as modal analysis. Information on the importance of finite element modal analysis of satellite structures is given. Transient response analysis such as sinusoidal vibration analysis will follow the modal analysis. Then, by giving information on random vibration analysis and stress analysis, this chapter is going to be completed. All the information in this chapter is given by literature survey.

In the fourth chapter, the structural design specifications of RASAT are given. These specifications are based on the requirements given by the launcher companies. All the data presented in this chapter is going to be used during the structural analysis section.

In the fifth chapter, the studies which are done on RASAT satellite are presented. These studies cover both the finite element modeling and analyses sections. In the finite element modeling phase, the details for RASAT finite element model, such as meshing, material assignment, boundary conditions and constraints are given. Then, in the analysis section, the structural analyses including modal analysis, harmonic response analysis, random vibration analysis, and stress analysis are presented.

In the sixth chapter, the results of this study have been discussed in detail. Important conclusions are drawn on the corresponding analyses. The requirements which are to be taken into consideration and the results coming from the analyses have been compared to each other in order to understand whether the structural design of RASAT is reliable.

CHAPTER 2

MICRO SATELLITES AND STRUCTURE SUBSYSTEM

A satellite is a device which is made for communication, military, observation, meteorology, and similar purposes or scientific studies; launched by a rocket or a space transportation system to the space and landed onto an orbit of a space matter (especially the earth).

2.1 Satellite Classification

Satellites can be classified into many groups from different aspects. But, mainly they are classified by their masses. When considering the mass, it is more correct to include the propellant of the satellite. This is called as wet mass. Generally, the ones which are larger than 1000 kg are called as large satellites, the ones which are between 500 and 1000 kg are called as medium-sized satellites and those smaller than 500 kg are called as small satellites.

Small satellites are generally preferred in the applications whose developing and manufacturing times are relatively short. The developing and manufacturing time of a small satellite may be 6 to 36 months. Small satellites can be classified as in the Table 2.1.

2.2 Micro Satellite Subsystems

A satellite is composed of many different subsystems. These subsystems are often divided into two: the payload (the cameras, radars, or communication apparatus that does what the spacecraft is supposed to do), and the bus (all of the electronics and hardware used to support the payload).

Table 2.1. Types of small satellites

Satellite Type		**Wet Mass**
Small Satellites	Mini satellite	200 – 500 kg
	Micro satellite	10 – 200 kg
	Nano satellite	1- 10 kg
	Pico satellite	100 g – 1 kg
	Femto satellite	< 100 g

A bus typically consists of the following subsystems:

- Propulsion: It consists of thrusters, tanks, and a feed system. In some satellites, there are multiple propulsion subsystems (especially with electric propulsion).
- Power: It consists of solar panels, batteries, power processors and cables (harnessing).
- Thermal: It consists of radiators to keep the satellite electronics cool, and heaters to keep the propulsion system from freezing.
- Structure: It generally consists of some mechanical components and structural elements such as brackets, panels, cylinders, and struts to support the internals during launch and maneuvers.
- Attitude Determination and Control (ADCS): It consists of momentum wheels, gyros, reaction wheels, or other devices to keep the satellite steady during its mission on orbit.
- Communication: These are the antennae and electronics to act as the satellite's eyes and ears.
- Command and Control: These are the computers to provide the brains for the satellite. It sometimes processes the data collected by the payload

instruments as well, but not always.

None of the subsystem is any bit more important than any other. If any part does not function, the satellite will not work.

When designing a spacecraft, there are several other functional areas that are involved:

- Mission: This performs analysis related to the orbit of the satellite. It determines when and for how long the satellite will be looking at a given location on the Earth, how long the satellite will be in the dark with the Earth between it and the sun (called eclipse), and if multiple satellites should be used to get more complete or continuous coverage.
- Ground Systems: This is the mission control. Once the satellite is on orbit, they take care of commanding and controlling of the satellite. While they do not design hardware to go on the satellite, they need to be involved in the design of the satellite because the software, computers, and manpower needed to operate the satellite can be a significant source of expense.
- Systems Engineering: These are the people that make sure everything works together. Thus, they have to know a little bit about everything. In detail, systems engineering is the engineering of operational spacecraft including concept, configuration, specification, team organization, tasking timeline, preliminary design and review, simulation, costing, critical design review, subsystem construction and testing, system integration and test, calibration, documentation [1].

2.3 Structure Subsystem

Satellite structure is one of the most important subsystems of a micro satellite. Its function is to enclose, protect and support the other satellite subsystems and to provide a mechanical interface with the launch vehicle. The structural system of a satellite has three main functions:

- To provide the support of all the other subsystem and materialize the geometry of the satellite and its payloads
- To guarantee the necessary strength to survive all phases of the satellite life (in particular the most critical: e.g. the launch) without failures.
- To keep the structural stiffness in certain limits to guarantee the operational functionality of the overall system and avoid coupled resonant responses (e.g. between the satellite and its launcher) [2].

Since the cost of mass is very critical in a space mission, the structural system should be optimized with respect to it both in terms of material and in terms of the optimal structural geometries. Structural problems affect also other subsystems (e.g. propulsion, attitude and orbital control, on board data handling, telemetry and telecommand) and the payload itself. In fact every component of a satellite needs to withstand the mission environment and a structural failure could occur in a component of the system and might be critical for the success of the mission.

Micro satellite structures can be divided into three parts:

1-Primary structure: The mechanical parts holding the subsystems together, and being able to resist and support against the most critical load conditions to be met. In other words, primary structure is the system's backbone.

2-Secondary structure: The mechanical parts needed by each subsystem. That is it includes all the essential appendages and support structures (such as solar arrays, antennas, and fuel tanks).

3-Tertiary structure: Less-essential mounting hardware (brackets, component housing connector panels).

2.3.1 Micro Satellite Structures

For a micro satellite it is very important to survive and be operational during launch and in orbit. So, in order to do this the structure of the satellite must be designed very carefully. It must withstand the harsh environmental and launching conditions.

The design and development of a satellite is an engineering process that can be divided into identifiable phases. Regardless of how long it takes, satellite design and development typically occur in phases as: requirements definition, conceptual design, preliminary design, and detailed (or critical) design.

It is very logical to start satellite development by defining requirements which the system have to satisfy. For example, these could be the need to observe the earth, taking photographic images with predetermined resolution and transmitting the information in real time. The ground, launch, and space environments each impose their own specific requirements. Structural elements of a satellite must retain their integrity after exposure to these environmental conditions with minimum mass, minimum cost, maximum reliability.

The next step is the conceptual design phase. In this phase various system concepts which can satisfy the mission requirements are considered and subjected to analysis. The most proficient means to carry out the mission is selected and major risks, costs, and schedules are identified.

The preliminary design phase follows conceptual design, and may stretch over a couple of months. During this phase, variations of the concept chosen in the conceptual design phase are analyzed and refined. Subsystem and component level specifications are defined and major documents such as the interface control document are written. Anticipated performance of systems and subsystems is substantiated and, from the detailed specifications, a preliminary parts list is identified.

The final phase is the critical (or detailed) design phase. It is within this phase that the specific aspects of structural design are identified, such as finalizing the thickness of structures and load paths. The satellite design must accommodate everything that fits into the structure, including equipment and payload. Options for secondary structures (plumbing, wiring, etc.) are also analyzed and evaluated several times during the critical design phase. Design verification is an important part of this phase. Verification involves tests of electronic circuit models, software and engineering models. Design and performance margin estimates are refined and

test and evaluation plans are finalized.

Many factors influence the definition and selection of the structural design concept (e.g. strength, stiffness, mass, resilience, resistance to corrosion and the environment, fatigue, thermal properties, manufacturing, availability and cost). Structural design is an iterative process. The process starts with the conceptual design of possible alternatives which could be considered to satisfy the general performance requirements and are likely to meet the main mission constraints (e.g. mass, interfaces, operation and cost). The various concepts are then evaluated according to a set of prioritized criteria in order to select the one or more designs to be developed further in detail. The main purpose of the evaluation is to identify the main mission requirements and to establish whether the selected concepts meet the requirements. The selected concepts are evolved and evaluated in more detail against a comprehensive set of mechanical requirements and interface constraints which are came from the main mission and functional requirements.

The following structural design aspects shall be covered:

1. The structural design shall lead to an item that is proven to be strong and stiff enough for the intended purpose throughout its intended life time;

2. Practices used in structural design shall be in accordance with those stipulated or agreed by the controlling bodies to permit certification and qualification of structures;

3. All structural design concepts shall include provision for verification of the structural integrity during design, manufacture and once in service;

4. The structural materials used should be known, reliable and reproducible properties and should be proven resistance to the environmental factors considered;

5. The structural materials shall not be hazardous to the operators or mission;

6. The structure mass shall be minimized;

7. The design shall include balancing mass fixations;

8. The structure shall be cost effectively manufactured, by methods that do not alter

the designed characteristics (mechanical or environmental resistance) in an unknown way, and by methods proven to be reliable and repeatable;

9. The generation of space debris by structural break up shall be minimized [2].

All structural assemblies and components must be able to withstand the environment loads and conditions to which they are exposed during both manufacture and their complete service-life. Components and assemblies for space applications shall be compatible with the operational environment conditions and with the atmospheric conditions on earth in which they are manufactured and tested. Consideration shall be given to the effects of gravitation and the exposure of sensitive materials to manufacturing and atmospheric environments; suitable provisions (e.g. gravitational compensation and purging) shall be made where necessary for the protection of sensitive equipment or components.

The sensitivity of materials to the environment on earth can anticipate the requirements for quality control procedures. The natural environment generally covers the climatic, thermal, chemical and vacuum conditions, required cleanliness, levels of radiation and the meteoroid and space debris environment. The induced environments cover the mechanical loads induced by ground handling and pre-launch operations, launch, maneuvers and disturbances, re-entry, descent and landing. Additional induced environments include static pressure within the payload volume, temperature and thermal flux variations and the electromagnetic and humidity environments.

2.3.2 Design Loads

All relevant mechanical and thermal load events experienced throughout the service-life of the structure shall be identified. Loads shall be defined according to their nature, static or dynamic, their level and time corresponding to the events during the lifetime, and as a minimum the following load events shall be considered.

2.3.2.1 Ground and Test Loads

Ground loads are generally due to handling, transportation and storage loads, assembly and integration loads which occur when the satellite is on ground yet. Similarly test loads are ground test loads which exist during environmental test which is performed to check the behavior of the satellite. Such load types are listed in Table 2.2.

2.3.2.2 Launch Loads

The most important and effective load conditions are launching loads. Launching loads differ as relative to the launching system (rocket). In a time interval (a few minutes) when the engines of the launching system run, the satellite is exposed to extremely high dynamic loads.

The launch environment is generally the main satellite structural design driver. During launch, the satellite is subjected to:

• Low frequency sinusoidal vibration, generated by aerodynamic forces acting on the launch vehicle and transient events like staging, fairing jettison, and engine cutoff

• High frequency random vibration, produced by mechanical parts in motion like engine turbo-pumps, fuel combustion, and structural elements excited by acoustic noise.

• Acoustic noise, reflected off the ground and pad facilities at liftoff, and at "Max Q_a", which is the maximum aerodynamic load acting on the launch vehicle. In other words, it can be described as the maximum pressure and bending on the launch vehicle due to the aerodynamic conditions [2].

Table 2.2. Examples of ground load sources and corresponding indicative figures with ref [2]

OPERATION			**APPLIED ACCELERATIONS (g)**			**REMARKS**
			X	**Y**	**Z**	
Handling	Clean Room	Dolly In-door movements Vertical hoisting Launcher mate/demate	± 1.0 ± 0.2 ± 0.2 ±0.5	± 0.75 ± 0.2 ± 0.2 ± 0.5	-1 ± 0.5 -1 ± 0.2 -1 ± 0.5 -2 / 0	Any satellite orientation
	Container	Hoisting	± 0.5	± 0.5	-1 ± 0.5	Satellite horizontal
Road		Quasi-static	± 2	± 2	-3 / +1	40 km/h top speed
Air		Take-off Vertical maneuver Lateral gusts Landing	-1.5 0 0 ± 1.5	± 0.1 ± 1.5 ± 1.5 ± 1.5	-2.5 / +1.5 -2.5 -1.0 -2.5	
Barge / Ship		Slamming Waves	0 ± 0.3	0 ± 0.5	-1.8 / +0.2 -1.6 / +0.4	
Any Transportation Source		Continuous Vibration	± 0.1	± 0.1	± 0.1	Below 10 Hz, not including gravity effect
Transport Shock Load			± 2	± 2	± 3	

2.3.2.3 Natural Frequency

Another concept that must be taken into consideration is natural frequency. Natural frequencies of satellite structural elements must be kept separated to avoid resonant coupling caused by excitations from vibrating sources and with the control system. For each module, the value of natural frequency must be at least a $\sqrt{2}$ times of the system the module is mounted. This comes from the vibration (or frequency) isolation theory. This theory is explained in Appendix A.

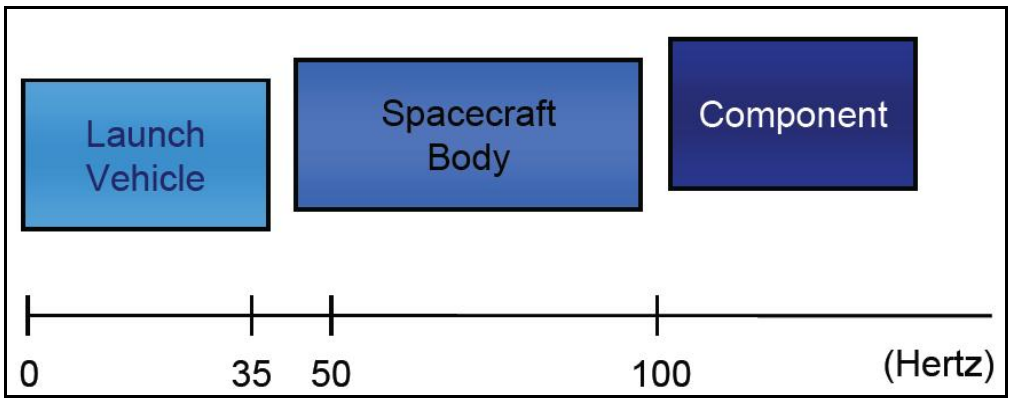

Figure 2.1. General satellite frequency separation with ref [3]

To prevent dynamic coupling between the low-frequency launch vehicle and satellite modes, the satellite should be designed with a structural stiffness which ensures that the requirements in Figure 2.1 are fulfilled.

Table 2.3. Lateral frequencies of a satellite

Satellite Mass (kg)	**Launcher interface diameter (mm)**	**1st fundamental lateral frequency (Hz)**	**Transverse inertia wrt. Separation plane ($kg.m^2$)**
< 4500 (covers small satellites)	< Ø 2600	≥ 10	≤ 50,000
	Ø 2600	≥ 9	

Lateral frequencies – The fundamental frequency in the lateral axis of a satellite hard-mounted at the interface must be as in Table 2.2 with an off-the-shelf adapter.

Longitudinal frequencies – The fundamental frequency in the longitudinal axis of a satellite hard-mounted at the interface must be as follows:

≥ 31 Hz for satellite mass < 4500 kg (i.e. covers small satellite)

2.3.2.4 Shocks

The satellite is subjected to shocks during launch vehicle stages of separation events, mainly fairing jettisoning, and during satellite separation. With respect to the launch vehicle shock events, the envelope of the shocks generated during the flight has to be considered. As examples, the separation shock levels of some launch vehicles are given in Figure 2.2.

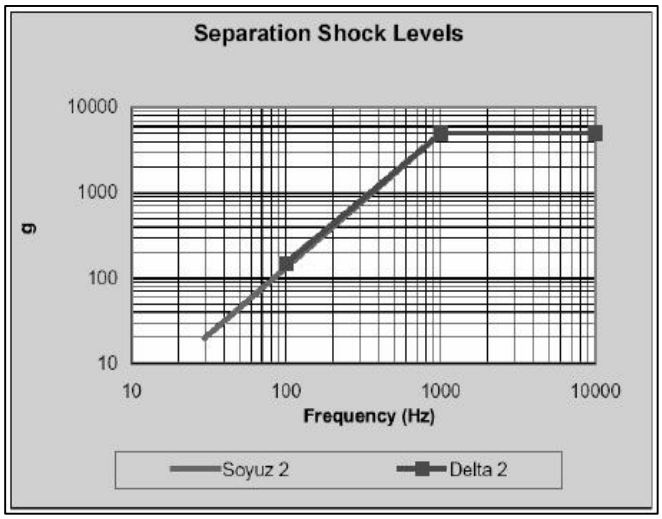

Figure 2.2. Separation Shock Levels of Soyuz 2 and Delta 2 Launch Vehicles with ref [2]

2.3.2.5 In-Orbit Loads

These loads are generally operational pressures, static and dynamic loads induced by thrusters, shocks due to pyrotechnical operation and deployment of appendages,

thermo-elastic loads induced by temperature variations, hygroscopic-induced load due to variations in moisture content, micro-vibrations induced by moving elements (e.g. momentum wheels) and thrusters, loads and shocks created by hitting of micrometeoroids and debris. In Figure 2.3, a general scale for this type of loads is given [2].

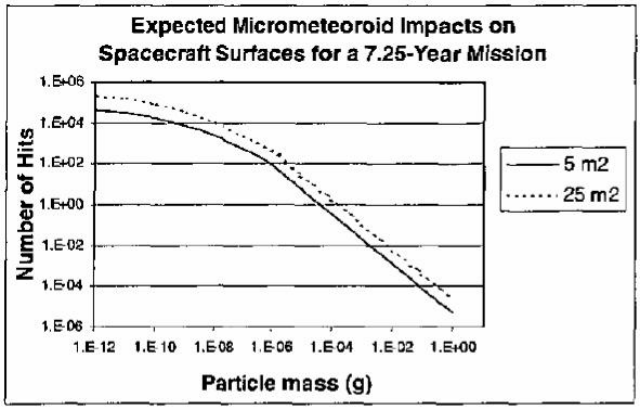

Figure 2.3. Expected Number of Impacts on Spacecraft Surfaces for a 7.25-Year Mission with ref [2]

2.3.2.6 Thermal Flux

During its on orbit life and according to the characteristics of the orbit, an earth orbiting satellite is subjected to sun radiation, albedo and earth radiation. The same is true for other space vehicles orbiting or flying by other planets. The thermal control subsystem is responsible for keeping the satellite in the admissible range of temperatures. The variations of temperature generate thermo elastic actions on the satellite structures. For a low-orbit satellite, thermal flux values may be shown as in Figure 2.4 [2].

2.4 Materials

The primary drivers for material selection are: Stiffness, strength, cost, availability, manufacturability, and effect of the space environment.

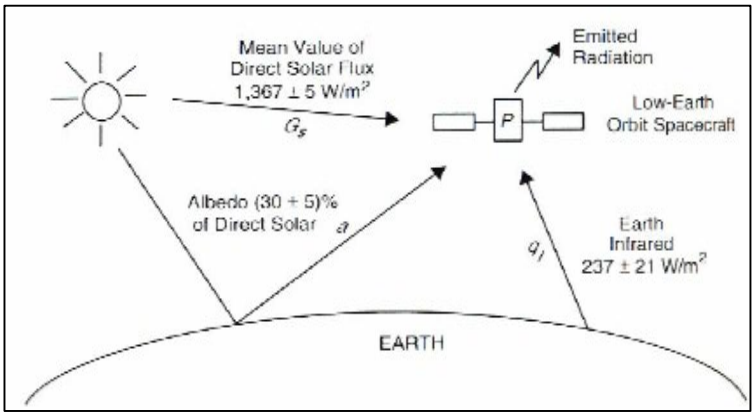

Figure 2.4. Thermal Flux Example of a Low-Earth Orbit Spacecraft with ref [2]

For satellite, aluminum alloys are still the most frequently used. Composites have more favorable characteristics and are becoming more common, but they require specific design and manufacture as well as protection from the space environment.

Table 2.4. Material Requirements for Satellite Structures with ref [3]

Categories	**Requirement**
Light Weight	• High Specific Strength • High Specific Stiffness • High Stability
Thermal Stability	• Low Thermal Expansion • Thermal Conductivity
Low Out-Gassing	• Total Mass Loss < 1.0% • CVCM < 0.1%
Environmental Resistance	• Radiation • Temperature Extremes • Atomic Oxygen
Manufacturing	• Cost & Availability • Ease of Fabrication

For all structural materials allowable stresses should be statistically derived, considering all operational environments. The scatter bands of the data shall be derived and allowable stresses defined in terms of fractions of their statistical distribution with prescribed levels of reliability and confidence. For each type of test the minimum number of test specimens should be ten to establish A-values, and five to establish B-values. (Note: A value is a mechanical property value above which at least 99% (90 % for B value) of the population of values is expected to fall, with a confidence level of 95 %). If the material is delivered in several batches, the allowable test program shall consider the probability of variations from batch to batch. In such cases, preliminary allowable stresses may be based on the initially small sample size, and upgraded as the sample size increases by tests of newly arriving batches. For satellite structures, the general material properties which are required for space conditions are given in Table 2.4. Similarly, the advantages and disadvantages of some materials which are used in space applications are listed in Table 2.5.

In making design, one of the most important criteria is the mass center of the satellite. The mass center should be chosen so that the propulsion vector will pass through it. If the propulsion vector does not pass through the mass center there will be a moment applied.

Table 2.5. Typical Features of Structural Materials for Space Applications with ref [4]

Material	Advantages	Disadvantages
Aluminum	• High strength vs. weight • Ductile; tolerant of concentrated stresses • Easy to machine • Low density; efficient in compression	• Relatively low strength vs. volume • Low hardness • High coefficient of thermal expansion
Steel	• High strength • Wide range of strength, hardness, and ductility obtained by treatment	• Not efficient for stability (high density) • Most are hard to machine • Magnetic
Heat-resistant	• High strength vs. volume • Strength retained at high temperatures • Ductile	• Not efficient for stability (high density) • Not as hard as some steels
Magnesium	• Low density—very efficient for stability	• Susceptible to corrosion • Low strength vs. volume
Titanium	• High strength vs. weight • Low coefficient of thermal expansion	• Hard to machine • Poor fracture toughness if solution treated and aged
Beryllium	• High stiffness vs. density	• Low ductility & fracture toughness • Low short transverse properties • Toxic
Composite	• Can be tailored for high stiffness, high strength, and extremely low coefficient of thermal expansion • Low density • Good in tension (e.g., pressurized tanks)	• Costly for low production volume; requires development program • Strength depends on workmanship; usually requires individual proof testing • Laminated composites are not as strong in compression • Brittle; can be hard to attach

CHAPTER 3

STRUCTURAL ANALYSIS THEORY OF MICRO SATELLITES

3.1 Finite Element Analysis of Satellite Structures

With the use of finite element analysis (FEA) software packages such as NASTRAN, ABAQUS, ANSYS etc., it is possible to model structures in great detail, and to examine their behavior under various static and dynamic load conditions. For instance, in a dynamic simulation, the structure's natural frequencies can be assessed and relative phase information of deflection shapes at different locations within the structure can be indicated. Once a complete set of finite element analyses has been performed on the whole structure and other subsystems, a reduced model, which demonstrates similar characteristics to the larger version, is used for incorporation into the overall satellite simulation. This model is then incorporated into a coupled analysis model of the launcher-satellite combination so that a full examination of the complete launch configuration can be made. However, the results of finite element analysis might present some important discrepancies with the actual data as small joints and mechanisms are difficult to model and subject to high concentration of stresses. The finite element analysis can sometimes lead to high errors such as 40 % if the number of elements used in the finite element model is very small. In dynamic models, where such details are less important, the average error rate is around a smaller percent rate such as 10%. The fact is that these error rates could be corrected by a more and more detailed model. Nevertheless, such an improvement requires time and money, which are actually the factors that define the limit of the use of finite element method (FEM) in satellite structure design. Usually a good solution to this problem is to use test data to correct the mathematical model.

In Figures 3.1 and 3.2, FE models of some satellite structures are shown.

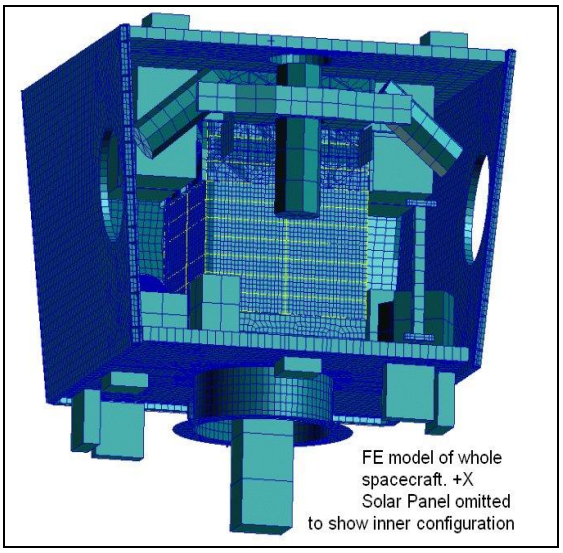

Figure 3.1. Finite Element Model of BILSAT Satellite with ref [5]

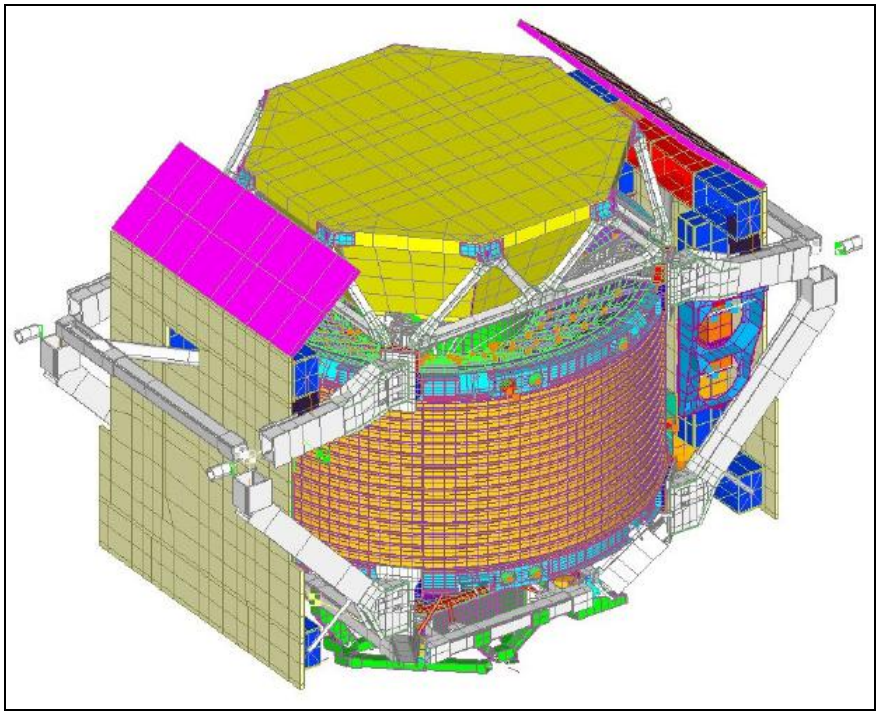

Figure 3.2. Finite Element Model of AMS-02 Satellite with ref [6]

3.2 Modal Analysis

3.2.1.1 Natural Frequencies

These are the frequencies of a structure at which the structure would vibrate if it are excited by a given transient load and then allowed to move freely.

We should note that a 1-degree-of-freedom system has 1 mode of vibration and 1 natural frequency, a 2-degree-of-freedom system has 2 modes of vibration and 2 natural frequencies, and a 3-degree-of-freedom system has 3 modes of vibration and 3 natural frequencies, and so on. But a continuous system has an infinite number of vibration modes natural frequencies.

Detailed modal analysis determines the fundamental vibration mode shapes and corresponding frequencies. This can be relatively simple for basic components of a simple system, and extremely complicated when qualifying a complex mechanical device or a complicated structure exposed to periodic wind loading. These systems require accurate determination of natural frequencies and mode shapes using techniques such as Finite Element Analysis (FEA).

The response of the structure is different at each of the different natural frequencies. These deformation patterns are called mode shapes. Now we can better understand what Modal Analysis is all about – it is the study of the natural characteristics of structures. Both the natural frequency (which depends on the mass and stiffness distributions in my structure) and mode shape are used to help design a structural system for noise and vibration applications. We use Modal Analysis to help design all types of structures including automotive structures, aircraft structures, spacecrafts, etc.

Modal Analysis is used in a vast range of applications including:

- Ensuring that resonances are away from excitation frequencies
- Prediction of the dynamic behavior of components and assembled structures
- Optimization of the structures dynamic properties (mass, stiffness, damping)

- Prediction of the forces from measured responses
- Prediction of the responses due to complex excitation
- Prediction of the effect of structural modifications
- Inclusion of damping in Finite Element Models
- Updating of Finite Element Models
- Damage detection and assessment

3.3 Sinusoidal Vibration Analysis

Several military specifications (MIL-E-5400, MIL-T-5422, and MIL-STD-810) recommend using sinusoidal sweeps through resonant points as part of a qualification test on many different types of electronic systems. A sine sweep test is also convenient for evaluating electronic subassemblies, such as PCBs, to determine their resonant frequencies and transmissibility. The test will usually start at a low frequency, around 10 Hz, with a sweep up to 2000 Hz, then back to 10 Hz once again. A logarithmic sweep is usually used, so that the time to sweep from 10 to 20 Hz is the same as the time to sweep from 1000 to 2000 Hz. The sweep rate is usually specified in terms of octaves per minute. An octave is a factor of 2 in frequency. This rate is thus related to the time it will take to sweep from 10 to 20 Hz, from 20 to 40 Hz, from 40 to 80 Hz, and so on.

Most of the damage accumulated during a sweep through the resonant points of an electronic structural assembly will occur near the peak response points. A convenient reference is the half-power points, used extensively by electrical engineers to characterize resonant peaks in electronic circuits. These are the points where the power that can be absorbed by damping is proportional to the square of the amplitude at a given frequency. For a lightly damped system, where the transmissibility Q is greater than about 10, the curve in the region of the resonance is approximately symmetrical. The half-power points are often taken to define the

bandwidth of the system.

The time it takes to sweep through the half-power points can be determined from the following expression:

$$t = \frac{\log_e \left(\frac{1 + (1/2Q)}{1 - (1/2Q)} \right)}{R \log_e 2} \tag{3.18}$$

Where t = time (minutes)

R = sweep rate (octaves/min)

Q = transmissibility at resonance (dimensionless) [7].

3.4 Random Vibration Analysis

A random vibration is one whose instantaneous value is not predictable with the available information. Such vibration is generated, for example, by rocket engines, turbulent flows, earthquakes, and motion over irregular surfaces. While the instantaneous vibration level is not predictable, it is possible to describe the vibration in statistical terms, such as the probability distribution of the vibration amplitude, the mean-square vibration level, and the average frequency spectrum.

A random process may be categorized as stationary (steady-state) or nonstationary (transient). A stationary random process is one whose characteristics do not change over time. For practical purposes a random vibration is stationary if the mean-square amplitude and frequency spectrum remain constant over a specified time period. A random vibration may be broad-band or narrow-band in its frequency content. Figure 3.3 shows typical acceleration-time records from a system with a mass resiliently mounted on a base subjected to steady, turbulent flow. The base vibration is broad-band with a Gaussian (or normal) amplitude distribution.

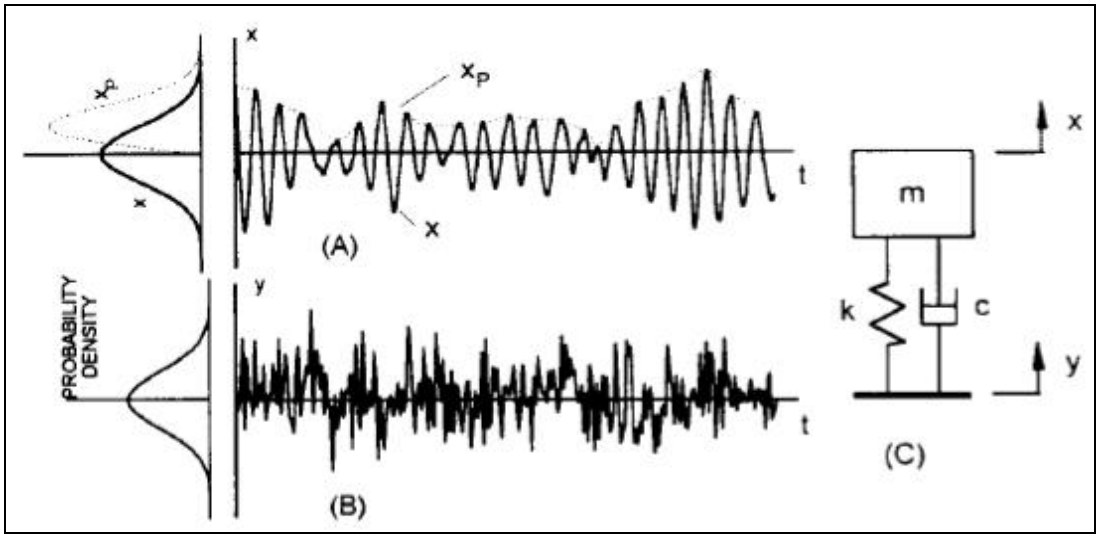

Figure 3.3. (A) Example of a narrow-band random signal x(t)

(B) Example of a broad-band random signal y(t)

(C) Resiliently mounted mass m with stiffness k and viscous damper c with ref [7]

The vibration of the mass is narrow-band (centered at the natural frequency of the mounted system) but also has a Gaussian amplitude distribution. The peaks of the narrow-band vibration have a distribution called the Rayleigh distribution. Technically, the statistical measures of a random process must be averaged over an ensemble (or assembly) of representative samples. For an arbitrary random vibration this means averaging over a set of independent realizations of the event. This is illustrated in Fig. 3.4 where four vibration-time records from a point on an internal combustion engine block are shown synchronized with the firing in a particular cylinder. Due to uncontrollable variations in the system, the vibration is not deterministically repeatable. The mean-square amplitude is also nonstationary. Therefore, the statistical parameters of the vibration are time dependent and must be determined from the ensemble of samples from each record at a particular time. For a stationary random process it may be possible to obtain equivalent ensemble averages by sampling over time if each time record is representative of the entire random process. Such a random process is called ergodic. However, not all stationary random processes are ergodic. For example, suppose it is desired to

determine the statistical parameters of the vibration levels of an aircraft fuselage during representative in-flight conditions. On a particular flight the vibration levels may be sufficiently stationary to obtain useful time averages. However, one flight is unlikely to encompass all of the expected variations in the weather and other conditions that affect the vibration levels. In this case it is necessary to combine the time averages with an ensemble average over a number of different flight conditions which represent the entire range of possible conditions [7].

3.4.1 Power Spectral Density (PSD)

The frequency content of a random variable x(t) is represented by the power spectral density $W_x(f)$, defined as the mean-square response of an ideal narrow-band filter to x(t), divided by the bandwidth Δf of the filter in the limit as $\Delta f \rightarrow 0$ at frequency

$$W_x(f) = \lim_{\Delta f \to 0} \frac{\overline{x_{\Delta f}^2}}{\Delta f} \tag{3.19}$$

By this definition the sum of the power spectral components over the entire frequency range must equal the total mean-square value of x:

$$\overline{x^2} = \int_0^\infty W_x(f)\, df \tag{3.20}$$

The term power is used because the dynamical power in a vibrating system is proportional to the square of the vibration amplitude.

An alternate approach to the power spectral density of stationary variables uses the Fourier series representation of x(t) over a finite time period $0 \leq t \leq T$, defined as:

$$x(t) = \bar{x} + \sum_{n=1}^{\infty} A_n \cos(2\pi f_n t) + \sum_{n=1}^{\infty} B_n \sin(2\pi f_n t) \tag{3.21}$$

where $f_n = n/T$.

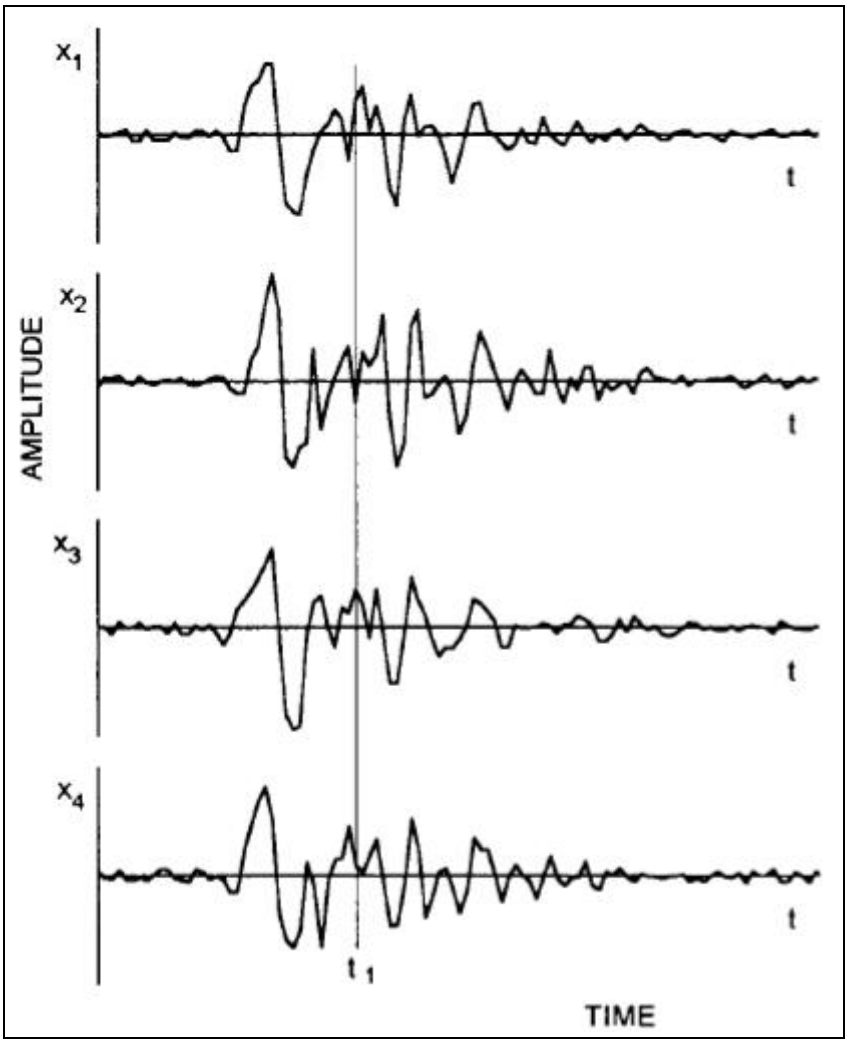

Figure 3.4. Ensemble of vibration responses (x1, x2, x3, x4) with ref [7]

The coefficients of the Fourier series are found by

$$A_n = \frac{2}{T}\int_0^T x(t)\cos(2\pi f_n t)\,dt \tag{3.22}$$

$$B_n = \frac{2}{T}\int_0^T x(t)\sin(2\pi f_n t)\,dt \tag{3.23}$$

It follows that the coefficients of the Fourier series are a measure of the correlation of x(t) with the cosine and sine waves at a particular frequency.

The relation between the Fourier series and the power spectral density can be found by evaluating $\overline{x^2}$ from Eq. (3.21):

$$\overline{x^2} = \frac{1}{T}\int_0^T \left\{ \bar{x} + \sum_{n=1}^{\infty} [A_n \cos(2\pi f_n t) + B_n \sin(2\pi f_n t)] \right\} \times \left\{ \bar{x} + \sum_{m=1}^{\infty} [A_m \cos(2\pi f_m t) + B_m \sin(2\pi f_m t)] \right\} dt \tag{3.24}$$

The integral over time cancels all cross terms in the product of the Fourier series leaving only the squares of each term:

$$\overline{x^2} = \frac{1}{T}\int_0^T \left\{ (\bar{x})^2 + \sum_{n=1}^{\infty} [A_n^2 \cos^2(2\pi f_n t) + B_n^2 \sin^2(2\pi f_n t)] \right\} dt$$

$$= (\bar{x})^2 + \sum_{n=1}^{\infty} \frac{1}{2}\left[A_n^2 + B_n^2 \right] \tag{3.25}$$

Each term in this series can be viewed as representing a component of the mean square value associated with a filter of bandwidth $\Delta f = 1/T$. The power spectral density is then approximated by

$$W_x(f_n) \simeq \frac{T}{2}\left(A_n^2 + B_n^2 \right) \tag{3.26}$$

Using a similar method the relation between $W_x(f)$ and $R_x(\tau)$ can be found. Equation (3.24) can be used to evaluate $R_x(\tau)$ by changing the factors $f_n(t)$ to $f_n(t + \tau)$. The time integration removes all terms except those of the form $\frac{1}{2}(A_n^2 + B_n^2)\cos(2\pi f_n \tau)$.

The autocorrelation is then given by

$$R_x(\tau) = (\bar{x})^2 + \sum_{n=1}^{\infty} \frac{1}{2}\left(A_n^2 + B_n^2 \right)\cos(2\pi f_n \tau)$$

$$= (\bar{x})^2 + \sum_{n=1}^{\infty} W_x(f_n)\cos(2\pi f_n \tau)\Delta f \tag{3.27}$$

In the limit as $T \rightarrow \infty$, $\Delta f \rightarrow 0$ and the summation approaches the continuous integral:

$$R_x(\tau) = \int_0^{\infty} W_x(f)\cos(2\pi f\tau)\, df \tag{3.28}$$

This is the Fourier cosine transform. The reciprocal relation is:

$$W_x(f) = 4\int_0^{\infty} R_x(\tau)\cos(2\pi f\tau)\, d\tau \tag{3.29}$$

For transient random variables the power spectral density is a function of time. However, if the power spectral density is integrated over the time duration of a transient x(t), an energy spectral density $E_x(f)$ can be obtained representing the frequency content of the total energy in x. Using the Fourier series approach, energy spectral density is:

$$E_x(f_n) = T\ W_x(f_n) \tag{3.30}$$

Alternately, the shock spectrum can be used to represent the frequency content of a transient. The shock spectrum represents the peak amplitude response of a narrow-band resonance filter to a transient event [8].

A PSD records the mean square value of the excitation and response as a function of frequency. There are two important concepts. First one is the area under a PSD curve is the variance of the response (square of the standard deviation). And the second one is the unit used in PSD is mean square/Hz (e.g. acceleration PSD will have units of G^2/Hz). Two samples of acceleration PSD curves can be seen in Figure 3.5.

3.4.2 Root-Mean-Square Acceleration (Grms)

It is very easy to describe the G_{rms} (root-mean-square acceleration, sometimes written as GRMS or Grms or grms) value as just the square root of the area under the Acceleration Spectral Density (ASD) vs. frequency curve. But to physically interpret this value we need to look at G_{rms} a different way. The easiest way to think of the G_{rms} is to first look at the mean square acceleration.

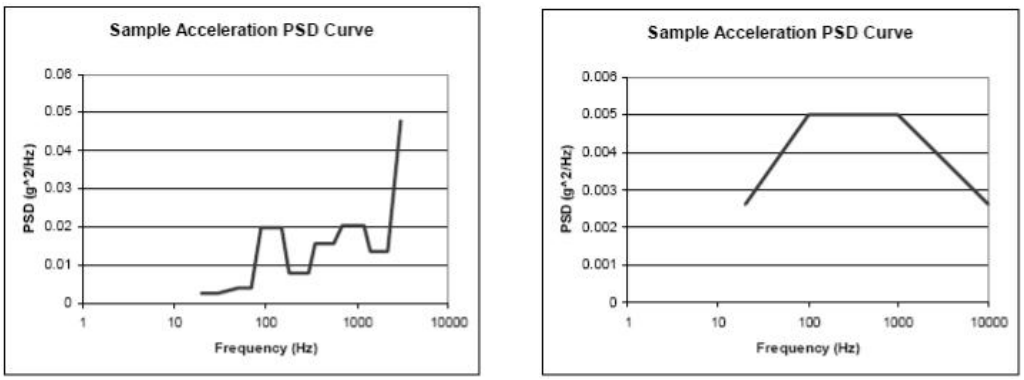

Figure 3.5. Sample Acceleration PSD Curves

Mean-square acceleration is the average of the square of the acceleration over time. That is, if a time history of an accelerometer trace are looked and this time history was squared and then it is possible to determine the average value for this squared acceleration over the length of the time history, which would be the mean square acceleration. Using the mean square value keeps everything positive.

The G_{rms} is the root-mean-square acceleration (or rms acceleration), which is just the square root of the mean square acceleration determined above.

If the accelerometer time history is a pure sinusoid with zero mean value, e.g., a steady-state vibration, the rms acceleration would be 0.707 times the peak value of the sinusoidal acceleration (if just a plain average are used, then the average would be zero). If the accelerometer time history is a stationary Gaussian random time history, the rms acceleration (also called the 1 sigma acceleration) would be related to the statistical properties of the acceleration time history,

68.3% of the time, the acceleration time history would have peaks that would not exceed the +/- 1 sigma (σ) accelerations.

95.4% of the time, the acceleration time history would have peaks that would not exceed the +/- 2 sigma (σ) accelerations.

99.7% of the time, the acceleration time history would have peaks that would not exceed the +/- 3 sigma (σ) accelerations.

There is no theoretical maximum value for the Gaussian random variable; however,

we typically design to 3 sigma since it would only be theoretically exceeded 0.3% of the time. In addition, from a practical point of view, we know that it would be physically impossible to achieve unreasonably high sigma values.

Below is presented the method to calculating the root-mean-square acceleration (G_{rms}) response from a random vibration ASD curve in Figure 3.6.

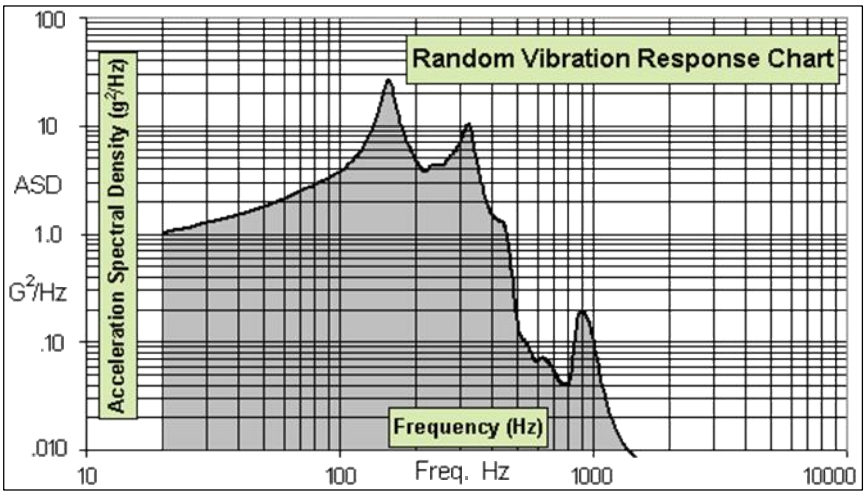

Figure 3.6. Typical random vibration response curve with ref [9]

G_{rms} values are determined by the square root of the area under an ASD vs. frequency response curve. The Acceleration Spectral Density values are in g^2/Hz and the frequencies are in Hz.

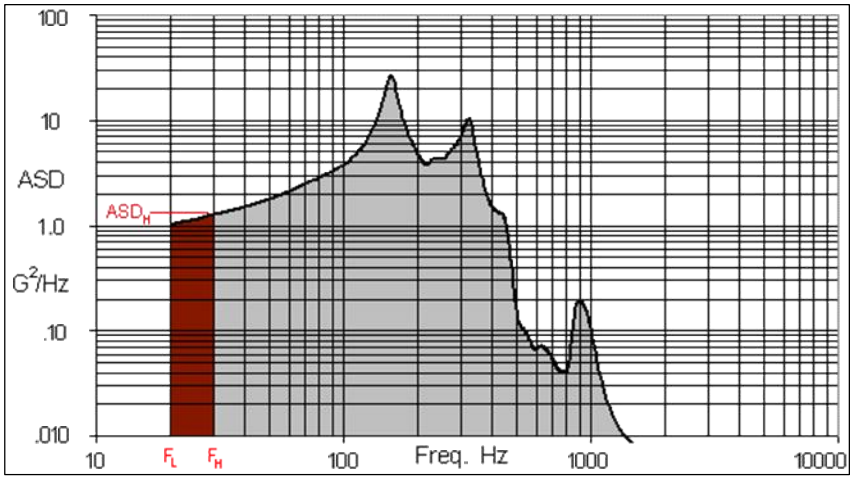

Figure 3.7. A bandwidth of 10 Hz with ref [9]

Figure 3.7 shows a bandwidth of 10 Hz, which will be used as an example for calculating G_{rms}.

First, calculate the number of octaves. From the plot, FL = 20Hz and FH = 30Hz. The equations below gives #octaves = 0.58.

$$\#Octaves = \frac{\log\left(F_H / F_L\right)}{\log(2)} \tag{3.31}$$

Second, calculate the dB value. For FL = 20 Hz, ASDL = 1.0 g^2/Hz, while ASDH = 1.1 g^2/Hz. The calculated value is 0.41 dB.

$$dB = 10\log\left(ASD_H / ASD_L\right) \tag{3.32}$$

Third, calculate the slope, m, of the segment between the frequencies FL and FH. Dividing the number of dB by the number of octaves gives m = 0.71 dB/oct.

$$m = dB/\#octaves \tag{3.33}$$

Fourth, calculate the area under the curve between the frequencies FL and FH. In our example, A = 10.53 g^2.

$$A = 10\log(2)\frac{ASD_H}{10\log(2)+m}\left[F_H - \left(F_L\right)\left(\frac{F_L}{F_H}\right)^{m/10\log(2)}\right] \tag{3.34}$$

NOTE - The above equation is invalid if the slope m = -10 log (2) because you would be dividing by zero. If m = -10 log (2), use the following equation for the area:

$$A = ASD_L \times F_L \times \ln\left(\frac{F_H}{F_L}\right) \tag{3.35}$$

(L'hôpital's Rule is used to solve the equation as the limit of [1 + m / (10log2)] goes to zero)

Finally, take the square root of the area for the G_{rms} value. To finish our example, the acceleration = 3.24 G_{rms}.

$$g_{rms} = \sqrt{A} \tag{3.36}$$

In order to calculate the G_{rms} value for the entire curve, sum up all the areas (A1 + A2 + A3 + ... + A_n = A) and take the square root of the sum.

NOTE: 3 dB is a factor of 2 for ASD curves (g^2/Hz) while 6 dB is a factor of 2 for G_{rms} values. For example, reducing a peak ASD value of 12 g^2/Hz by – 3 dB would give 6 g^2/Hz; reducing a value of 12 G_{rms} -3dB results in a value of 9 G_{rms} and reducing it -6 dB results in a value of 6G_{rms} [9].

CHAPTER 4

DESIGN SPECIFICATIONS OF RASAT

As described in the previous sections, RASAT satellite is going to be examined. RASAT is a scientific earth observation purposed satellite which is being designed by the engineers of TÜBİTAK UZAY. Basically, it is a micro satellite and all the requirements and constraints have been taken into consideration according to the general specifications of a micro satellite.

From the mechanical point of view, the main requirements and constraints are those of given by the possible launchers. At the beginning of the mechanical design, since the launcher of RASAT is not certain, it is a good idea to take the worst cases of the possible launcher. For instance, if the volume envelope of COSMOS-3M is smaller than that of DNEPR, it is better to take the volume envelope design requirement of COSMOS-3M. Other design constraints should be taken into consideration by the same philosophy.

4.1 Mass property Requirements

The mass of the whole spacecraft is a criterion in satellite design. Many launchers give their maximum payload mass for the satellites to be launched. Also, the mass-related specifications (e.g. center of mass, inertia) are also important. For instance, COSMOS-3M and ARIANE rockets give the following criteria:

- The maximum mass of a micro Auxiliary Payload without its separation system to ASAP 5 must be less or equal to 120 kg.
- Center of gravity position : $X_G \leq 450$ mm (from the mounting plan of the spacecraft) Y_G , $Z_G \leq \pm 5$ mm
- Inertia: I_{XX}, I_{YY} and $I_{ZZ} \leq 20$ m^2 kg. (w.r.t. C. o. G.)

So, in each phase of the structural design, the constraints given above must be satisfied. Generally, these values are checked at the end of the structural design or in the structural analysis phase. But, during the design, all these constraints must be kept in mind and it is necessary to be within these limits.

4.2 Stiffness Criteria (Frequency Requirements)

In order to avoid dynamic coupling between the low frequency vehicle and spacecraft modes, the spacecraft should be designed with a structural stiffness, which ensures that the values of fundamental frequency of the spacecraft, hard mounted at the separation plane, are not less than given launcher limits.

Frequency requirements of DNEPR rocket are:

The fundamental frequency of the spacecraft must be bigger than 20 Hz in the longitudinal axis and 10 Hz in the lateral axes.

Frequency requirements of COSMOS-3M rocket are:

The fundamental frequency of the spacecraft in the longitudinal axis is $\geq$ 90 Hz and the fundamental frequencies of the spacecraft in the lateral axes are $\geq$ 45 Hz. This applies for the spacecraft hard mounted at the ASAP 5 Payload separation plane.

So, during and after the structural design, the frequency requirements of COSMOS-3M should be taken into consideration since its limits are much higher than those of DNEPR. During the design, these values must be kept in mind and after the compilation of the design; the analysis checks must be valid according to these requirements.

4.3 Quasi-Static and Dynamic Loads

During flight, various static and dynamic loads are superimposed. The design and dimensioning of the satellite primary structure must therefore allow for the most severe load combination that can be encountered at a given instant of flight.

The quasi-static and dynamic flight limit loads of COSMOS-3M and ARIANE rockets are given in Table 4.1:

Table 4.1. The flight limit loads of COSMOS-3M with ref [10]

	Longitudinal	**Lateral**
	Static + Dynamic	**Static + Dynamic**
Acceleration (g)	- 7.5 / + 5.5	± 6

NOTES:

- The minus sign with longitudinal axis values indicates compression.
- Lateral loads may act in any direction simultaneously with longitudinal loads,
- The quasi static loads (QSL) apply on payload C of G,
- The gravity load is included,
- These loads apply for micro Auxiliary Payload complying with the frequency requirements.

Similarly, the quasi-static and dynamic components of accelerations that act on the spacecraft/launch vehicle (SC/LV) interface during the ground handling, launch and in-flight of DNEPR rocket are given in the Tables 4.2 and 4.3. Spacecraft dimensioning and testing must take into account safety factors, which are defined by the spacecraft authority, but should be no less than the values given below:

- 2.0 for ground handling;
- 1.5 during launch while LV is moving inside the transport and launch canister (TLC);
- 1.3 during launch after the LV exits from the TLC;
- 1.3 during the LV flight.

The spacecraft should remain operable after the effect of the given accelerations.

Table 4.2. Accelerations at SC/LV Interface during Transportation with ref [11]

Load Source	**Acceleration (g)**		
	Longitudinal (X)	**Lateral (Y)**	**Lateral (Z)**
SHM Transportation	±0.4	-1.0±0.7	±0.5

Table 4.3. Maximum Quasi-static and Dynamic Accelerations at SC/LV Interface with ref [11]

	Acceleration (g)	
Load Source	**Longitudinal (X)**	**Lateral (Y, Z)**
LV movement inside TLC	2.5±0.7	±0.3
After LV exit from TLC	±1.0	±0.8
1st stage burn		
Maximum dynamic head	3.0±0.5	0.5±0.5
Maximum longitudinal acceleration	7.5±0.5	0.1±0.5
2nd stage burn – maximum longitudinal acceleration	7.8±0.5	0.2
3rd stage burn	-0.3...-0.5	0.25

Notes to Tables 4.2 and 4.3:

- Lateral accelerations may act in any direction, simultaneously with longitudinal ones;
- The above values are inclusive of gravity force component;

- Dynamic accelerations are preceded by "±" symbol;
- The above values are correct for the spacecraft complying with the fundamental frequency requirements.

So, during the design, the quasi-static and dynamic load limits of COSMOS-3M rocket must be considered. Once the design is completed, all the structural analysis and tests must be according to these values.

4.4 Vibration Loads

Described below are vibrations acting on the spacecraft attachment points during the LV flight. Two types of vibrations are as follows:

- Harmonic oscillations; and
- Random vibrations.

The harmonic oscillations are characterized by the amplitude of vibro-accelerations and frequency. The parameters of harmonic oscillations of DNEPR rocket are given in Tables 4.4 and 4.5, and those for ARIANE-5 rocket are given in Table 4.6.

The random vibrations are characterized by spectral density of vibro-accelerations and the duration of influence. The random vibration parameters of DNEPR rocket are given in Table 4.7 and those of COSMOS-3M rocket are given in Table 4.8. The random vibrations are spatial with approximately equal intensity of vibro-accelerations in each of the three randomly selected mutually perpendicular directions.

The values of amplitude and spectral densities are given in the extreme octave points. The change of these values within the limits of each octave is linear in the logarithm frequency scale.

Table 4.4. Amplitude of Harmonic Oscillations at SC/LV Interface with ref [11]

Frequency sub-band (Hz)	5-10	10-15	15-20
Amplitude (g)	0.5	0.6	0.5
Duration (sec)	10	30	60

Table 4.5. Amplitude of Harmonic Oscillations at SC/LV Interface. Lateral Axes (Y, Z) with ref [11]

Frequency sub-band (Hz)	2-5	5-10	10-15
Amplitude (g)	0.2-0.5	0.5	0.5-1.0
Duration (sec)	100	100	100

Table 4.6. Sinusoidal vibration design levels with ref [12]

	Frequency range (Hz)	**Qualification levels (0-peak)**	**Acceptance levels (0-peak)**
Longitudinal	4-5	12.4 mm	9.9 mm
	5-100	1.25 g	1 g
Lateral	2-5	9.9 mm	8.0 mm
	5-25	1 g	0.8 g
	25-100	0.8 g	0.6 g
Sweep rate		2 oct./min	4 oct./min

Table 4.7. Spectral Density of Vibro-accelerations at SC/LV Interface with ref [11]

	Load Source	
Frequency sub-band (Hz)	**Liftoff, LV flight segment where M=1, q_{max} 1st stage burn (except for LV flight segment where M=1, q_{max}), 2nd and 3rd stage burn**	
	Spectral Density (g^2/Hz)	
20 to 40	0.007	0.007
40 to 80	0.007	0.007
80 to 160	0.007-0.022	0.007
160 to 320	0.022-0.035	0.007-0.009
320 to 640	0.035	0.009
640 to 1280	0.035-0.017	0.009-0.0045
1280 to 2000	0.017-0.005	0.0045
Root Mean Square Value, σ (g)	6.5	3.6
Duration (sec)	35	831

Table 4.8. Vibration loads near sonic velocity (including safety factor of +6dB) with ref [12]

Frequency Band (Hz)	**Spectral Density of Vibration Acceleration (g^2/Hz)**	**Duration (sec)**
10 to 20	0,006 to 0,004	80
20 to 40	0,004	
40 to 80	0,004 to 0,0062	
80 to 160	0,0062 to 0,02	
160 to 320	0,02 to 0,046	
320 to 640	0,046 to 0,084	
640 to 1280	0,084 to 0,074	
1280 to 2000	0,074 to 0,036	

4.5 Mechanical Concept of RASAT

The structural design of RASAT is based on a module-stack frame type. There is a main module-stack which is composed of several micro trays. On both sides of the stack there are stiffened facing plates. The one that looks through the earth on orbit is called as “Earth Facing Facet (EFF)” and the other one that looks through the outer space is called as “Space Facing Facet (SFF)“. The earth facing facet is connected to the stack from the bottom on which there is a stiffened module (called as BCR). The space facing facet is connected to the main stack by means of some stiffened panels, which are called as “Shear Panels”. Lastly the solar panels are mounted between SFF and EFF. All the primary structure of RASAT is formed as above. In Fig. 4.1, the main module-stack, the space facing facet, the earth facing facet, the shear panels and the solar panels are shown as an exploded view.

The main module-stack is composed of 10 micro trays. These micro trays are assembled by means of 8 tie-bars which are made of titanium in order to obtain a good strength, stiffness and due to having a good ductile behavior.

RASAT satellite is going to be attached to the launcher rocket from its separation system ring. The picture of the separation ring is shown in Fig.4.2.

This separation ring is intended to fasten a micro satellite to the launch vehicle, to separate it and then to send it up. It is activated by an electric order coming from the launcher the detonators initiate the pyrotechnics fuse. At the same time detonation’s wave bends the tube and causes the structure to break. The springs loose their tension and send up the micro satellite. In Fig. 4.3, this separation motion before the separation and after the separation is shown.

So, by mounting all the primary structural elements (SFF, EFF, shear panels), the main module-stack, the nano-stacks, their modules and solar panels the overall design of RASAT is completed as shown in Fig. 4.4. And also the main dimensions of RASAT are shown in Fig. 4.5 as an isometric view.

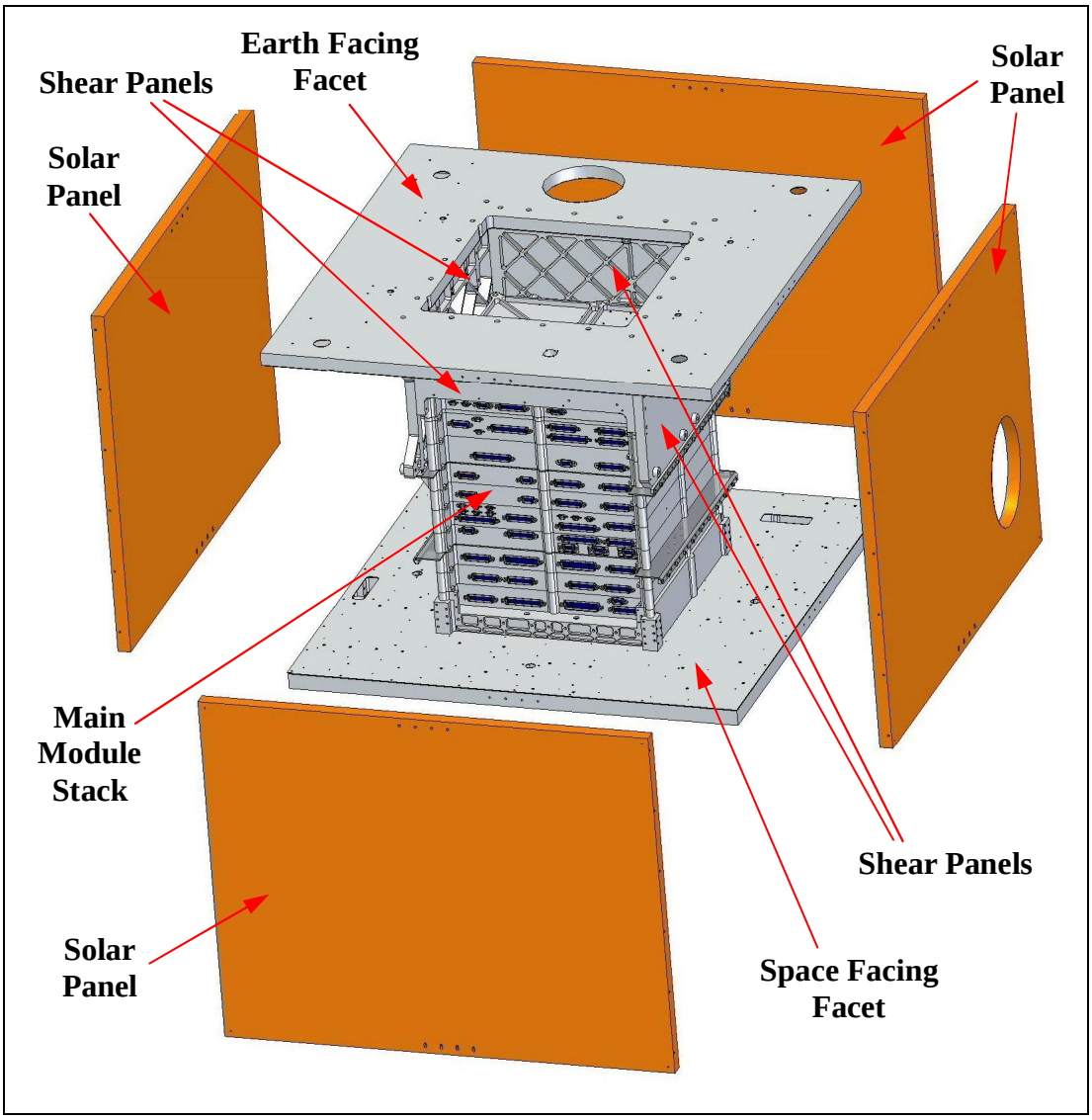

Figure 4.1. Main Structure of RASAT

Figure 4.2. Dassault Separation System for Micro Satellites with ref [13]

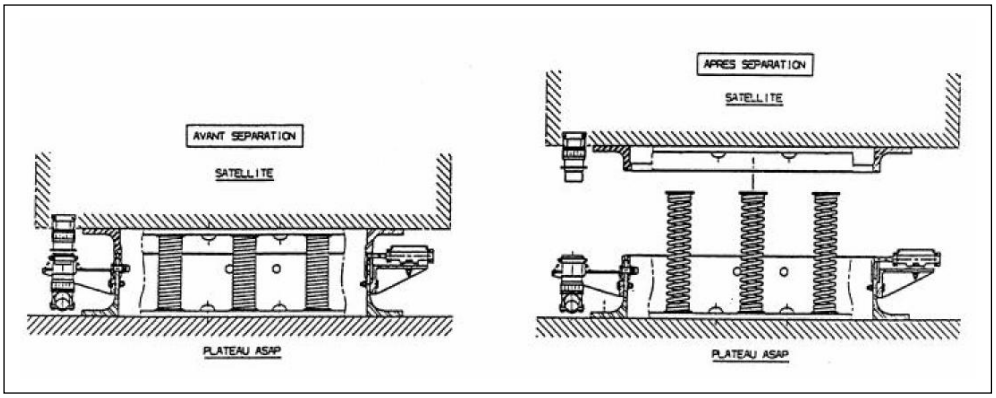

Figure 4.3. Separation system mechanism with ref [14]

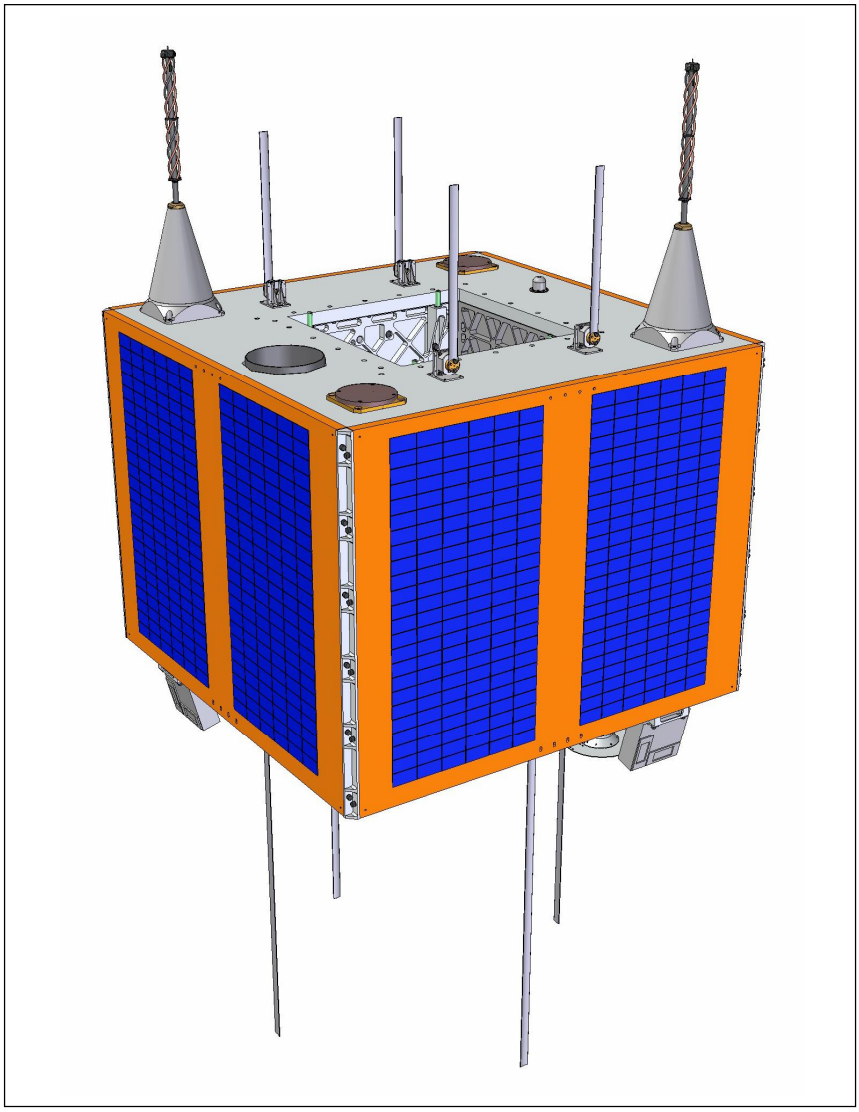

Figure 4.4. Solid Model of the RASAT Satellite

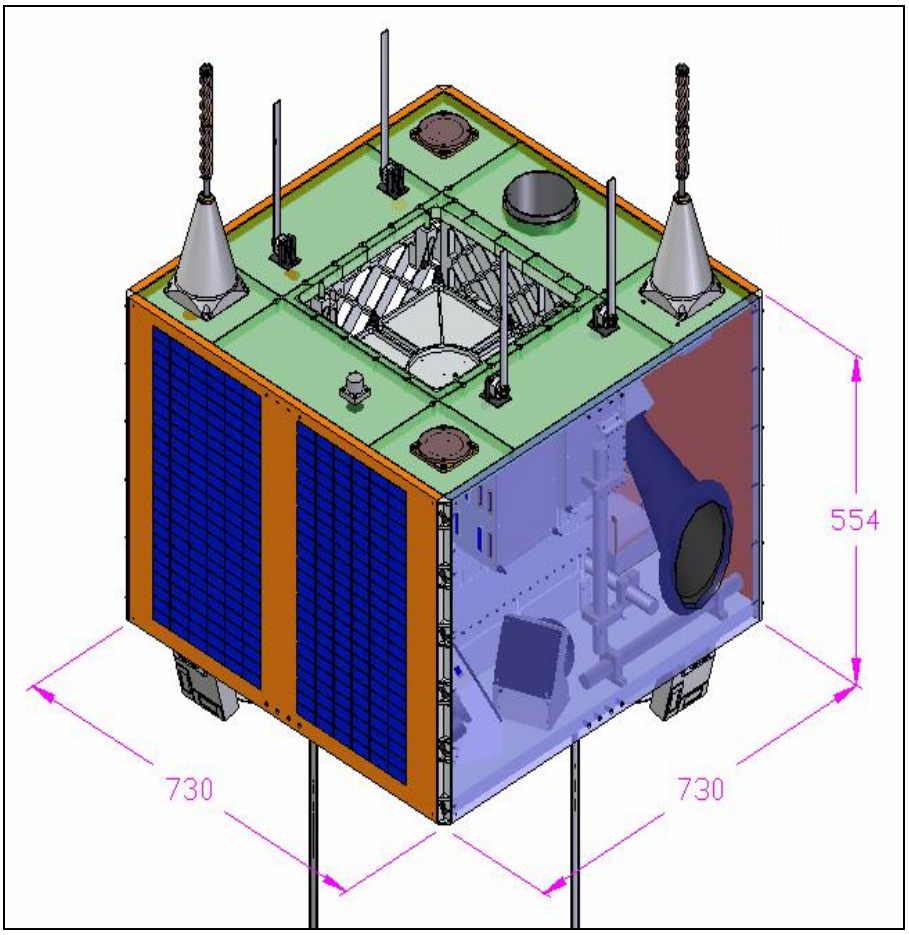

Figure 4.5. Main Dimensions of RASAT (in millimeters)

4.6 Mass Properties

Another concept which is to be kept in mind during design is the total mass and the mass-related properties of the micro satellite. The requirements are given in the previous chapters. The weight of RASAT must not exceed 120 kg. During and after the design, mass of RASAT is checked regularly by keeping the given constraint in mind. After the design is completed, it is seen that the overall calculated weight of RASAT is about 104.63 kg, not exceeding 120 kg.

The mass budget of RASAT is summarized in Table 4.9. The percentages are quite logical as compared to the suggested values. This table shows us that structural mass of the satellite is about 26% of the total mass by taking the most important role in the total mass as shown in Fig. 4.6.

Table 4.9. RASAT Mass Budget

SUBSYSTEM	MASS [kg]	PERCENTAGE
Communication	12.437	12%
Power	12.35	12%
ADCS	12.97	12%
OBC	5.993	6%
Other Modules	0.551	1%
Sep. System	3.5	3%
Camera	6.38	6%
Solar Panels	8	8%
Harness	15	14%
Structural	27.45	26%
Total	104.631	100%

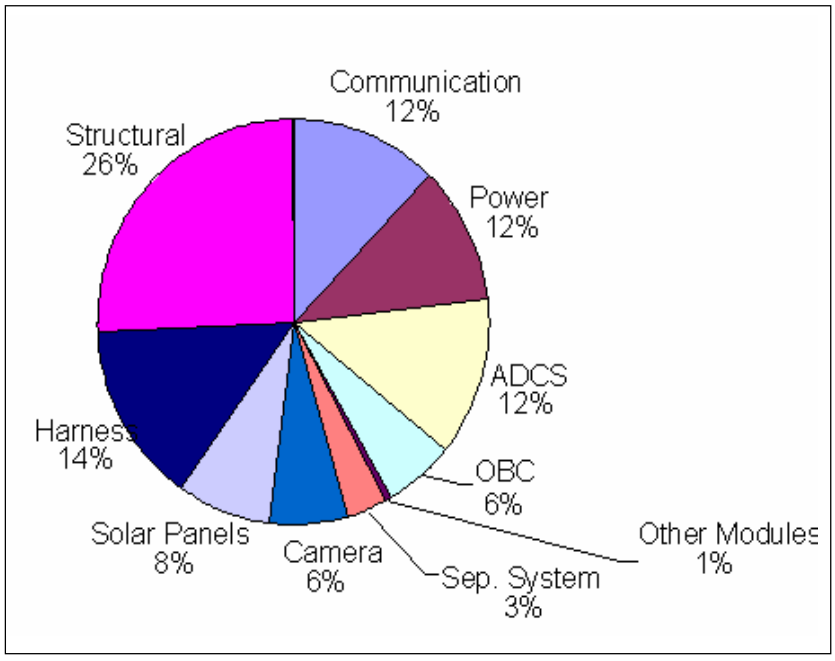

Figure 4.6. Mass Allocation of RASAT

The other mass-related properties, which are the center of mass and the mass moment of inertia, are also important in design as indicated before. These values are must also be kept within the specified limits. But in order to specify and calculate these values, the coordinate axes of RASAT must be specified. These coordinate axes are also used in finite element analysis and environmental tests in order to make the analyses correctly.

The coordinate axes of RASAT are specified as,

+ Z axis: From the space facing to the earth facing facet;

+ X axis: To the main camera side from the other side;

+ Y axis: From the star tracker camera side to the other side;

Origin: On the contact surface between the space facing facet and the separation ring and on the separation ring center, as shown in Fig. 4.7.

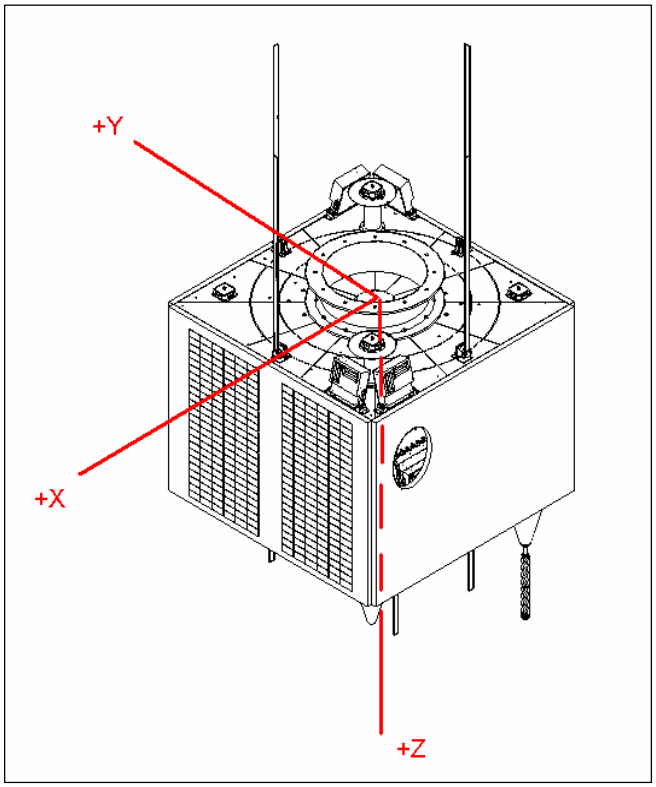

Figure 4.7. Coordinate Axes of RASAT

The Center of Gravity Location of RASAT is calculated as:

X: 6.372 mm

Y: -2.105 mm

Z: 236.023 mm

and the Mass Moments of Inertia w.r.t. Center of Gravity are calculated as:

I_{xx}: 7814621 kg-mm^2

I_{yy}: 7521425 kg-mm^2

I_{zz}: 8034486 kg-mm^2

I_{xy}: 202672.8 kg-mm^2

I_{xz}: -50658.02 kg-mm^2

I_{yz}: 40257.59 kg-mm^2

These values are within the limits of the launcher as specified before.

CHAPTER 5

STRUCTURAL FINITE ANALYSIS OF THE RASAT SATELLITE

In order to verify the mechanical design, a structural finite element analysis is performed as part of the mechanical qualification process. In this chapter the analysis is going to be detailed. The top-level structural analysis based on an FE model of the complete spacecraft is carried out. Results from this whole-spacecraft analysis are going to be used in the component-level analysis of some modules and structural elements.

All the finite element analyses are performed by using ABAQUS software. It is chosen due to its superior CAD interface, higher mesh quality, and user-friendly graphical interface.

5.1 Finite Element Model

The finite element model of RASAT is formed by transferring the CAD solid model from CAD software to the finite element software. Almost all of the parts which have structural importance are included in the finite element model. After transferring the part models, they are prepared to make the required analyses.

First of all, all the parts are assembled in the FEA software as in the CAD assembly. All the locations, placements and constraints are done according to the real case. The next step is to mesh the assembly. While meshing, the assembly is not meshed as a whole body since the parts forming the assembly do not have the same structure and similar geometry. For instance some parts are in the solid structure and some are in the shell structure. So, all the parts are meshed independently. While meshing, firstly, lower number of elements is selected according to the size of the component being meshed. Then, the number of

elements is increased in order to obtain the results so that two successive results should have a relative error of 10%. In other words, Then the RASAT assembly model is meshed to perform analyses as shown in Fig.5.1. The inner configuration of the mesh is shown in Fig.5.2 by removing the solar panels. The coordinate axes are chosen consistent with those used in mass calculations.

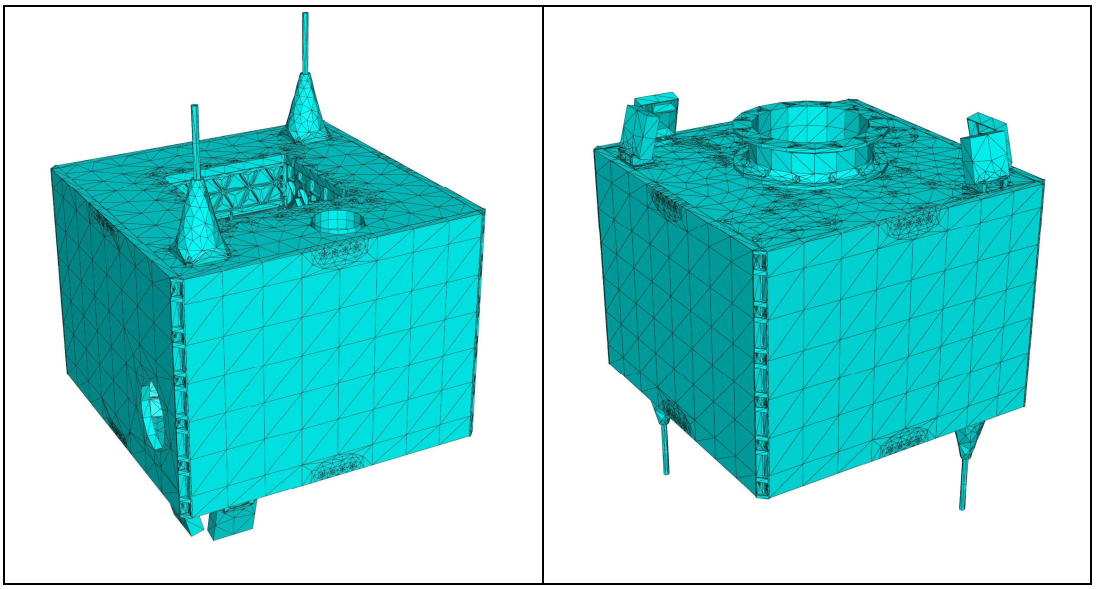

Figure 5.1. RASAT Finite Element Model

The parameters of the finite element model are as follow:

- The number of elements defined by the user and the tie constraints: 205129
- The number of internal elements generated for contact: 8448
- **The total number of elements: 213577**
- The number of nodes defined by the user: 76916
- The number of internal nodes generated by the program: 20352
- **The total number of nodes: 97268**

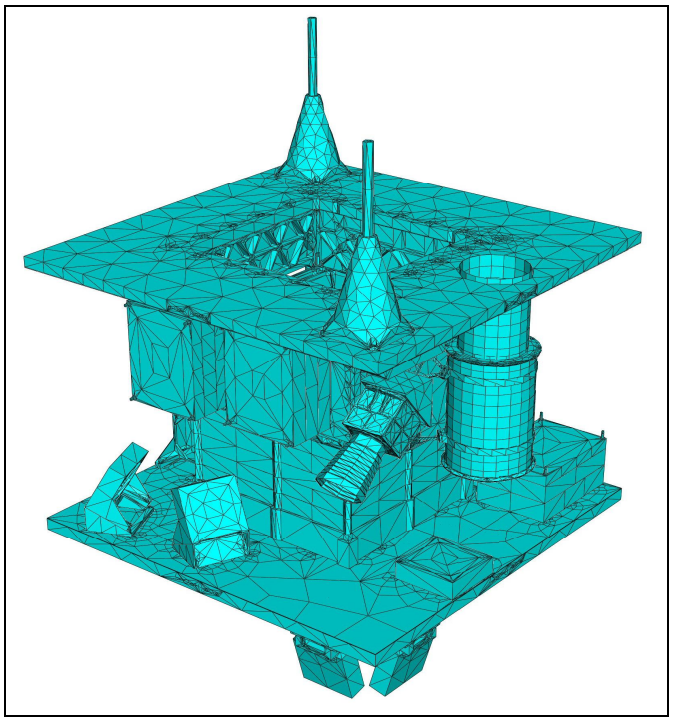

Figure 5.2. Inner View of the RASAT Finite Element Model

5.1.1 Material Properties

Various materials are used in the FE model of the whole spacecraft. Generally aluminum alloys are selected due to their easy provision, easy machining, good strength/weight ratio and good thermal properties. Most of the structural elements like SFF, EFF, shear panels, module boxes, and brackets are made of aluminum alloys. In addition to aluminum alloys, titanium is selected for tie-bars due to its good strength and mass properties. The isotropic materials used in RASAT are listed in Table 5.1. Other than the isotropic materials, there are some materials having orthotropic properties. For instance, the structure used for the solar panels is honeycomb. The honeycomb core material has a 3-D orthotropic property as listed in Table 5.2. Similarly, the skin material for the solar panels is Carbon Fiber Reinforced Plastic (CFRP). Since these skins are modeled as shell elements, a 2-D orthotropic material property is used as listed in Table 5.3.

Table 5.1. Isotropic materials used in the model with ref [15]

Material	**Modulus of Elasticity (GPa)**	**Poisson's Ratio**	**Density (kg/m^3)**	**Ultimate Tensile Stress (MPa)**
Aluminum 5050	68.9	0,33	2,69	172
Aluminum 6061-T6	68.9	0,33	2,70	310
Aluminum 7075-T6	71.7	0,33	2,81	572
Stainless Steel 416	200	0,33	7,80	760
Titanium 6Al 4V(Grade 5)	113.8	0,342	4,43	950
PEEK 450G	3.5	0,40	1,30	97 (Yield stress)

Table 5.2. Honeycomb core material properties (3-D orthotropic) with ref [15]

Property		**Value**
Moduli of Elasticity (MPa)	E_{11}	0.264
	E_{22}	0.264
	E_{33}	1034
Poisson's Ratios	ν_{12}	0.40
	ν_{23}	-
	ν_{31}	-
Shear Moduli (MPa)	G_{12}	1
	G_{23}	214
	G_{31}	214
Density (kg/m^3)		0.0190

Table 5.3. CFRP-M18/45%/193P/AS-4-3K material properties (2-D orthotropic) with ref [16]

Property	Value
E_{11} (GPa)	101.92
E_{22} (GPa)	101.92
ν_{12}	0.30
G_{12} (GPa)	3
Density (kg/m^3)	1.4349

The material assignment is shown in Fig 5.3 as each material type is corresponded to a color. As it can be seen that the most used material type is Aluminum 7075-T6, then Aluminum 6061-T6 is the next one.

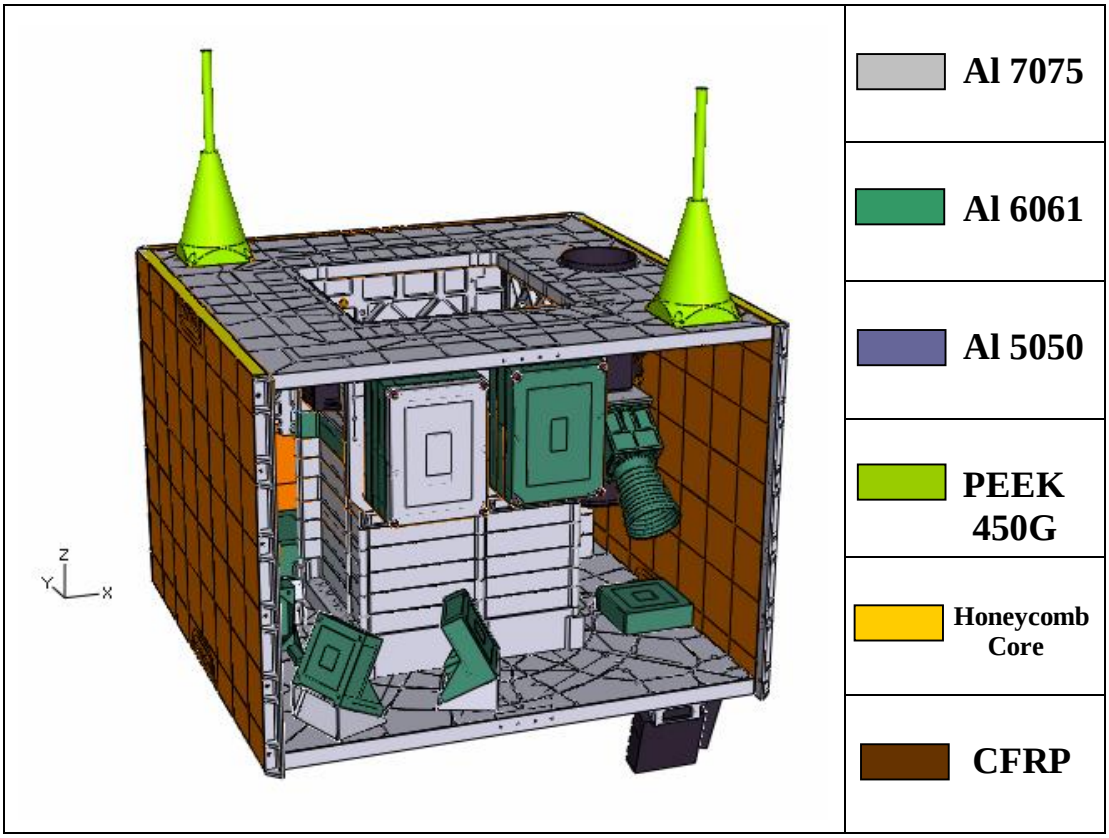

Figure 5.3. Materials used in the Finite Element Model (the solar panel on the near side removed for clarity)

5.1.2 Boundary Conditions

After meshing all the parts and assigning all the corresponding materials, the next step is defining the boundary conditions in order to carry out the analyses. Since, the satellite is attached to the launch vehicle from its separation ring, normally; the boundary condition is going to be the 12 cylindrical holes of the separation ring on the launch vehicle side. Boundary conditions consisted of nodes on the bottom flange of the Separation System are being constrained in all degrees of freedom. These constraints are applied at 12 equally spaced angular locations around the Separation System, corresponding to the actual bolted connections to the launch vehicle. In Fig.5.4, these holes are shown by a marker plot with these boundary conditions.

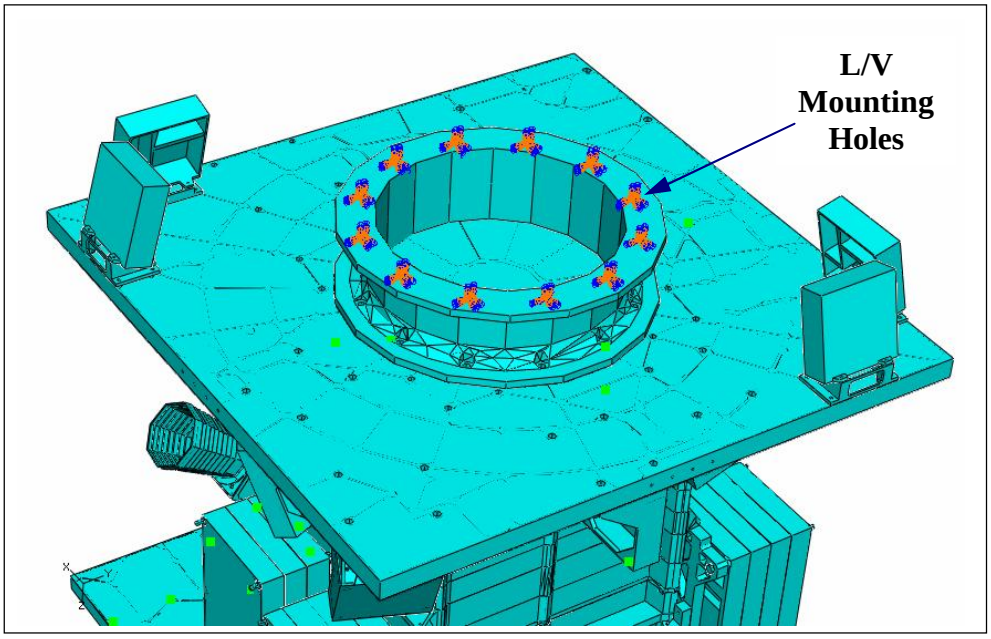

Figure 5.4. Boundary Condition of the Model

5.1.3 Element Types and Constraints

When preparing the model, different element types are used. These elements are either 2-D or 3-D. For the main structural elements, like SFF, EFF, shear panels,

separation ring, nano and micro trays, brackets, etc., 3-D solid elements are used. For the solar panel skins and main camera enclosure, 2-D shell elements are used since their structure is made of sheet material.

Since the geometry of the solid structures like SFF, EFF, micro trays, shear panels, and so on are quite complex, it is not possible to mesh them with brick-type elements. So in such structures, 6-node linear triangular prism and 4-node linear tetrahedron elements are used. In the solid structures having regular geometry, like tie-bars and fasteners, 8-node brick elements are used. In the shell-type structures, 6-node quadratic plane stress shell elements are used where appropriate. In Table 5.4, the element types used in the finite element model and their corresponding ABAQUS element codes are listed.

Table 5.4. Element Types Used in the Model with ref [17]

C3D8R	8-node linear brick, reduced integration with hourglass control 3-D solid element
C3D6	6-node linear triangular prism 3-D solid element
C3D4	4-node linear tetrahedron 3-D solid element
CPS6	6-node quadratic plane stress elements

The parts are connected to each other by using the “TIE” constraint of ABAQUS software. This is a multi-point constraint (MPC). In this type connection, the nodes of master and slave bodies are tied to each other from the selected nodes or surfaces. For instance, as shown in Fig.5.5, the upper part is to be tie-connected to the lower part from its cylindrical holes lower circle (pink circle in the figure) to the upper surface of the lower part (red surface). In this case, the circle nodes become slave nodes and the surface of lower part becomes the master surface.

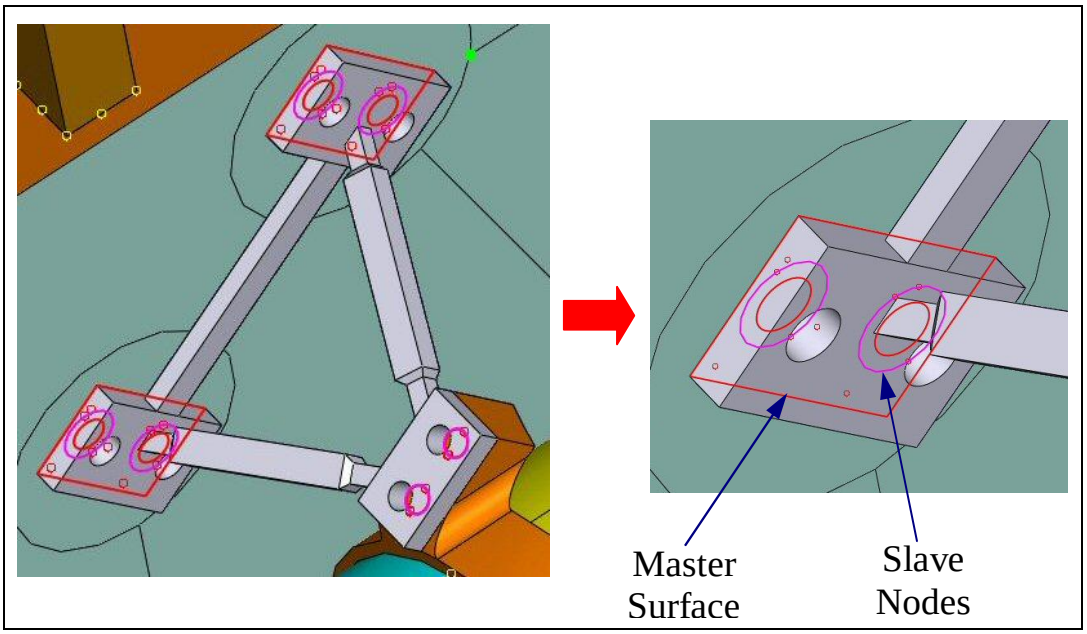

Figure 5.5. Presentation of TIE constraint

The mass properties and mass budget of the finite element model are prepared as based on the mass budget and properties calculated before (Chapter 4.6). But, since all the parts, like printed circuit boards, electronic hardware, cable harness, etc. used in the real model are not considered in the finite element model, the weight of the finite element model is lower than the real one. In order to equate both models, mass inertias are used. These inertias are connected to the parts from the location of the absent masses. In Fig.5.6, an example of a mass inertia and its connection are shown.

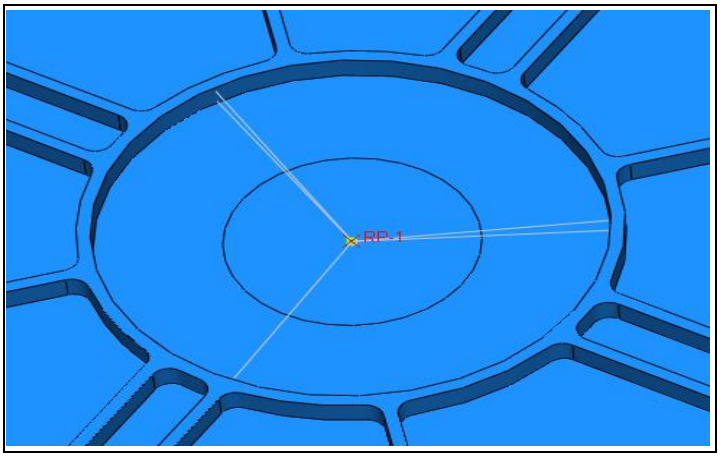

Figure 5.6. Presentation of Mass Inertia

5.2 Modal Analysis

The purpose of the normal modes analysis at the spacecraft top level is to assess the overall key lateral and axial resonant frequencies of the craft as a whole. Although there are no rigid specifications for lateral resonant frequency of the spacecraft, it is conventional for a craft of this size to aim for a value larger than 45 Hz, preferably within the range 50 Hz to 60 Hz. Similarly, the first axial mode of the spacecraft as a whole should be at least 90 Hz, and preferably about 120 Hz.

When the model is analyzed, the results showed suggested behavior of the spacecraft. The first two normal modes are predicted to be lateral swaying of the spacecraft as a whole. The frequencies are very close to each other, the first mode being a sway along the Y axis at about 53.45 Hz and the second being a sway along the X axis of the spacecraft at about 54.98 Hz as shown in Figures 5.7 and 5.8. Since the preferable range is 50 Hz to 60 Hz it can said that the results are very logical and reliable.

The first axial (Z axis translation) normal mode of the satellite had been calculated as 134.84 Hz as shown in Figure 5.11. Actually, this result is also logical when compared to the given stiffness requirement. But, there are two normal modes between the X axis sway and the axial normal modes. The first one is the first rotation mode of the satellite about Z axis. Its value is 97.27 Hz and shown in Figure 5.9. The other one is a local mode. It is the mode of main observation camera, which is swaying along X axis. Its value is 106.18 Hz and shown in Figure 5.10. Actually, as specified before, the component mode should be at least $\sqrt{2}$ times of the system to which the component is mounted. So, the mode value of the camera should be checked according to this rule. It is known that the largest normal bending mode is 54.98 Hz. So, the minimum value that the camera mode should have is about $\sqrt{2} * 54.98$ Hz = 77.75 Hz. Since the result after the analysis is 106.18, much higher than 77.75 Hz, there is no resonance coupling, so that there will be no problem with the main camera.

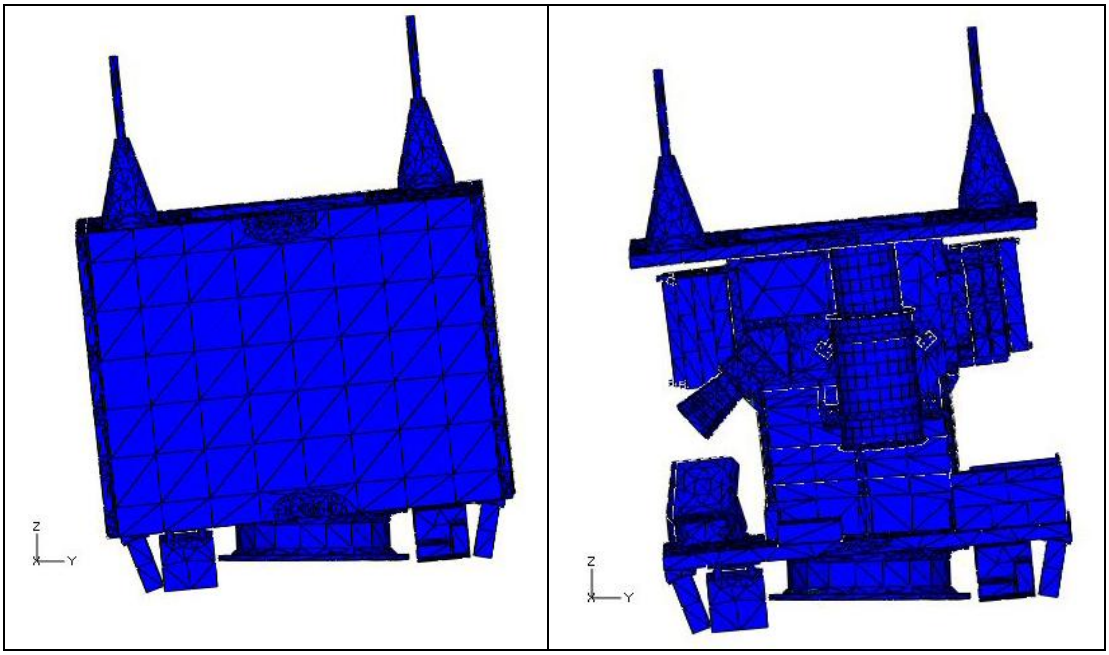

Figure 5.7. MODE 1 - 53.447 Hz – YZ BENDING MODE

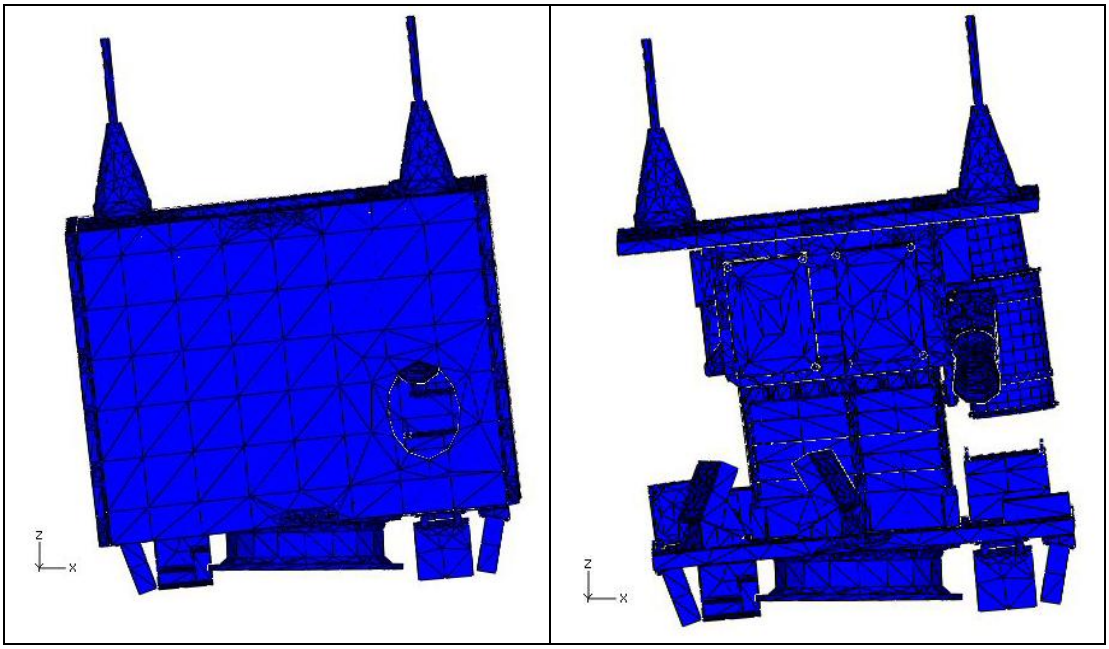

Figure 5.8. MODE 2 - 54.981 Hz – XZ BENDING MODE

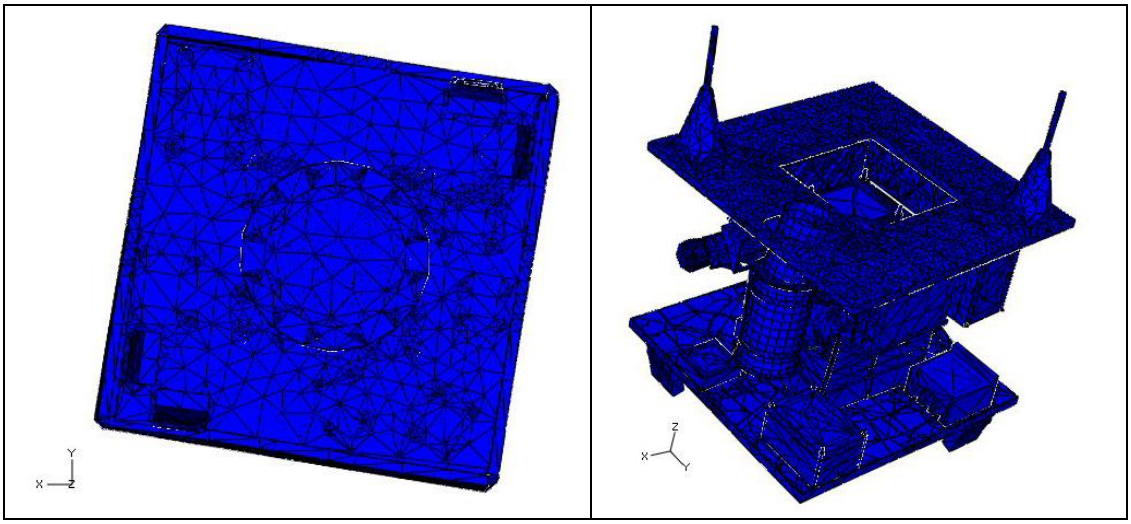

Figure 5.9. MODE 3 - 97.270 Hz- ROTATION MODE ABOUT Z

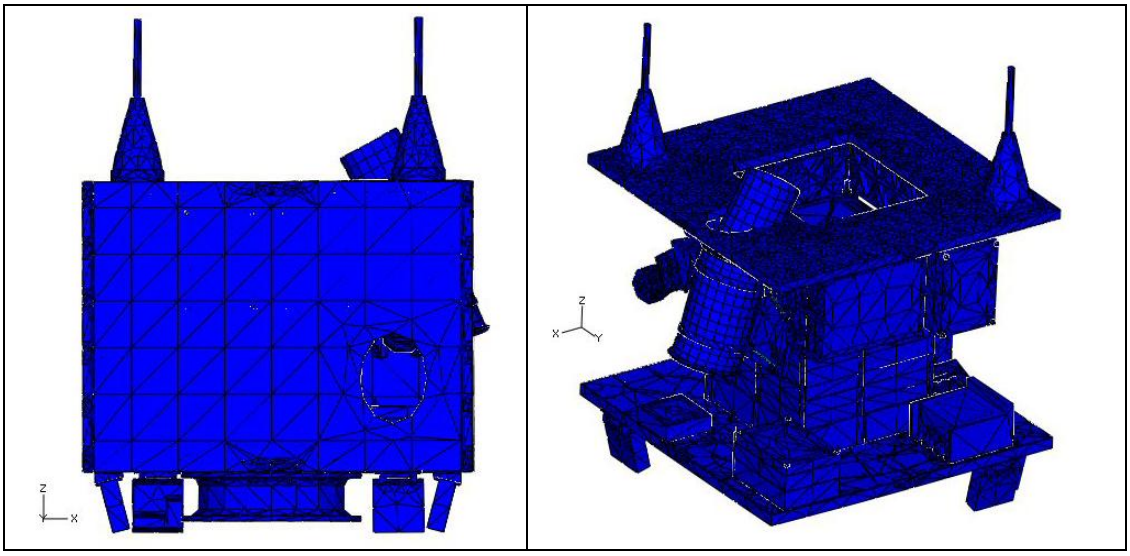

Figure 5.10. MODE 4 - 106.18 Hz – MAIN CAMERA LOCAL MODE

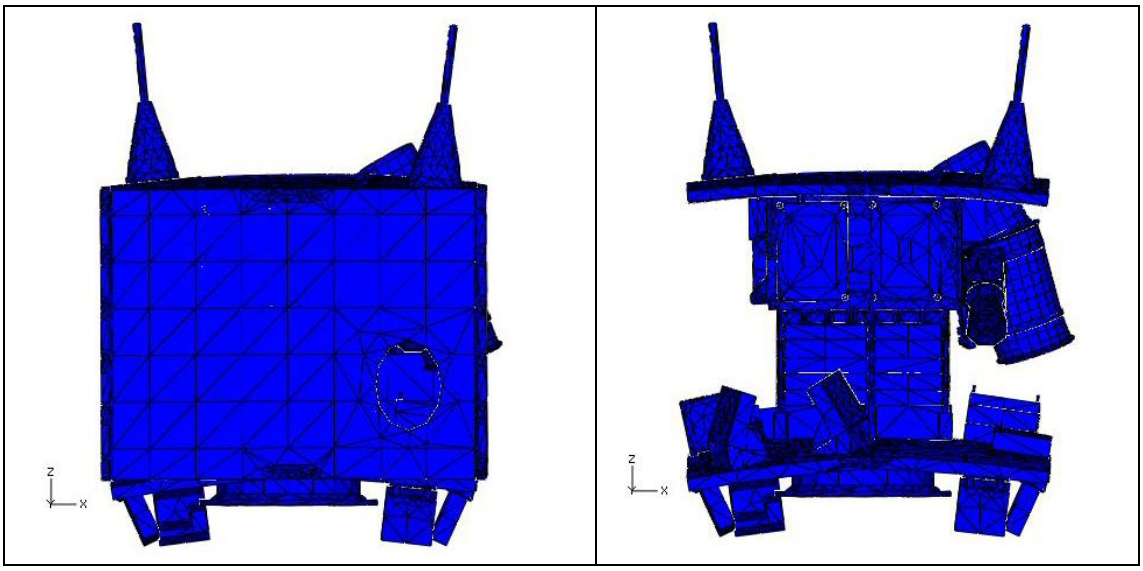

Figure 5.11. MODE 5 - 134.84 Hz – TRANSLATION MODE IN Z

Between 0 Hz and 2000 Hz, 444 normal modes of the satellite are found according to the modal analysis. The first 10 modes are given in Table 5.5. Whole list including eigenvalues and frequencies is given in the Appendix B.

Most of the normal modes are local modes not affecting the whole body. In order to see which mode is effective for the whole spacecraft, it is necessary to make an effective mass calculation. This calculation is going to be useful for the response analysis related to modal analysis. Since there are many numbers of modes, it may be useful to specify the most representative modes for the whole structure. The details about this subject are given in Appendix C. In Figure 5.12, the cumulative masses for each axis are given as a line chart. So, it can be seen that, for the X and Y axes, about the 100th mode, the normal modes are sufficient to represent almost 96% of the response of the whole satellite. For the Z axis, it can be said that, about 200th mode, the normal modes are sufficient to represent almost 95% of the response of the whole satellite.

Table 5.5. First 10 Normal Modes of RASAT

MODE NO	EIGENVALUE	FREQUENCY	
		(RAD/TIME)	(CYCLES/TIME)
1	1,12774E+05	335.82	53.447
2	1,19340E+04	345.46	54.981
3	3,73523E+05	611.17	97.270
4	4,45101E+05	667.16	106.18
5	7,17797E+05	847.23	134.84
6	8,90127E+05	943.47	150.16
7	1,07786E+06	1038.2	165.23
8	1,25975E+06	1122.4	178.63
9	1,29439E+06	1137.7	181.07
10	1,37042E+06	1170.7	186.31

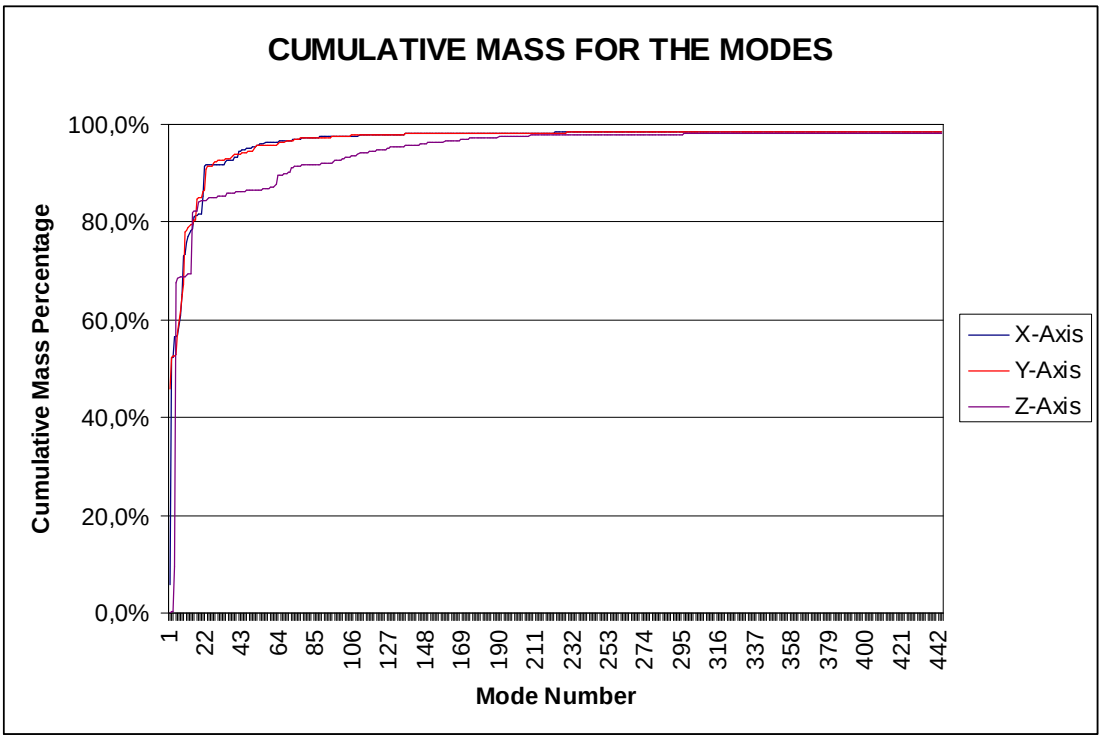

Figure 5.12. Cumulative Mass for the Modes

5.3 Harmonic Response Analysis

In order to determine the steady-state response of the satellite to loads that vary sinusoidally (harmonically) with time, it is necessary to make a harmonic response analysis, thus enabling us to verify whether or not our design will successfully overcome resonance, fatigue, and other harmful effects of forced vibrations due to launch vehicle.

In the mechanical design requirements chapter the specified harmonic oscillation and amplitude values of a typical launch vehicle are given. The most severe one is chosen to make a reliable analysis, and it is listed in Table 5.6.

Table 5.6. Sinusoidal Vibration Analysis Levels

	Frequency range (Hz)	**Qualification levels (0-peak)**
Longitudinal	4-5 5-100	12.4 mm 1.25 g
	2-5	9.9 mm
Lateral	5-25	1 g
	25-100	0.8 g
Sweep rate		2 oct./min

During the analysis, the same boundary condition is applied. The critical damping ratio is chosen as 0.02 which is given by the ref [18]. After the analysis is completed, some responses are determined. For instance, the sine vibration responses of some critical components, which have structural importance, are determined as in Fig.5.13 for z axis.

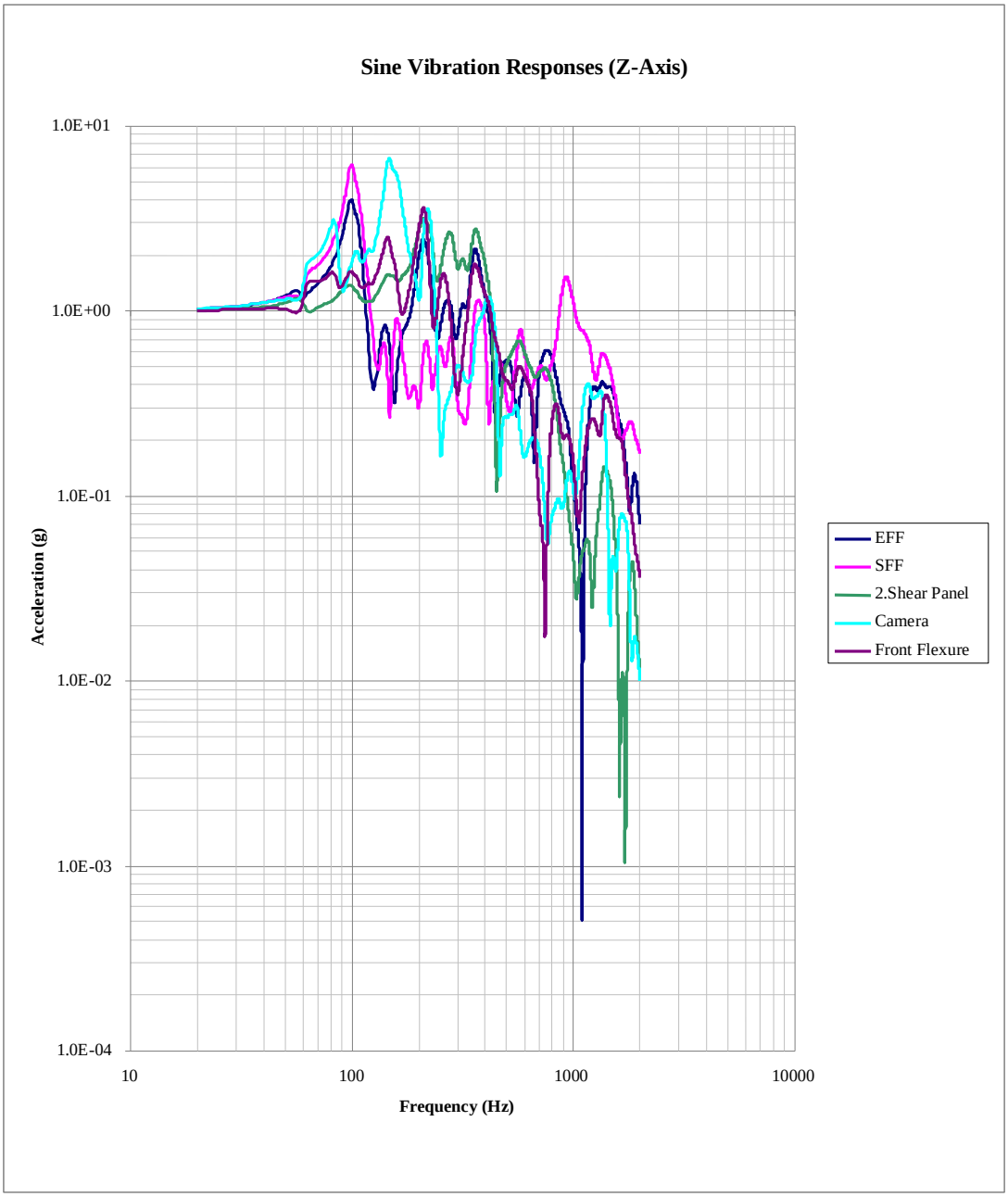

Figure 5.13. Sinusoidal Vibration Responses of some critical components

5.4 Random Vibration Analysis

Another analysis that should be done is random vibration analysis. By this analysis there is the opportunity to calculate the component responses for the applied random load. These results will be used for the environmental test and structural

analysis requirements of those components.

In order to do the random vibration analysis, it is necessary to have a PSD input. For this reason we have to calculate the Grms values of the possible launch vehicles to see which one is more severe for the design requirements. In Table 5.7, the PSD input values of COSMOS-3M rocket are given.

Table 5.7. PSD inputs of COSMOS-3M

Frequency (Hz)	**PSD (g^2/Hz)**
10	0,0060
20	0,0040
40	0,0040
80	0,0062
160	0,0200
320	0,0460
640	0,0840
1280	0,0740
2000	0,0360

By using these values, it is possible to prepare a PSD curve to calculate the Grms value of the given PSD input. In Fig.5.14, the PSD curve of COSMOS-3M rocket is given.

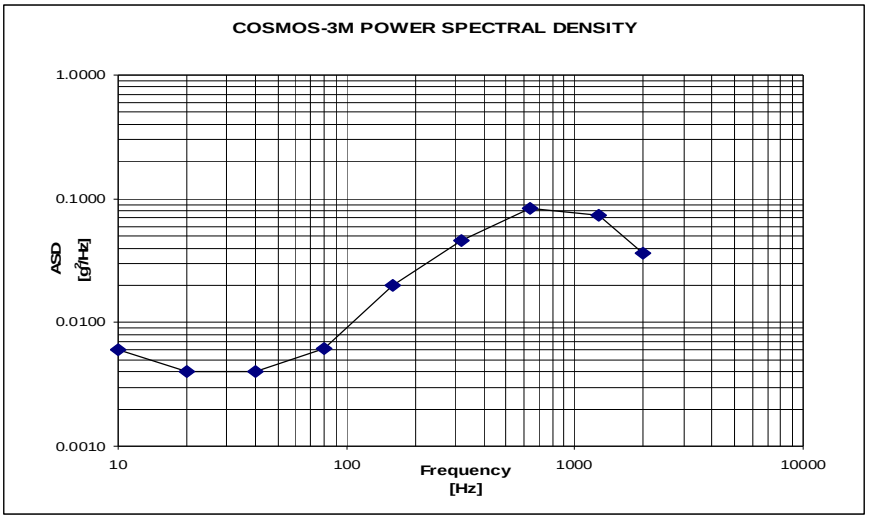

Figure 5.14. PSD Curve of COSMOS-3M

After drawing the PSD curve, it is possible to make a table and by formulating the cells as square root of the AREA column, we can get the Grms values of all frequency bands. At the end of the frequency bands, we have the total Grms value of COSMOS-3M rocket. As it can be seen from the Table 5.8., the Grms value of COSMOS-3M is 10.70.

Table 5.8. Grms Calculation of COSMOS-3M

				Slope		Acceleration
FREQ(Hz)	**PSD(G^2/Hz)**	**dB**	**OCT**	**dB/OCT**	**AREA**	**Grms**
10	0,0060	*	*	*	*	*
20	0,0040	-1,76	1,00	-1,76	0,05	0,22
40	0,0040	0,00	1,00	0,00	0,13	0,36
80	0,0062	1,90	1,00	1,90	0,33	0,58
160	0,0200	5,09	1,00	5,09	1,34	1,16
320	0,0460	3,62	1,00	3,62	6,57	2,56
640	0,0840	2,62	1,00	2,62	27,46	5,24
1280	0,0740	-0,55	1,00	-0,55	77,59	8,81
2000	0,0360	-3,13	0,64	-4,86	114,56	10,70

Now, a similar calculation can be done for DNEPR rocket. Its PSD input values are given in Table 5.9.

Table 5.9. PSD inputs of DNEPR

Frequency (Hz)	**PSD (g^2/Hz)**
20	0,007
40	0,007
80	0,007
160	0,022
320	0,035
640	0,035
1280	0,017
2000	0,005

By means of these inputs, the PSD curve can be drawn as shown in Fig.5.15.

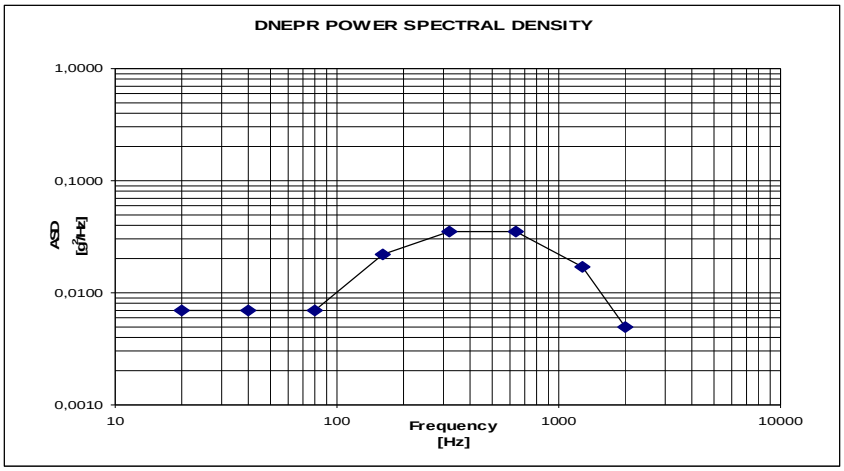

Figure 5.15. PSD Curve of DNEPR

After drawing the PSD curve, again it is possible to make a table and by formulating the cells as square root of the AREA column, we can get the Grms values of all frequency bands. At the end of the frequency bands, we have the total Grms value of DNEPR rocket. As it can be seen from the Table 5.10., the Grms value of DNEPR is 6.28.

Table 5.10. Grms Calculation of DNEPR

				Slope		Acceleration
FREQ(Hz)	**PSD(G^2/Hz)**	**dB**	**OCT**	**dB/OCT**	**AREA**	**Grms**
20	0,007	*	*	*	*	*
40	0,007	0,00	1,00	0,00	0,14	0,37
80	0,007	0,00	1,00	0,00	0,42	0,65
160	0,022	4,97	1,00	4,97	1,54	1,24
320	0,035	2,02	1,00	2,02	6,14	2,48
640	0,035	0,00	1,00	0,00	17,34	4,16
1280	0,017	-3,14	1,00	-3,14	32,64	5,71
2000	0,005	-5,31	0,64	-8,25	39,39	6,28

So, it is better to use the values of COSMOS-3M since its PSD values are more severe. By inputting these PSD values into the program in the random response

analysis module, and by selecting the critical damping coefficient as 0.02, we can make the analysis. After the analysis, we get some response curves for different components.

For instance, for some critical components, the Z direction responses, which are assumed as the most critical are drawn. In Figures 5.16 and 5.17, the DNEPR and the COSMOS 3-M response charts are shown respectively.

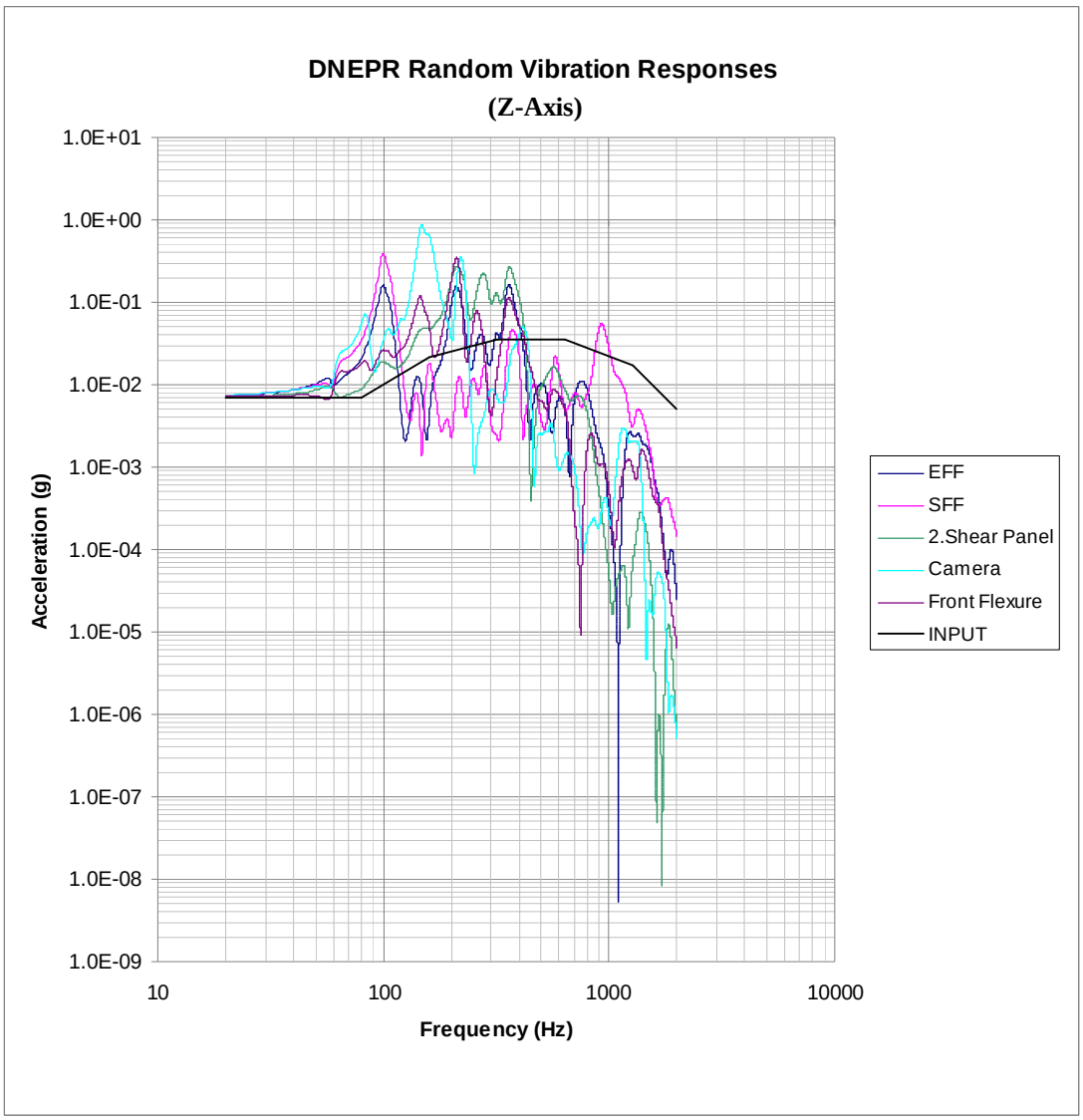

Figure 5.16. DNEPR Random Vibration Z-direction responses of some critical components

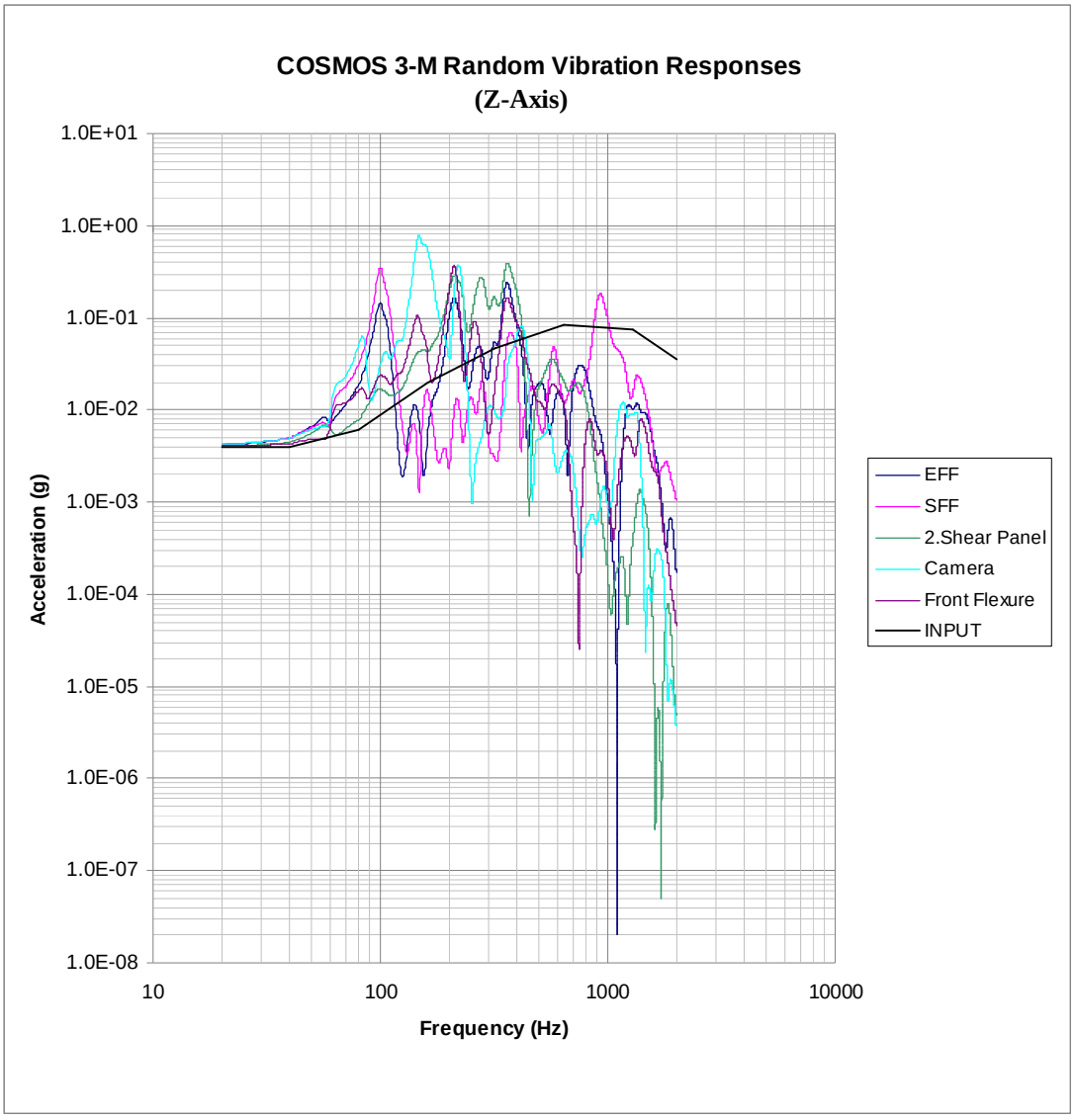

Figure 5.17. COSMOS 3-M Random Vibration Z-direction responses of some critical components

5.5 Stress Analysis

In cases where loads produced by different launching environments can occur simultaneously, these loads shall be combined in a rational manner to define the limit load for that flight event. Types of load combinations vary dependent upon the particular launch vehicle. For a shuttle, common types of load combinations are

quasi-static loads with random vibration loads due to liftoff events and quasi-static loads with thermally induced loads due to landing.

For liftoff, the following specific requirements shall apply to design loads for components and their supporting interface structure:

a. The effects of low frequency quasi-static loads and random vibration/acoustic loads shall be combined in a rational manner to determine the total load environment for liftoff.

b. For components weighing less than 500 kg, the appropriate method of load combination is dependent on how the low frequency and the random vibration/acoustic design environments of the event are specified. Typically, the maximum levels are defined as requirements for a flight event, such as liftoff, even if these maxima do not necessarily occur at the same time. The relative timing of the quasi-static and random vibration environments is unique for each launch vehicle, but simultaneous occurrence of maximum low frequency quasi-static and maximum random vibration load is improbable. Therefore, a root-sum-square (RSS) approach is acceptable for combining the maximum low frequency and maximum random vibration loads for the liftoff flight event. When the low frequency quasi-static and random vibration environments are specified in a time correlated manner, a time consistent approach is also acceptable for combining the low frequency quasi-static loads and the random vibration loads.

d. When an RSS approach to defining component loads is utilized, the maximum low frequency and maximum random vibration load factor are root sum squared. The root sum squared values are then applied in all axes simultaneously. When the load combination is directly applied to member loads, the maximum random vibration and low frequency member forces are root sum squared.

e. When a time consistent approach to defining component loads is utilized, the low frequency quasi-static load factor and random vibration load factor are combined in a time consistent manner. When the load combination is directly applied to member loads, the member loads due to low frequency and random vibration are combined

in a time consistent manner.

Because quasi-static and transient events have positive and negative load factors, all possible combinations must be considered when combined with respective random vibration loads.

Table 5.11 describes how the random vibration loads are superimposed, one axis at a time, with quasi-static and transient loads. The impacts of other loads, such as acoustic, thermal, and misalignment, shall also be considered where applicable. Resulting design load factors for each axis can be calculated and applied simultaneously in a stress analysis.

Table 5.11. Combination of Load Factors with ref [18]

LOAD CASE	X AXIS	Y AXIS	Z AXIS
LC 1-8	$\pm ((QSL_x)^2 + (RVLF_x)^2)^{1/2}$	QSL_x	QSL_x
LC 9-16	QSL_x	$\pm ((QSL_x)^2 + (RVLF_x)^2)^{1/2}$	QSL_x
LC 17-24	QSL_x	QSL_x	$\pm ((QSL_x)^2 + (RVLF_x)^2)^{1/2}$

Where QSL is the respective axis quasi-static load factor and RVLF is the respective axis random vibration load factor.

5.5.1 Random Vibration Load Factor (RVLF)

The Random Vibration Load Factors (RVLF) acting on payload flight equipment results from the resonant structural response of the equipment to random vibration environments (input from rocket engines mechanically and acoustically induced

vibrations) during launch. Therefore, random load factors shall be combined with low frequency load factors and other loads which apply during the launch phase of flight operations. Also, the RVLF's do not apply to large mass items since they will not respond to random vibrations (at frequencies significantly above those included in the low frequency load factor range). RVLF's shall be calculated for lower mass items such as rack mounted payloads / components and cargo bay items below 1000 lb or 454 kg. Specific RVLF's for payload flight equipment may be calculated using the following procedure:

A. By calculation or test, the first system natural frequency, (f_n), in each axis is determined.

B. The resonant amplification factor, (Q), (equal to 1/2x, where x is the structural damping coefficient) is determined.
1. from test data, if available
2. 10 is used if no data is available.

C. Using the natural frequency, f_n calculated in step A, and the applicable random vibration input criteria defined in the applicable IDD or payload-specific ICD (for the particular location of the equipment item), the applicable acceleration Power Spectral Density (PSD_n in g^2/Hz) corresponding to the natural frequency f_n can be determined. If f_n falls on a sloped portion of the curve, PSD_n can be interpolated using the following relationship:

$$PSD_n = PSD_1(f_n/f_1)^{.3322s} \quad (5.1)$$

Where:
PSD_n = PSD value which corresponds to f_n
PSD_1 = PSD value corresponding to f_1
s = The slope of the PSD function (dB per octave)
f_1 = lowest frequency given for the portion of the PSD table being interpolated

f_n = Natural frequency of system in the direction in which the load factor is being calculated.

D. The peak RVLF in each axis is determined using the Miles' relationship:

$$\text{RVLF} = 3\sqrt{\frac{\Pi}{2} Q f_n PSD_n} \tag{5.2}$$

The factor of three in each of the above equations is a statistical factor applied because the load factors calculated from the power spectral density curves are standard deviation amplitude for random vibrations, and design shall be based upon three standard deviations. In other words, the results obtained are the RMS stress values. But these values cannot be used in stress analysis due to they just give 1 sigma, or 68.3% certainty. In order to be on the safe side, we have to increase this certainty value and find the effective stress values.

The simplest and most effective way of converting these RMS stress values to the effective stress values is to multiply the RMS values by a greater sigma value. This sigma value is selected according the application type on which the analyzed components are being used. Generally for spacecrafts, sigma value is chosen as 3, in order to estimate with 99.737% certainty.

For the given PSD spectrum, the RVLF is calculated for each resonant frequency. In this case, in order to find the overall RVLF for the whole spectrum, each RVLF is multiplied by the effective mass of the corresponding frequency and the multiplication is divided by the overall mass. So, by this procedure, the mass weighted RVLF (i.e. RVLF_{MW}) for each frequency is determined with the following formula:

$$RVLF_{mw} = \frac{RVLF_i \cdot EFFM_i}{M} \tag{5.3}$$

Finally, for every direction the RVLF is calculated with the relation of RSS:

$$RVLF_{(x,y,z)} = \sqrt{\sum_i^n RVLF_{MW}^2} \tag{5.4}$$

After making the calculations using the above relations, the RVLF's of RASAT for all three axes are shown in Table 5.12.

Table 5.12. Random Vibration Load Factors

Random Vibration Load Factor	Value (g)
$RVLF_x$	5.19
$RVLF_y$	5.26
$RVLF_z$	11.61

After finding all the RVLF's, which are shown in Table 5.12, these are combined with the quasi-static load factors as shown in Table 5.11 and the load combination table is determined. In Table 5.13 all these 24 load cases are presented.

In order to calculate the stresses occurred on the structure during launching, all these load combinations are applied on the satellite model and the most effective one is going to be selected for the strength case. In this case there are 24 load cases. All these 24 load cases are applied on the finite element model of RASAT respectively. In other words all the margins of safety for each 24 case are determined and the smallest margin of safety for the satellite is obtained. The formulas used in calculating yield and ultimate margin of safety are given below as Formula (5.5) and (5.6) [18].

$$MoS_y = \left[\frac{\sigma_{yield}}{SF_{yield} \times stress_{\max}^{VonMises}} - 1 \right] \tag{5.5}$$

$$MoS_u = \left[\frac{\sigma_{ultimate}}{SF_{ultimate} \times stress_{\max}^{VonMises}} - 1 \right] \tag{5.6}$$

In calculations, the yield safety factor is chosen as 1.25 and the ultimate safety factor is chosen as 1.4. These values are taken for metallic structures from Table-1 of ref [19].

Table 5.13. Load Cases of RASAT Stress Analysis

LOAD CASE	X (g's)	Y (g's)	Z (g's)
LC1	9.121	7.5	6
LC2	9.121	7.5	-6
LC3	9.121	-7.5	6
LC4	-9.121	7.5	6
LC5	9.121	-7.5	-6
LC6	-9.121	7.5	-6
LC7	-9.121	-7.5	6
LC8	-9.121	-7.5	-6
LC9	7.5	9.161	6
LC10	7.5	9.161	-6
LC11	7.5	-9.161	6
LC12	-7.5	9.161	6
LC13	7.5	-9.161	-6
LC14	-7.5	9.161	-6
LC15	-7.5	-9.161	6
LC16	-7.5	-9.161	-6
LC17	7.5	7.5	13.069
LC18	7.5	7.5	-13.069
LC19	7.5	-7.5	13.069
LC20	-7.5	7.5	13.069
LC21	7.5	-7.5	-13.069
LC22	-7.5	7.5	-13.069
LC23	-7.5	-7.5	13.069
LC24	-7.5	-7.5	-13.069

It is known that to pass for the stress analysis, the required safety margins are: $MoS_y > 0$ and $MoS_u > 0$. It is observed after the analyses that all the yield and ultimate margins of safety are all positive as shown in Table 5.14. So, the stress analysis has been finished with satisfactory results.

Table 5.14. Results of Stress Analysis

Load Case	Component	Max. Von Mises Stress Value (MPa)	Material	Allowable Stress Value		Minimum Margin of Safety (MoS)	
				σ_{ty} (MPa)	σ_{tu} (MPa)	MoS_y	MoS_u
1	Rear Left E-Flexure	149.1	Titanium 6Al4V	890	950	3.78	3.55
2	Rear Left E-Flexure	133.2	Titanium 6Al4V	890	950	4.35	4.09
3	Shear Panel 5	61.6	Aluminum 7075-T6	475	572	5.17	5.63
4	Rear Right E-Flexure	78.6	Titanium 6Al4V	890	950	8.06	7.63
5	Rear Right E-Flexure	78.6	Titanium 6Al4V	890	950	8.06	7.63
6	Shear Panel 5	61.6	Aluminum 7075-T6	475	572	5.17	5.63
7	Rear Left E-Flexure	133.2	Titanium 6Al4V	890	950	4.35	4.09
8	Rear Left E-Flexure	149.1	Titanium 6Al4V	890	950	3.78	3.55
9	Rear Left E-Flexure	147.4	Titanium 6Al4V	890	950	3.83	3.60
10	Rear Left E-Flexure	131.0	Titanium 6Al4V	890	950	4.44	4.18

(Table 5.14 continued)

Load Case	Component	Max. Von Mises Stress Value (MPa)	Material	Allowable Stress Value		Minimum Margin of Safety (MoS)	
				σ_{ty} (MPa)	σ_{tu} (MPa)	MoS_y	MoS_u
11	Shear Panel 5	64.2	Aluminum 7075-T6	475	572	4.92	5.36
12	Rear Right E-Flexure	82.4	Titanium 6Al4V	890	950	7.64	7.24
13	Rear Right E-Flexure	82.4	Titanium 6Al4V	890	950	7.64	7.24
14	Shear Panel 5	64.2	Aluminum 7075-T6	475	572	4.92	5.36
15	Rear Left E-Flexure	131.0	Titanium 6Al4V	890	950	4.44	4.18
16	Rear Left E-Flexure	147.4	Titanium 6Al4V	890	950	3.83	3.60
17	Rear Left E-Flexure	144.2	Titanium 6Al4V	890	950	3.94	3.71
18	Rear Left E-Flexure	109.9	Titanium 6Al4V	890	950	5.48	5.17
19	Shear Panel 5	68.2	Aluminum 7075-T6	890	950	9.44	8.95
20	Rear Left E-Flexure	89.6	Titanium 6Al4V	890	950	6.95	6.57

(Table 5.14 continued)

Load Case	Component	Max. Von Mises Stress Value (MPa)	Material	Allowable Stress Value		Minimum Margin of Safety (MoS)	
				σ_{ty} (MPa)	σ_{tu} (MPa)	MoS_y	MoS_u
21	Rear Left E-Flexure	109.9	Titanium 6Al4V	890	950	5.48	5.17
22	Rear Left E-Flexure	89.6	Titanium 6Al4V	890	950	6.95	6.57
23	Rear Left E-Flexure	109.9	Titanium 6Al4V	890	950	5.48	5.17
24	Rear Left E-Flexure	144.2	Titanium 6Al4V	890	950	3.94	3.71

From Fig. 5.18 to 5.29, the Von Mises stress contour plots are represented in order to show the maximum stress nodes and locations. In some cases, the maximum stress locations are the same. The maximum stress locations are generally on the rear left e-flexure, the rear right e-flexure and the shear panel #5. But when the corresponding material properties are considered, all these components left on the safe side.

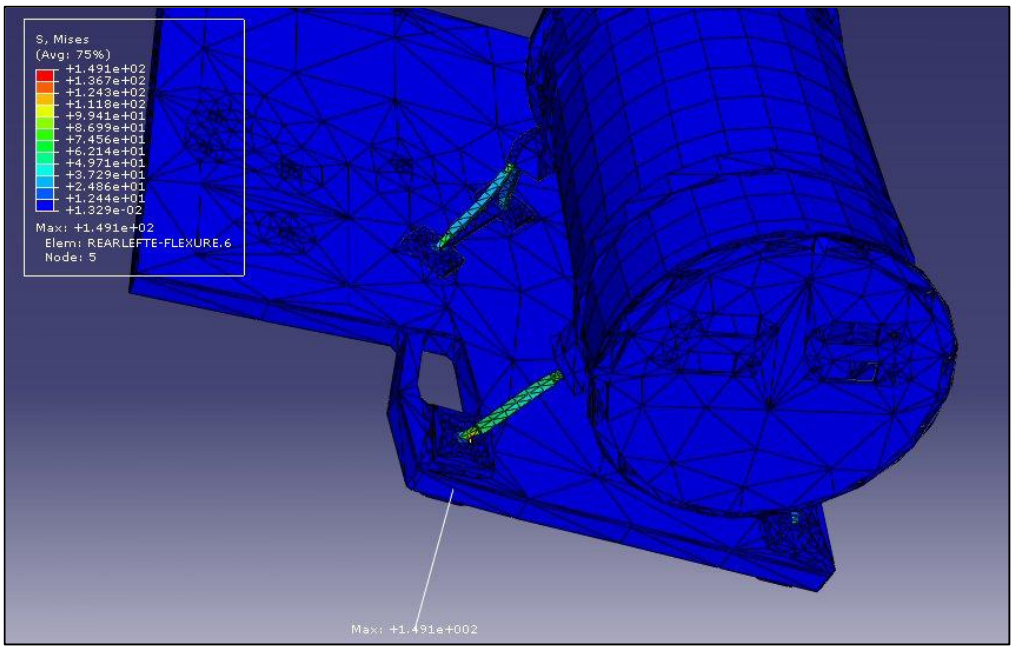

Figure 5.18. Von Mises Stress contours of LC 1 & 8

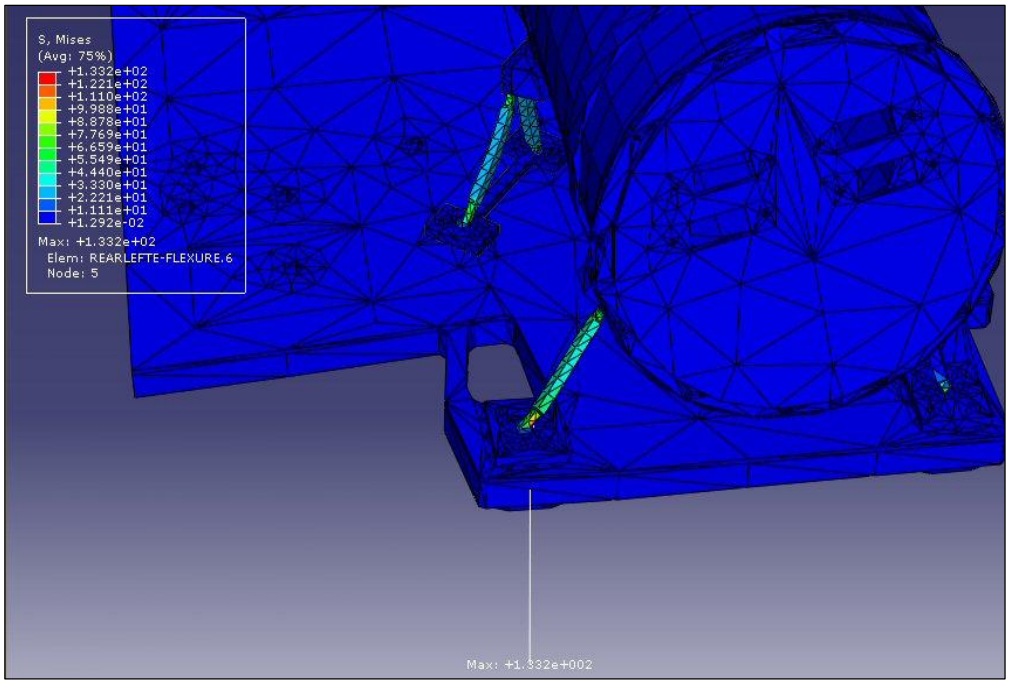

Figure 5.19. Von Mises Stress contours of LC 2 & 7

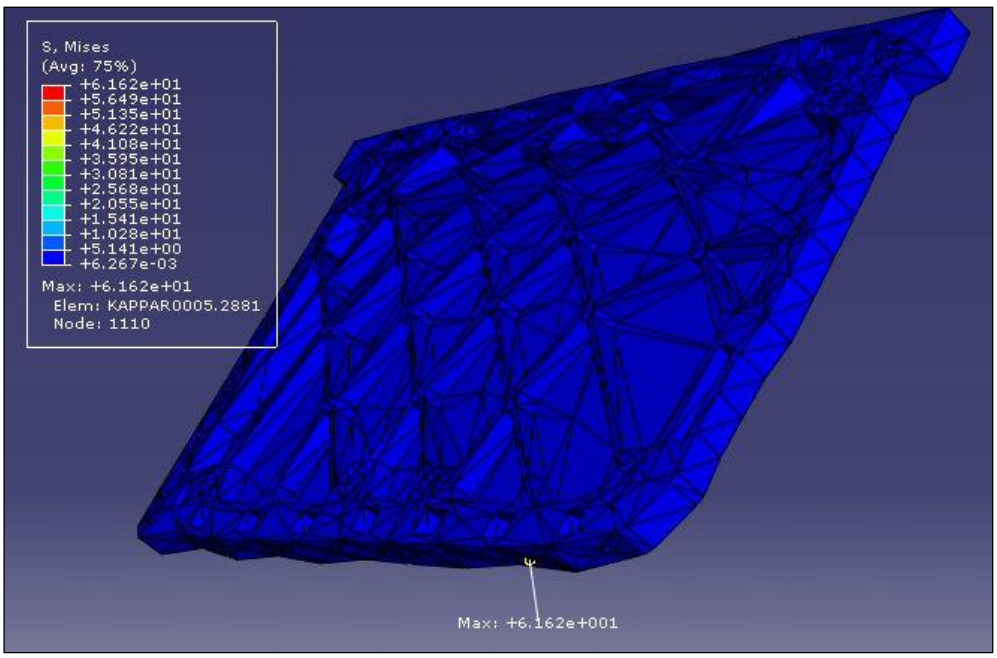

Figure 5.20. Von Mises Stress contours of LC 3 & 6

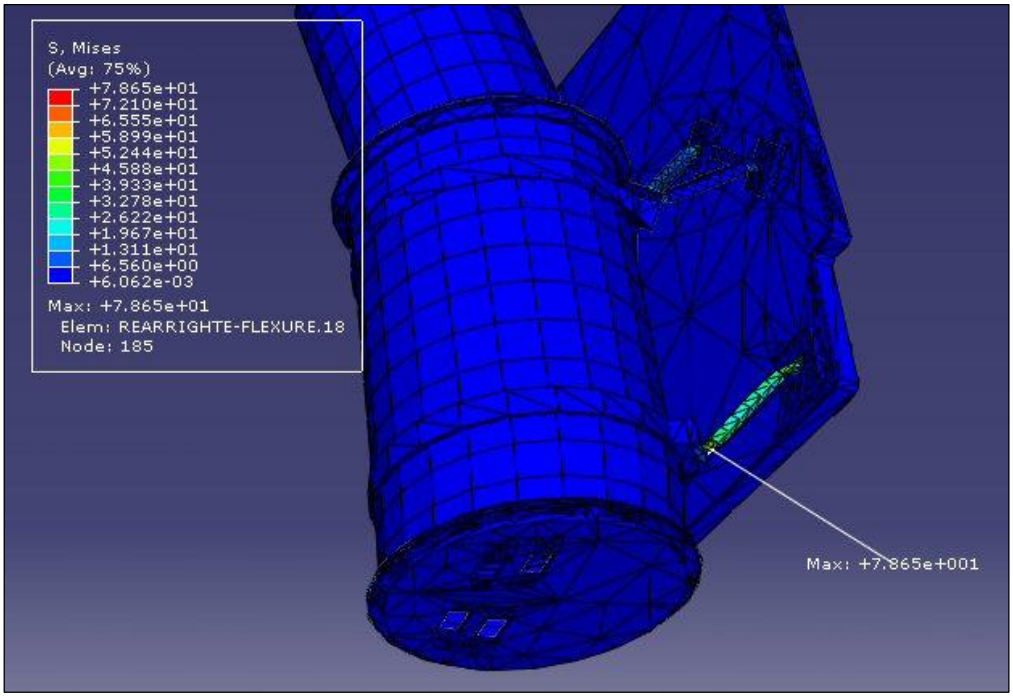

Figure 5.21. Von Mises Stress contours of LC 4 & 5

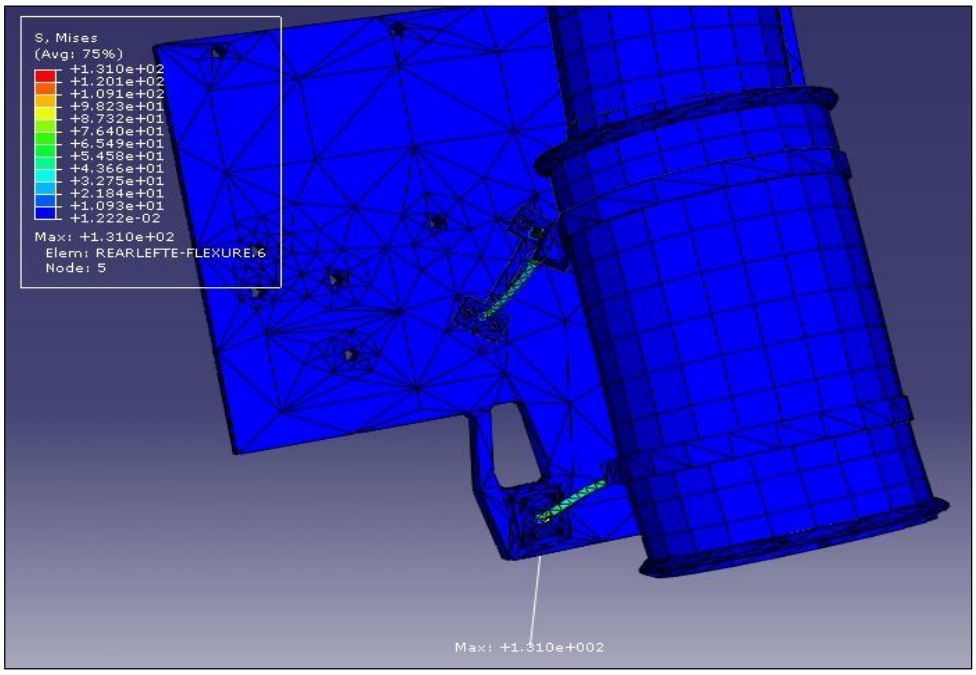

Figure 5.22. Von Mises Stress contours of LC 9 & 16

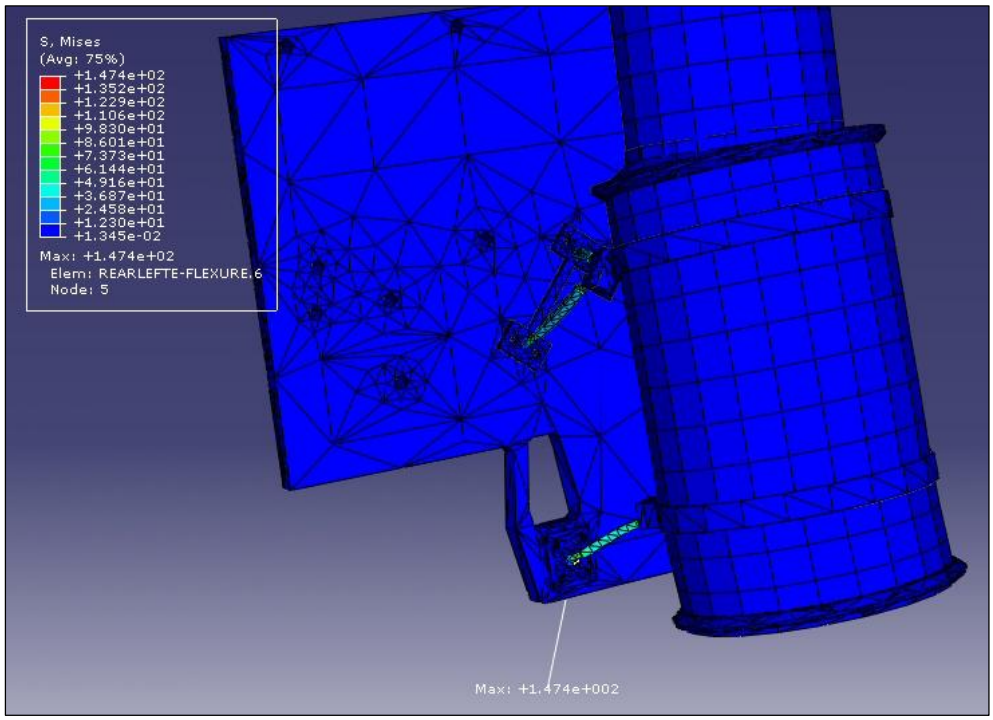

Figure 5.23. Von Mises Stress contours of LC 10 & 15

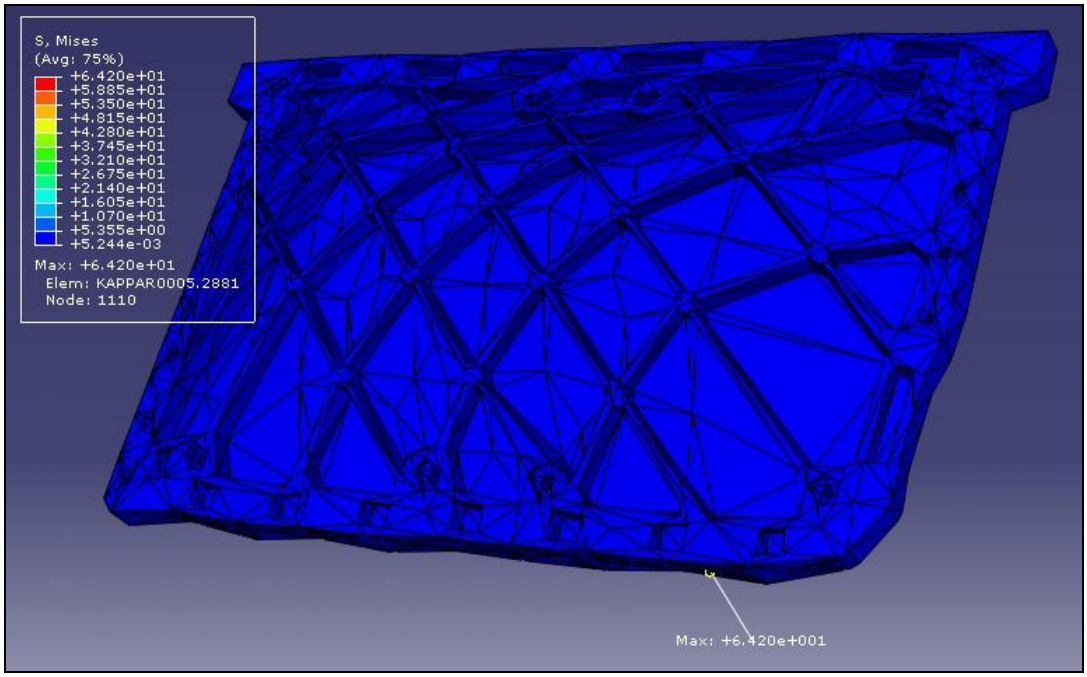

Figure 5.24. Von Mises Stress contours of LC 11 & 14

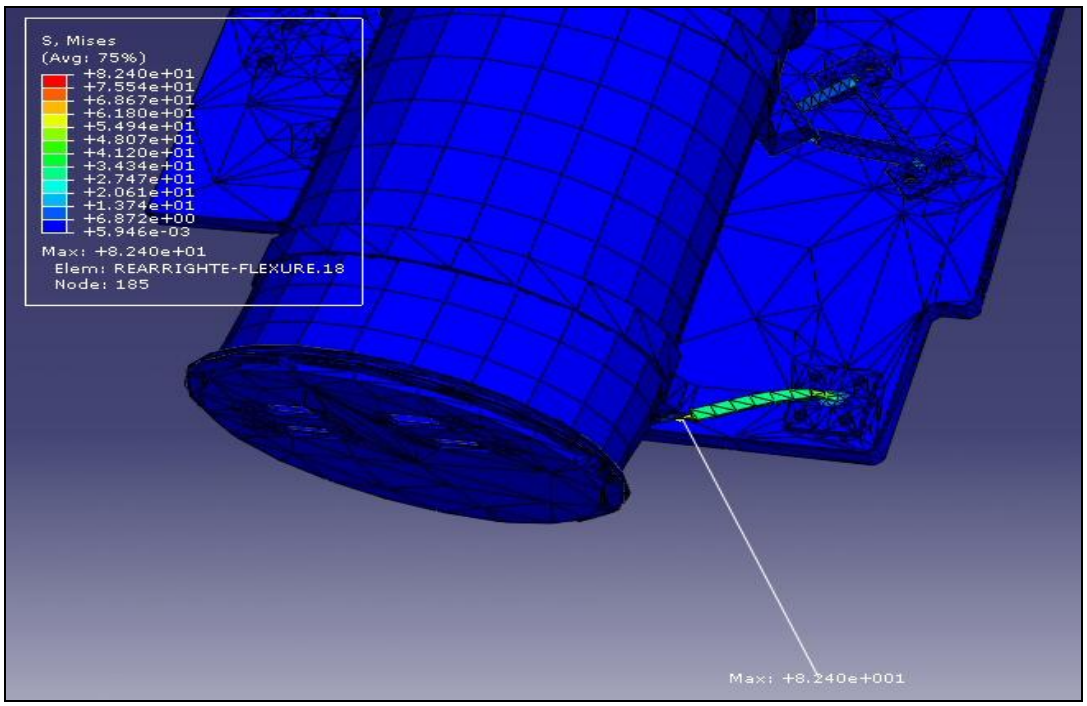

Figure 5.25. Von Mises Stress contours of LC 12 & 13

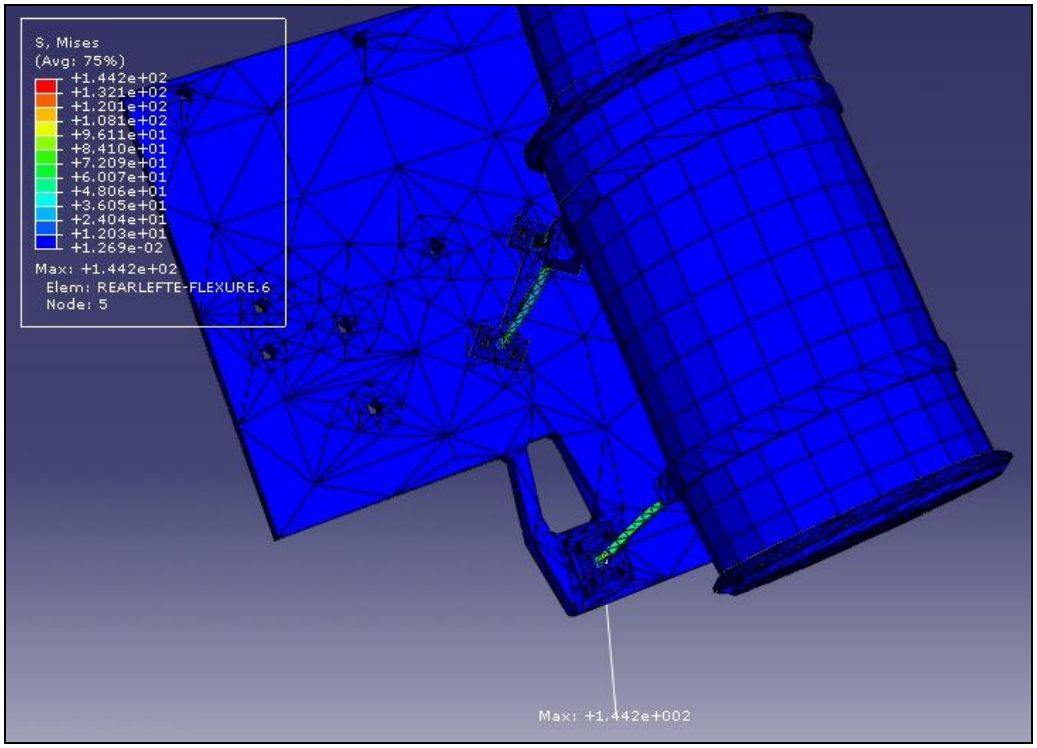

Figure 5.26. Von Mises Stress contours of LC 17 & 24

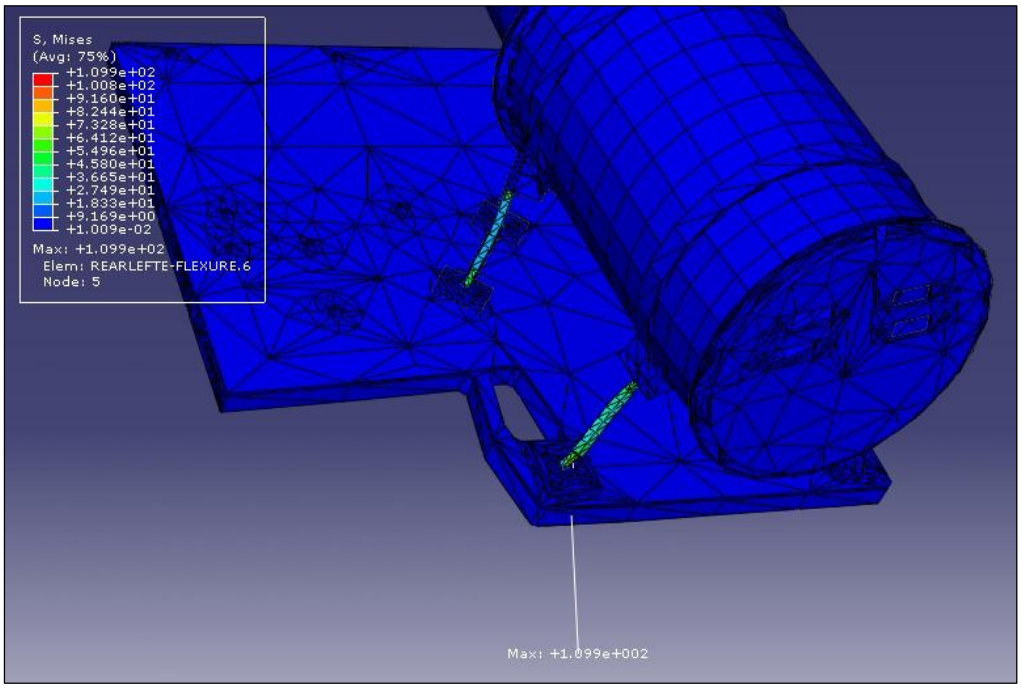

Figure 5.27. Von Mises Stress contours of LC 18 & 21 & 23

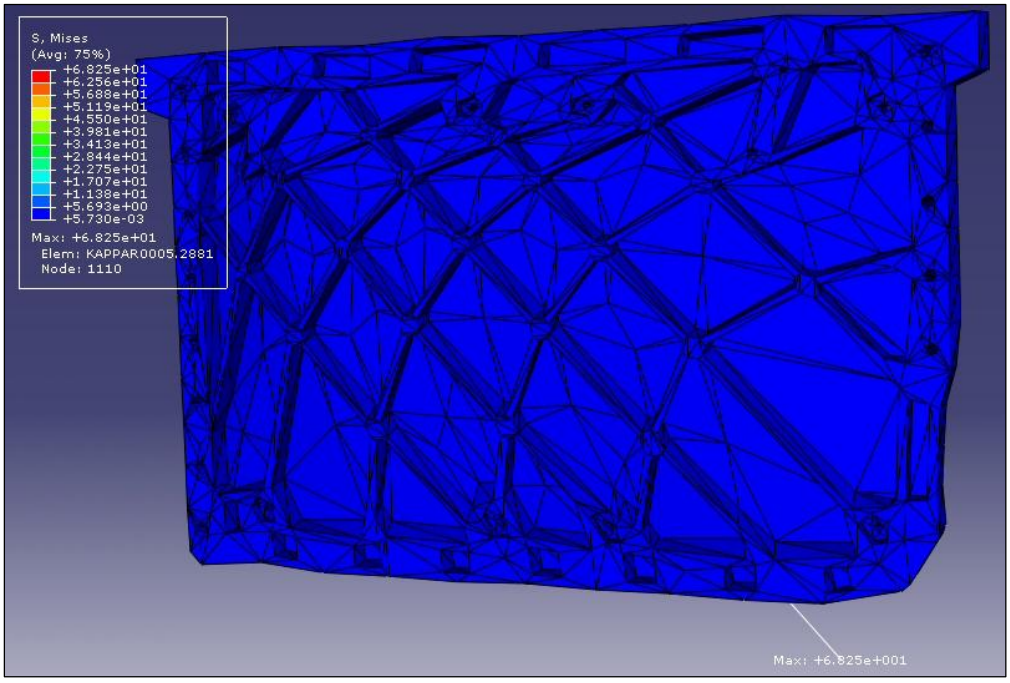

Figure 5.28. Von Mises Stress contours of LC 19

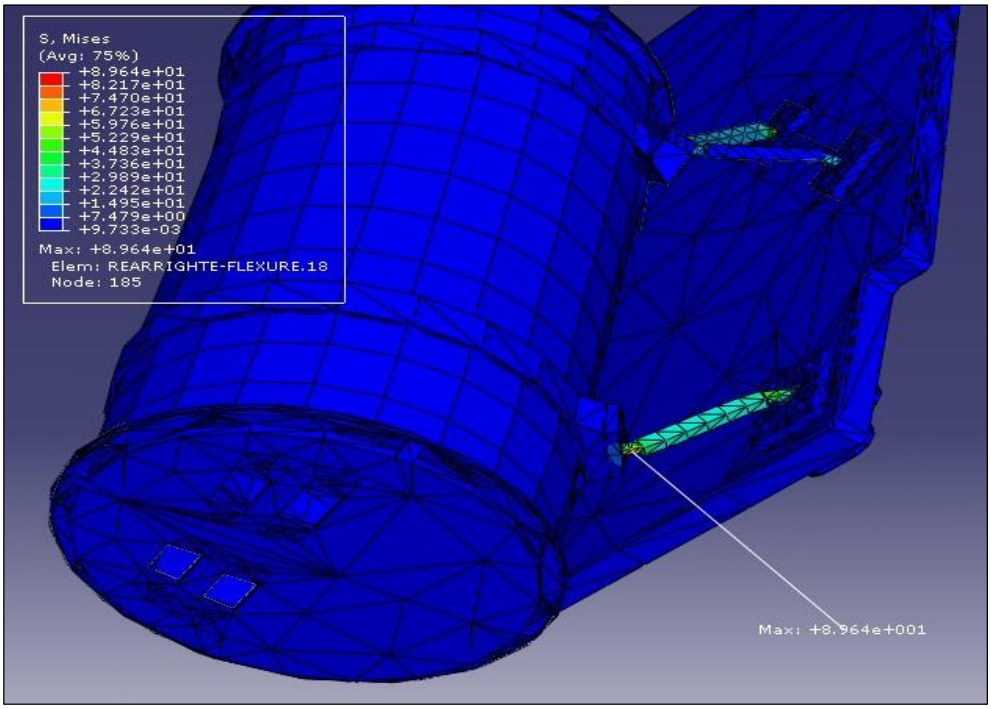

Figure 5.29. Von Mises Stress contours of LC 20 & 22

CHAPTER 6

CONCLUSIONS

6.1 General Conclusions

This study is on the finite element analysis of a micro satellite structure. The study describes the definition of a load envelope, main available launchers and provides an analysis philosophy that will satisfy qualification and launcher rocket requirements. The mechanical designers must take some factors into consideration in order to reach these requirements. All the possible parameters and factors are explained in this study step by step.

The first thing to keep in mind before starting the mechanical design is to stay within the design limitations and requirements. These limitations and requirements are coming from the launch vehicle. The satellites need to be launched according to these limitations and requirements.

In this study, since the launcher is not certain yet, some possibilities are taken into account. In other words, some possible launchers are determined, their limitations and requirements are specified, and the design is performed according to the most severe limitations and requirements.

When dealing with the mechanical design, the first limitation is about the volume of the micro satellite. Launchers give their fairing cover envelope volume capacity values for the satellites which they launch. So, the volume of the model satellite is designed so that it will not exceed the launcher capacity. After describing the maximum volume dimensions, the structural elements are started to be designed.

The main structure of the model satellite is chosen so that there is a main stack which is fixed between two structural facing panels. The panel that looks through the earth on orbit is called the Earth Facing Facet. The opposite panel is called the Space Facing Facet. The main observation camera system and other nano stacks are

mounted to the shear panel assembly which connects the main stack to the earth facing facet. The satellite is attached to the launch vehicle from the separation system ring which is mounted on the space facing facet.

The next requirement for the mechanical design is about mass-related properties. The weight of the satellite must not exceed the capacity given by the launcher. So, for this reason a mass budget is formed and maximum possible masses for each subsystem are allocated. The launch cost is directly proportional to the weight of the whole satellite. So, during the design, the weight of the satellite is required to be minimum as much as possible. For this reason, much of the structural elements are designed so that they have smaller weights but greater stiffness and strength. This is provided by placing stiffeners, webs and ribs on the structural elements so that they can easily be machined during manufacturing. So, the much of the structural elements have great weight/stiffness ratios.

Another concept that should be taken into consideration is material selection. Most of the materials used are aluminum alloys such as Al 7075-T6 and Al 6061-T6. These are chosen due to their good mechanical properties (like weight/strength ratio), good thermal properties, good machinability and easy availability in the market. Where the higher strength requirements are needed some other materials having greater strength values are used such as titanium and stainless steel. For instance, in order to integrate the main-stack modules, titanium tie-bars are used.

Satellites are exposed to different load conditions after the compilation of production. Their structures must be checked so that they will resist to these load conditions and provide surviving of the satellite’s mission. Most of these load conditions are vibration loads during the launching and transportation. So, structural analyses are generally based on these types of load sources.

These analyses are done either by computer or by environmental tests. Computer analyses are based on finite element analysis. A finite element model of the satellite is prepared and necessary analyses are performed in order to see whether the design is suitable or not by using a finite element software.

For this purpose, in this study, a finite element model of the pilot satellite is prepared by using ABAQUS finite element software. While preparing the finite element model, solid models from CAD software of the parts generating the satellite are used in order to make the analysis more logical. All of the structural elements and some important components like main camera, star tracker camera, battery pack, etc are modeled. All these component models are meshed by appropriate finite elements and connected to each other by using TIE constraint of ABAQUS software.

Then all the material assignments are completed on the assembly model. After assigning the materials, the mass properties of the model are checked. It is seen that the weight of the finite element model is lower than the real model due to non-existing components like electronic hardware, harness, fasteners, etc. Instead of modeling these elements having no structural importance, mass inertias are used in order to simulate the non-existing components. With the included mass inertias, the finite element model has the appropriate mass properties and can be used in the analyses.

First structural analysis done is modal analysis. This is important in case of determining the fundamental global modes and mode shapes of the satellite. Actually, frequency stiffness properties are also required by the launcher. Launchers provide some values and they require the satellite to be launched to have greater modal properties which are appropriate. After the modal analysis is completed, it is shown that the first global normal modes of the micro satellite RASAT are very appropriate when compared to the possible launchers' requirements. So, the design is appropriate for modal requirements.

Then harmonic response analysis is performed. The requirements for this analysis are also given by the launchers. The most severe ones are taken into consideration and all the analyses are done according to these values. After the analysis the response of the satellite due to harmonic excitation is determined. The results are to be used in component-based analyses and tests. Some structurally critical components and locations are determined and the harmonic responses of these

components are tabulated in graphical form.

Another analysis type performed is random vibration analysis. This is similar to the harmonic response analysis. The main difference is the input values. Instead of giving g values, PSD values are given for the specified frequency spectrum. The PSD values of both COSMOS-3M and DNEPR rockets are taken into consideration and analyses are done for both of the launcher rockets. As similar to the harmonic response analysis, PSD responses of the satellite and its components are determined. Some of the critical components are determined and their random vibration response charts are generated in order to use them in component-based analyses.

The last quantity to be determined is equivalent stress values from the stress analysis. For this purpose, all the loads acting on the satellite structure during the launching are combined. These loads are quasi-static loads and random vibration loads. Random vibration load factors are determined by using Miles' formula and taking the root sum squares of them the load combinations are obtained. There are 24 load cases possibly acting on the structure. Each load case is applied on the satellite structure and the maximum Von Mises stress values found in order to check the margin of safety values of the structure components. It is determined that all the 24 load cases have positive safety margins. This means that after the stress analysis the resulting stress values are on the safe side. So, the satellite and its components satisfy the requirements on stress analysis.

But, although all the margins of safety obtained from the stress analysis are positive, their values are much greater than the optimum ones. Actually, safety margins are accepted as optimum if they are between 0 and 0.5, and not efficient if they are greater than 1.5 [20]. So, the stress analysis of RASAT can be considered so that the RASAT structural design is not efficient since the minimum margin of safety found is 3.55, which is much greater than the optimum interval. So, some design improvements should be made in order to get a more efficient structural design. These improvements are explained in the future work section below.

In conclusion, it can be said that the structural design has maintained the micro satellite project's low-cost requirements and optimized the system compatibility rather than adopting a conventional weight-critical design approach. The performance of the structure under the loads prescribed shows the structural integrity and its compatibility with the possible launch vehicles that may have more severe structural requirements.

6.2 Future Work

There are several improvements those can be made on the structural design as future work. First of all, the high level margins of safety obtained from the stress analysis shows that these structural elements are over-designed. So, the most critical structural elements those have the minimum margins of safety can be redesigned so that their margins of safety are going to be between 0 and 0.5. Then, in general, weight and design optimization should be made on the structural elements of RASAT in order to have a more efficient design. By decreasing the margins of safety to the optimum interval, the structure is going to decrease in weight. By taking the stiffness, modal frequency and volume requirements into consideration, the weight of the RASAT satellite may be reduced in certain level. This requires a multi optimization approach. An optimization on structure may be going to give a better and more efficient design.

REFERENCES

[1] Bryce Harrington Propulsion Website, "http://bryce.homelinux.org/site/Propulsion/bus.htm", Last Access date: April 2008

[2] Gaudenzi P., The ESA SME Initiative Training Courses, "Design criteria and procedures of space structures"

[3] Mosher T., 2004. "Spacecraft Structures and Testing", Utah State University, Utah, U.S.A.

[4] Gaudenzi P., The ESA SME Initiative Training Courses, "Mechanical behavior of structural materials and structures for space"

[5] 36071 BILSAT-1 - Top-Level FE Analysis of Spacecraft, SSTL

[6] Lauritzen C., 2007, "AMS-02 Structural Analysis Overview", ESC Group, Jacobs Engineering, U.S.A.

[7] Steinberg, D. S., 2000. "Vibration Analyses for Electronic Equipment", John Wiley, New York

[8] Newland, D. E., 1993, "An Introduction to Random Vibrations, Spectral and Wavelet Analysis", Third Edition, Longman Scientific&Technical, England

[9] NASA Finite Element Modeling Continuous Improvement Website, "http://femci.gsfc.nasa.gov/", Last Access date: April 2008

[10] Cosmos USA Assured Space Access Cosmos-3M Guide, Revision 1, January 1997

[11] DNEPR User's Guide, Issue 2, November 2001

[12] Arianespace Ariane 5 User's Manual, Issue 2, Revision February 1998

[13] DASSAULT Aviation Micro-Satellite Support Website, "http://www.dassault-aviation.com/en/space/pyrotechnics-catalogue/micro-satellite-support.html?L=1", Last Access date: April 2008

[14] Arianespace ASAP 5 User's Manual, Issue 0, Revision February 1998

[15] Material Property Data Website, "http://www.matweb.com", Last Access date: April 2008

[16] GAM 215/07 Volume I, Galileo Avionica Milano

[17] Abaqus Analysis User's Manual, Volume IV: Elements

[18] NASA-SSP5200B, Payload Flight Equipment Requirements and Guidelines for Safety Critical Structures, International Space Station Program, (December 10, 1998)

[19] NASA-STD-(I)-5001A, Structural Design and Test Factors of Safety for Spaceflight Hardware, (December 09, 2006)

[20] Fraser D., Kleespies H., Vasicek C., 1991, "Spacecraft Structures"

[21] Sarafin T. P., 2003, "Spacecraft Structures and Mechanisms From Concept to Launch" Fourth Edition, Space Technology Series, United States of America

[22] Finite Element Analysis Domain - Modal Effective Mass Website, "http://feadomain.com/content76.html", Last Access date: April 2008

APPENDIX A

VIBRATION (FREQUENCY) ISOLATION

The purpose of vibration isolation is to control unwanted vibration so that its adverse effects are kept within acceptable limits. Vibrations originating from machines or other sources are transmitted to a support structure such as a facility floor, causing a detrimental environment and unwanted levels of vibration.

If the equipment requiring isolation is the source of unwanted vibration, the purpose of isolation is to reduce the vibration transmitted from the source to the support structure. Conversely, if the equipment requiring isolation is a recipient of unwanted vibration, the purpose of isolation is to reduce the vibration transmitted from the support structure to the recipient.

Natural frequency and damping are the basic properties of isolation which determine the transmissibility of a system designed to provide vibration isolation. Resonance occurs when the natural frequency of the component coincides with the frequency of the source vibration.

The ideal isolation would have as little damping as possible in the isolation region and as much as possible at the natural frequency to reduce amplification at resonance.

The ratio of vibration transmitted after isolation to the disturbing vibration is described as "transmissibility" and is expressed in its basic form in

$$TR = \sqrt{1 + \left(\frac{2\zeta\Omega}{\omega_n}\right)^2} D_{max} \qquad \text{(A.1)}$$

where Ω is the disturbing frequency of vibration in rad/s, ω_n is the undamped natural frequency of the component which is connected to the main system and D_{max} is the maximum dynamic amplification factor.

When considering damping, the equation above is rewritten as below, where ζ represents the damping ratio of the component.

$$\mathbf{TR} = \sqrt{\frac{1+\left(\frac{2\zeta\Omega}{\omega_n}\right)^2}{\left(1-\left(\frac{\Omega}{\omega_n}\right)^2\right)^2+\left(\frac{2\zeta\Omega}{\omega_n}\right)^2}} \qquad \text{(A.2)}$$

Maximum transmissibility of a component occurs at resonance when the ratio of the disturbing frequency to the natural frequency is almost equal to 1 (i.e. $\Omega / \omega_n \approx 1$). At resonance the transmissibility is given by

$$T = \frac{1}{2\zeta} \qquad \text{(A.3)}$$

It should be noted that the magnitude of a component's amplification at resonance is a function of that component's damping.

The figure below graphically shows the transmissibility of a component as a function of the frequency ratio for various damping ratios.

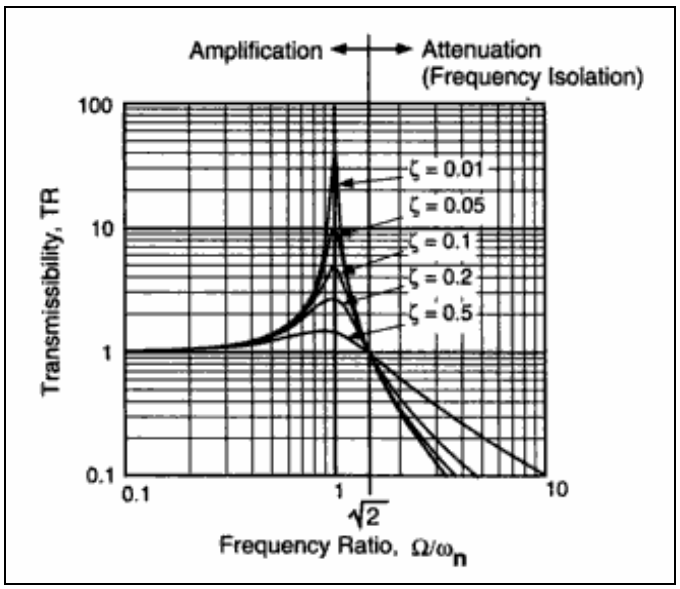

Figure A.1. Transmissibility Chart with ref [21]

Several percentages of critical damping are displayed to show the effect of damping in the attenuation region and the amplification region, including the maximum amplification at resonance ($\Omega / \omega_n = 1$). It should be noted that below a frequency ratio Ω / ω_n of $\sqrt{2}$, the response exceeds the input (TR>1) for all damping values. For frequency ratios above $\sqrt{2}$, the response is less than the input. This latter condition is known as vibration (frequency) isolation and is often a design goal [21].

APPENDIX B

FEA NORMAL MODES RESULTS OF RASAT

Table B.1. All Normal Modes of RASAT from 0 Hz to 2000 Hz

MODE NO	EIGENVALUE	FREQUENCY		MODE NO	EIGENVALUE	FREQUENCY	
		(RAD/TIME)	(HZ)			(RAD/TIME)	(HZ)
1	1.13E+10	335.82	53,447	32	4.43E+11	2105.6	335.12
2	1.19E+10	345.46	54,981	33	4.56E+11	2134.6	339.73
3	3.74E+10	611.17	97,270	34	4.71E+11	2170.3	345.41
4	4.45E+10	667.16	106.18	35	4.73E+11	2175.9	346.30
5	7.18E+10	847.23	134.84	36	4.85E+11	2201.3	350.35
6	8.90E+10	943.47	150.16	37	5.18E+11	2275.6	362.17
7	1.08E+11	1038.2	165.23	38	5.27E+11	2296.6	365.52
8	1.26E+11	1122.4	178.63	39	5.65E+11	2376.4	378.21
9	1.29E+11	1137.7	181.07	40	5.73E+11	2394.4	381.09
10	1.37E+11	1170.7	186.31	41	5.89E+11	2427.5	386.35
11	1.53E+11	1235.1	196.58	42	6.08E+11	2465.8	392.45
12	1.79E+11	1337.4	212.85	43	6.21E+11	2492.1	396.62
13	1.80E+11	1341.0	213.43	44	6.33E+11	2515.8	400.40
14	1.88E+11	1371.1	218.22	45	6.54E+11	2557.2	406.99
15	2.20E+11	1483.5	236.11	46	6.87E+11	2621.6	417.24
16	2.26E+11	1502.9	239.19	47	7.17E+11	2678.1	426.23
17	2.33E+11	1526.4	242.94	48	7.26E+11	2694.6	428.86
18	2.36E+11	1537.4	244.68	49	7.28E+11	2698.5	429.48
19	2.55E+11	1596.5	254.09	50	7.36E+11	2713.6	431.88
20	2.62E+11	1618.5	257.59	51	7.39E+11	2719.3	432.80
21	2.71E+11	1646.2	262.00	52	7.57E+11	2750.6	437.77
22	2.82E+11	1679.5	267.31	53	7.67E+11	2770.3	440.90
23	3.05E+11	1746.1	277.90	54	8.42E+11	2901.5	461.78
24	3.32E+11	1822.5	290.06	55	8.47E+11	2911.2	463.33
25	3.55E+11	1883.8	299.82	56	9.00E+11	2999.9	477.45
26	3.83E+11	1956.7	311.41	57	9.26E+11	3042.4	484.21
27	3.92E+11	1979.4	315.03	58	9.76E+11	3123.5	497.12
28	4.04E+11	2010.5	319.98	59	9.83E+11	3135.8	499.07
29	4.08E+11	2020.7	321.61	60	1.01E+12	3176.2	505.51
30	4.33E+11	2081.7	331.31	61	1.03E+12	3210.0	510.88
31	4.37E+11	2090.2	332.66	62	1.07E+12	3268.1	520.14

(Table B.1 continued)

MODE NO	EIGENVALUE	FREQUENCY		MODE NO	EIGENVALUE	FREQUENCY	
		(RAD/TIME)	(HZ)			(RAD/TIME)	(HZ)
63	1.09E+12	3299.9	525.20	103	1.95E+12	4410.8	702.00
64	1.11E+12	3336.0	530.95	104	1.97E+12	4443.1	707.14
65	1.12E+12	3344.6	532.30	105	2.01E+12	4487.8	714.25
66	1.16E+12	3412.1	543.06	106	2.03E+12	4510.5	717.86
67	1.17E+12	3423.0	544.79	107	2.10E+12	4582.1	729.27
68	1.19E+12	3444.0	548.13	108	2.14E+12	4625.0	736.09
69	1.22E+12	3494.8	556.21	109	2.16E+12	4649.9	740.05
70	1.24E+12	3520.6	560.32	110	2.18E+12	4673.8	743.86
71	1.28E+12	3573.8	568.78	111	2.21E+12	4698.0	747.72
72	1.30E+12	3604.5	573.68	112	2.24E+12	4728.6	752.59
73	1.32E+12	3639.6	579.27	113	2.27E+12	4760.6	757.68
74	1.33E+12	3647.1	580.45	114	2.29E+12	4786.7	761.82
75	1.36E+12	3683.1	586.19	115	2.34E+12	4837.8	769.96
76	1.36E+12	3691.4	587.50	116	2.37E+12	4867.5	774.68
77	1.38E+12	3709.7	590.42	117	2.38E+12	4874.0	775.72
78	1.41E+12	3750.5	596.91	118	2.43E+12	4926.2	784.03
79	1.42E+12	3770.2	600.04	119	2.50E+12	5003.9	796.40
80	1.44E+12	3801.1	604.96	120	2.54E+12	5043.4	802.69
81	1.46E+12	3825.1	608.78	121	2.56E+12	5055.0	804.52
82	1.48E+12	3848.2	612.46	122	2.57E+12	5073.7	807.51
83	1.50E+12	3876.0	616.88	123	2.63E+12	5133.2	816.97
84	1.51E+12	3891.7	619.38	124	2.66E+12	5154.4	820.34
85	1.53E+12	3909.2	622.17	125	2.68E+12	5176.3	823.84
86	1.57E+12	3962.8	630.69	126	2.73E+12	5228.2	832.09
87	1.58E+12	3976.7	632.92	127	2.74E+12	5233.7	832.98
88	1.59E+12	3993.6	635.60	128	2.80E+12	5289.0	841.77
89	1.65E+12	4063.1	646.67	129	2.84E+12	5330.4	848.36
90	1.67E+12	4092.4	651.32	130	2.85E+12	5337.7	849.53
91	1.70E+12	4125.7	656.62	131	2.87E+12	5357.2	852.63
92	1.74E+12	4166.3	663.09	132	2.90E+12	5380.8	856.38
93	1.76E+12	4200.1	668.47	133	2.93E+12	5409.8	861.00
94	1.77E+12	4207.1	669.59	134	2.94E+12	5417.7	862.26
95	1.79E+12	4231.5	673.47	135	2.96E+12	5444.3	866.49
96	1.82E+12	4264.2	678.67	136	2.98E+12	5458.3	868.72
97	1.83E+12	4276.0	680.55	137	3.02E+12	5494.4	874.46
98	1.85E+12	4297.0	683.89	138	3.06E+12	5530.8	880.25
99	1.86E+12	4312.8	686.41	139	3.07E+12	5539.0	881.56
100	1.88E+12	4340.4	690.80	140	3.17E+12	5628.9	895.87
101	1.91E+12	4374.0	696.15	141	3.19E+12	5644.5	898.34
102	1.92E+12	4385.4	697.96	142	3.21E+12	5666.9	901.92

(Table B.1 continued)

MODE NO	EIGENVALUE	FREQUENCY		MODE NO	EIGENVALUE	FREQUENCY	
		(RAD/TIME)	(HZ)			(RAD/TIME)	(HZ)
143	3.23E+12	5687.2	905.14	183	4.88E+12	6982.9	1111.4
144	3.25E+12	5703.4	907.72	184	4.93E+12	7023.4	1117.8
145	3.28E+12	5730.6	912.05	185	4.97E+12	7048.0	1121.7
146	3.34E+12	5781.0	920.07	186	5.05E+12	7103.0	1130.5
147	3.36E+12	5797.4	922.69	187	5.09E+12	7132.0	1135.1
148	3.39E+12	5819.8	926.25	188	5.11E+12	7151.8	1138.2
149	3.46E+12	5880.4	935.90	189	5.14E+12	7172.7	1141.6
150	3.52E+12	5932.2	944.15	190	5.24E+12	7239.1	1152.1
151	3.52E+12	5934.4	944.49	191	5.25E+12	7245.7	1153.2
152	3.58E+12	5982.1	952.08	192	5.27E+12	7259.1	1155.3
153	3.69E+12	6073.8	966.67	193	5.32E+12	7293.1	1160.7
154	3.72E+12	6097.3	970.42	194	5.38E+12	7331.5	1166.8
155	3.74E+12	6113.5	973.00	195	5.46E+12	7390.2	1176.2
156	3.80E+12	6165.1	981.20	196	5.50E+12	7418.7	1180.7
157	3.86E+12	6214.2	989.01	197	5.51E+12	7422.0	1181.2
158	3.87E+12	6221.0	990.10	198	5.54E+12	7445.6	1185.0
159	3.96E+12	6290.0	1001.1	199	5.60E+12	7486.5	1191.5
160	3.97E+12	6298.0	1002.4	200	5.68E+12	7537.1	1199.6
161	3.99E+12	6312.9	1004.7	201	5.68E+12	7539.7	1200.0
162	4.04E+12	6352.4	1011.0	202	5.70E+12	7550.4	1201.7
163	4.06E+12	6370.5	1013.9	203	5.82E+12	7630.9	1214.5
164	4.06E+12	6375.0	1014.6	204	5.85E+12	7645.9	1216.9
165	4.11E+12	6414.2	1020.8	205	5.87E+12	7664.3	1219.8
166	4.18E+12	6467.5	1029.3	206	5.91E+12	7688.9	1223.7
167	4.22E+12	6497.8	1034.1	207	5.97E+12	7727.4	1229.8
168	4.24E+12	6509.8	1036.1	208	6.06E+12	7786.9	1239.3
169	4.25E+12	6516.1	1037.1	209	6.11E+12	7817.4	1244.2
170	4.29E+12	6548.3	1042.2	210	6.15E+12	7843.5	1248.3
171	4.30E+12	6559.8	1044.0	211	6.21E+12	7881.7	1254.4
172	4.34E+12	6589.2	1048.7	212	6.29E+12	7932.9	1262.6
173	4.36E+12	6605.1	1051.2	213	6.35E+12	7965.8	1267.8
174	4.41E+12	6639.9	1056.8	214	6.38E+12	7986.3	1271.1
175	4.49E+12	6697.9	1066.0	215	6.41E+12	8005.7	1274.1
176	4.53E+12	6729.7	1071.1	216	6.45E+12	8033.6	1278.6
177	4.54E+12	6738.8	1072.5	217	6.51E+12	8071.0	1284.5
178	4.63E+12	6803.6	1082.8	218	6.59E+12	8115.3	1291.6
179	4.72E+12	6870.4	1093.5	219	6.62E+12	8138.2	1295.2
180	4.73E+12	6873.9	1094.0	220	6.66E+12	8162.3	1299.1
181	4.83E+12	6948.0	1105.8	221	6.70E+12	8182.4	1302.3
182	4.86E+12	6973.4	1109.9	222	6.73E+12	8201.2	1305.3

(Table B.1 continued)

MODE NO	EIGENVALUE	FREQUENCY		MODE NO	EIGENVALUE	FREQUENCY	
		(RAD/TIME)	(HZ)			(RAD/TIME)	(HZ)
222	6.73E+12	8201.2	1305.3	262	8.59E+12	9268.0	1475.0
223	6.90E+12	8305.1	1321.8	263	8.62E+12	9285.2	1477.8
224	6.91E+12	8314.7	1323.3	264	8.63E+12	9288.4	1478.3
225	6.98E+12	8354.4	1329.6	265	8.63E+12	9288.4	1478.3
226	7.01E+12	8372.0	1332.4	266	8.63E+12	9288.4	1478.3
227	7.08E+12	8415.8	1339.4	267	8.63E+12	9288.4	1478.3
228	7.10E+12	8426.7	1341.1	268	8.63E+12	9290.1	1478.6
229	7.16E+12	8460.1	1346.5	269	8.66E+12	9306.9	1481.2
230	7.17E+12	8465.3	1347.3	270	8.69E+12	9322.5	1483.7
231	7.27E+12	8528.1	1357.3	271	8.72E+12	9338.9	1486.3
232	7.30E+12	8541.6	1359.4	272	8.77E+12	9363.7	1490.3
233	7.34E+12	8565.9	1363.3	273	8.87E+12	9417.1	1498.8
234	7.35E+12	8571.7	1364.2	274	8.88E+12	9422.2	1499.6
235	7.36E+12	8580.5	1365.6	275	8.88E+12	9422.4	1499.6
236	7.39E+12	8598.5	1368.5	276	8.88E+12	9422.4	1499.6
237	7.40E+12	8600.3	1368.8	277	8.88E+12	9422.4	1499.6
238	7.44E+12	8623.9	1372.5	278	8.88E+12	9422.4	1499.6
239	7.45E+12	8632.9	1374.0	279	8.88E+12	9422.4	1499.6
240	7.48E+12	8650.5	1376.8	280	8.91E+12	9440.1	1502.4
241	7.52E+12	8673.2	1380.4	281	8.92E+12	9442.3	1502.8
242	7.62E+12	8729.9	1389.4	282	8.95E+12	9460.8	1505.7
243	7.68E+12	8765.3	1395.0	283	9.00E+12	9489.4	1510.3
244	7.70E+12	8776.8	1396.9	284	9.01E+12	9494.2	1511.0
245	7.77E+12	8815.5	1403.0	285	9.05E+12	9514.2	1514.2
246	7.82E+12	8841.5	1407.2	286	9.07E+12	9524.3	1515.8
247	7.90E+12	8890.9	1415.0	287	9.13E+12	9556.9	1521.0
248	7.92E+12	8897.1	1416.0	288	9.21E+12	9594.9	1527.1
249	7.97E+12	8927.5	1420.9	289	9.23E+12	9606.8	1529.0
250	8.00E+12	8945.7	1423.8	290	9.25E+12	9616.3	1530.5
251	8.07E+12	8985.0	1430.0	291	9.31E+12	9650.7	1536.0
252	8.11E+12	9003.4	1432.9	292	9.33E+12	9658.8	1537.2
253	8.20E+12	9053.7	1440.9	293	9.42E+12	9703.1	1544.3
254	8.30E+12	9111.8	1450.2	294	9.45E+12	9718.7	1546.8
255	8.33E+12	9128.3	1452.8	295	9.50E+12	9747.4	1551.3
256	8.36E+12	9144.3	1455.4	296	9.58E+12	9787.5	1557.7
257	8.41E+12	9172.4	1459.8	297	9.60E+12	9795.5	1559.0
258	8.48E+12	9206.7	1465.3	298	9.63E+12	9813.0	1561.8
259	8.49E+12	9216.3	1466.8	299	9.66E+12	9828.6	1564.3
260	8.53E+12	9233.6	1469.6	300	9.77E+12	9882.0	1572.8
261	8.56E+12	9251.3	1472.4	301	9.83E+12	9915.0	1578.0

(Table B.1 continued)

MODE NO	EIGENVALUE	FREQUENCY		MODE NO	EIGENVALUE	FREQUENCY	
		(RAD/TIME)	(HZ)			(RAD/TIME)	(HZ)
302	9.89E+12	9943.9	1582.6	342	1.15E+13	10742.	1709.6
303	9.92E+12	9959.4	1585.1	343	1.16E+13	10774.	1714.7
304	1.00E+13	10002.	1591.8	344	1.17E+13	10795.	1718.1
305	1.00E+13	10011.	1593.2	345	1.17E+13	10795.	1718.1
306	1.00E+13	10025.	1595.5	346	1.17E+13	10795.	1718.1
307	1.01E+13	10025.	1595.5	347	1.17E+13	10795.	1718.1
308	1.01E+13	10061.	1601.3	348	1.17E+13	10802.	1719.2
309	1.01E+13	10074.	1603.3	349	1.17E+13	10802.	1719.2
310	1.02E+13	10115.	1609.8	350	1.17E+13	10802.	1719.2
311	1.03E+13	10144.	1614.4	351	1.17E+13	10802.	1719.2
312	1.03E+13	10156.	1616.4	352	1.17E+13	10802.	1719.2
313	1.04E+13	10182.	1620.5	353	1.17E+13	10809.	1720.3
314	1.04E+13	10217.	1626.1	354	1.17E+13	10809.	1720.3
315	1.04E+13	10220.	1626.6	355	1.17E+13	10809.	1720.3
316	1.05E+13	10252.	1631.6	356	1.17E+13	10809.	1720.3
317	1.05E+13	10267.	1634.1	357	1.17E+13	10815.	1721.2
318	1.06E+13	10285.	1636.9	358	1.17E+13	10815.	1721.2
319	1.06E+13	10294.	1638.4	359	1.17E+13	10815.	1721.2
320	1.06E+13	10317.	1642.0	360	1.17E+13	10815.	1721.2
321	1.07E+13	10324.	1643.2	361	1.18E+13	10840.	1725.3
322	1.07E+13	10329.	1643.8	362	1.18E+13	10846.	1726.2
323	1.07E+13	10358.	1648.5	363	1.18E+13	10857.	1728.0
324	1.07E+13	10364.	1649.4	364	1.18E+13	10876.	1730.9
325	1.08E+13	10380.	1652.1	365	1.19E+13	10888.	1732.8
326	1.08E+13	10402.	1655.6	366	1.19E+13	10906.	1735.8
327	1.09E+13	10418.	1658.1	367	1.19E+13	10915.	1737.1
328	1.09E+13	10427.	1659.5	368	1.20E+13	10940.	1741.1
329	1.09E+13	10444.	1662.2	369	1.20E+13	10972.	1746.3
330	1.10E+13	10492.	1669.8	370	1.21E+13	11007.	1751.9
331	1.10E+13	10507.	1672.3	371	1.22E+13	11038.	1756.8
332	1.11E+13	10535.	1676.6	372	1.22E+13	11052.	1759.0
333	1.11E+13	10536.	1676.8	373	1.23E+13	11083.	1763.9
334	1.12E+13	10569.	1682.1	374	1.23E+13	11090.	1765.1
335	1.12E+13	10589.	1685.2	375	1.23E+13	11090.	1765.1
336	1.12E+13	10603.	1687.6	376	1.23E+13	11090.	1765.1
337	1.13E+13	10620.	1690.2	377	1.23E+13	11090.	1765.1
338	1.13E+13	10639.	1693.3	378	1.23E+13	11108.	1767.9
339	1.14E+13	10669.	1698.0	379	1.24E+13	11141.	1773.2
340	1.14E+13	10680.	1699.8	380	1.25E+13	11173.	1778.2
341	1.15E+13	10718.	1705.8	381	1.25E+13	11183.	1779.9

(Table B.1 continued)

MODE NO	EIGENVALUE	FREQUENCY		MODE NO	EIGENVALUE	FREQUENCY	
		(RAD/TIME)	(HZ)			(RAD/TIME)	(HZ)
382	1.26E+13	11205.	1783.3	414	1.43E+13	11956.	1902.8
383	1.26E+13	11220.	1785.8	415	1.43E+13	11975.	1905.8
384	1.26E+13	11240.	1788.9	416	1.44E+13	12010.	1911.4
385	1.27E+13	11280.	1795.3	417	1.44E+13	12017.	1912.6
386	1.28E+13	11296.	1797.8	418	1.45E+13	12043.	1916.7
387	1.28E+13	11307.	1799.6	419	1.45E+13	12060.	1919.3
388	1.29E+13	11345.	1805.6	420	1.46E+13	12084.	1923.3
389	1.29E+13	11356.	1807.4	421	1.46E+13	12103.	1926.2
390	1.30E+13	11387.	1812.3	422	1.47E+13	12124.	1929.6
391	1.31E+13	11426.	1818.6	423	1.47E+13	12133.	1931.1
392	1.31E+13	11441.	1820.9	424	1.47E+13	12142.	1932.4
393	1.31E+13	11462.	1824.2	425	1.48E+13	12175.	1937.7
394	1.32E+13	11477.	1826.7	426	1.49E+13	12196.	1941.0
395	1.32E+13	11497.	1829.7	427	1.49E+13	12210.	1943.3
396	1.34E+13	11564.	1840.4	428	1.50E+13	12235.	1947.2
397	1.34E+13	11589.	1844.5	429	1.50E+13	12265.	1952.0
398	1.34E+13	11591.	1844.7	430	1.51E+13	12273.	1953.3
399	1.35E+13	11613.	1848.3	431	1.52E+13	12321.	1960.9
400	1.36E+13	11648.	1853.8	432	1.52E+13	12344.	1964.6
401	1.37E+13	11690.	1860.5	433	1.53E+13	12367.	1968.2
402	1.37E+13	11697.	1861.7	434	1.54E+13	12414.	1975.7
403	1.37E+13	11726.	1866.2	435	1.54E+13	12414.	1975.8
404	1.38E+13	11750.	1870.1	436	1.54E+13	12424.	1977.3
405	1.38E+13	11763.	1872.1	437	1.55E+13	12451.	1981.7
406	1.39E+13	11771.	1873.5	438	1.56E+13	12481.	1986.5
407	1.39E+13	11783.	1875.4	439	1.56E+13	12483.	1986.8
408	1.40E+13	11813.	1880.0	440	1.56E+13	12505.	1990.3
409	1.40E+13	11826.	1882.2	441	1.56E+13	12508.	1990.8
410	1.40E+13	11842.	1884.7	442	1.57E+13	12545.	1996.6
411	1.41E+13	11870.	1889.1	443	1.58E+13	12553.	1997.9
412	1.42E+13	11896.	1893.3	444	1.58E+13	12573.	2001.0
413	1.43E+13	11944.	1900.9				

APPENDIX C

USING MODAL EFFECTIVE MASS TO DETERMINE MODES FOR FREQUENCY RESPONSE ANALYSIS

The response of a structure due to dynamic loads can be determined using either a direct frequency analysis or modal frequency analysis. Of these two methods, the modal approach is popular due to its efficiency and can approximate the response using only a small number of modes. When dealing with small models all the modes in the frequency range of interest are included for the response solution. But for larger structures, including all the modes in the frequency range can be computationally expensive. Therefore it is important to understand the modes with large contributions to the overall response of the structure.

The first step in calculating the modal frequency response is to compute the normal modes of the structure. The results from the normal modes analysis are the mode shapes and natural frequencies. Observing the mode shapes reveals how the structure will deform at natural frequencies. However, the modal displacements / deformation information does not provide a good insight to the response since the Eigenvectors are arbitrarily scaled and the displacements seen in the postprocessor can be deceiving.

One method employed to understand the response is by examining the so-called "modal effective mass". The modal effective mass associated with each deformation mode represents the amount of system mass participating in that mode. Therefore, a mode with a large effective mass is usually a significant contributor to the system's response. These criteria are in other words used to find the important system modes. A typical requirement for the selection of target modes is that modes with a translational effective mass equal to or greater than 2 percent of the total mass are target modes. It should be noted that the 2% criteria can vary with application and proper engineering judgment should be used while applying it. In this article, the use of modal effective mass is demonstrated using a simple

example. This example problem is solved using MSC.Nastran but can be used in all flavors of Nastran with minor modifications. The readers are encouraged to read the references provided at the bottom of this page in order to understand the theoretical basis of this method.

Consider a cantilever beam modeled with CBAR elements. The problem is to find the important modes for consideration in a subsequent modal frequency response analysis. The normal modes analysis is performed for a frequency range of 0 Hz to 650 Hz. The modal effective mass can be printed out during the normal modes solution by providing the MEFFMASS in the case control section for MSC.Nastran Rel 2004 and above and NX Nastran. For earlier version of MSC.Nastran this feature is available through the DMAP. For other flavors of Nastran, proper user manuals should be consulted.

A trial run is conducted to determine the number of modes needed to represent the response of the entire structure. One way to determine this is to calculate the cumulative modal effective mass. If the cumulative sum of modal effective mass is more than 80%, then the modes are sufficient to represent 80% of the response of the structure. In some applications, the requirement is to use 98%.The modal effective mass table is printed out along all directions in the f06 file as requested in the input file shown above. A modified version of this table is shown in Table C.1. The sum along each direction should be compared with the effective mass matrix shown below. In this example the mass along the translation directions represent 100% of the effective mass matrix. This means the first 30 modes are sufficient to represent 100% of the structural response seen in Table C.1.

The results of the analysis are shown in Table C.1 and Figure C.1. It can be seen that modes 7 10 and 13 represents 80 % of the response in T1 direction. Similarly modes 1, 2 and 4 represent the response in T2 and T3 directions [22].

Table C.1. Modal Effective Mass from Print-out F06 File with ref [22]

MODE NO.	FREQUENCY, (Hz)	T1	%T1	T2	% T2	T3	% T3
1	2.86E+02	6.48E-34	0.00	4.38E-04	46.66	1.66E-04	17.64
2	2.86E+02		0.00	1.66E-04	17.64	4.38E-04	46.66
3	1.78E+03	4.90E-35	0.00	1.95E-06	0.21	1.84E-04	19.64
4	1.78E+03	1.26E-34	0.00	1.84E-04	19.64	1.95E-06	0.21
5	4.92E+03	1.27E-30	0.00	1.48E-05	1.57	4.92E-05	5.24
6	4.92E+03	6.37E-32	0.00	4.92E-05	5.24	1.48E-05	1.57
7	5.06E+03	7.98E-04	84.99	1.35E-33	0.00	2.77E-32	0.00
8	9.54E+03	3.06E-32	0.00	2.35E-05	2.50	9.18E-06	0.98
9	9.54E+03	1.62E-32	0.00	9.18E-06	0.98	2.35E-05	2.50
10	1.51E+04	8.58E-05	9.13	9.32E-32	0.00	6.98E-32	0.00
11	1.56E+04	4.21E-31	0.00	5.95E-07	0.06	1.91E-05	2.03
12	1.56E+04	4.43E-32	0.00	1.91E-05	2.03	5.95E-07	0.06
13	2.30E+04	2.64E-31	0.00	4.62E-06	0.49	8.38E-06	0.89
14	2.30E+04	2.93E-32	0.00	8.38E-06	0.89	4.62E-06	0.49
15	2.47E+04	2.88E-05	3.07	3.43E-32	0.00	2.19E-33	0.00
16	3.15E+04	9.41E-32	0.00	2.88E-06	0.31	6.10E-06	0.65
17	3.15E+04	3.76E-32	0.00	6.10E-06	0.65	2.88E-06	0.31
18	3.37E+04	1.32E-05	1.40	1.76E-33	0.00	9.85E-32	0.00
19	4.04E+04	4.05E-32	0.00	5.97E-06	0.64	1.21E-07	0.01
20	4.04E+04	5.08E-31	0.00	1.21E-07	0.01	5.97E-06	0.64
21	4.19E+04	6.78E-06	0.72	5.26E-31	0.00	6.80E-31	0.00
22	4.87E+04	5.42E-29	0.00	9.09E-07	0.10	2.64E-06	0.28
23	4.87E+04	2.56E-31	0.00	2.64E-06	0.28	9.09E-07	0.10
24	4.90E+04	3.61E-06	0.38	1.17E-29	0.00	1.64E-29	0.00
25	5.46E+04	1.80E-28	0.00	1.72E-07	0.02	9.85E-07	0.10
26	5.46E+04	1.29E-31	0.00	9.85E-07	0.10	1.72E-07	0.02
27	5.50E+04	1.86E-06	0.20	1.49E-29	0.00	8.68E-29	0.00
28	5.96E+04	8.48E-07	0.09	2.52E-33	0.00	3.78E-32	0.00
29	6.27E+04	2.85E-07	0.03	1.87E-31	0.00	8.57E-32	0.00
30	6.43E+04	3.06E-08	0.00	1.82E-32	0.00	2.15E-31	0.00
	TOTAL	9.39E-04		9.39E-04		9.39E-04	

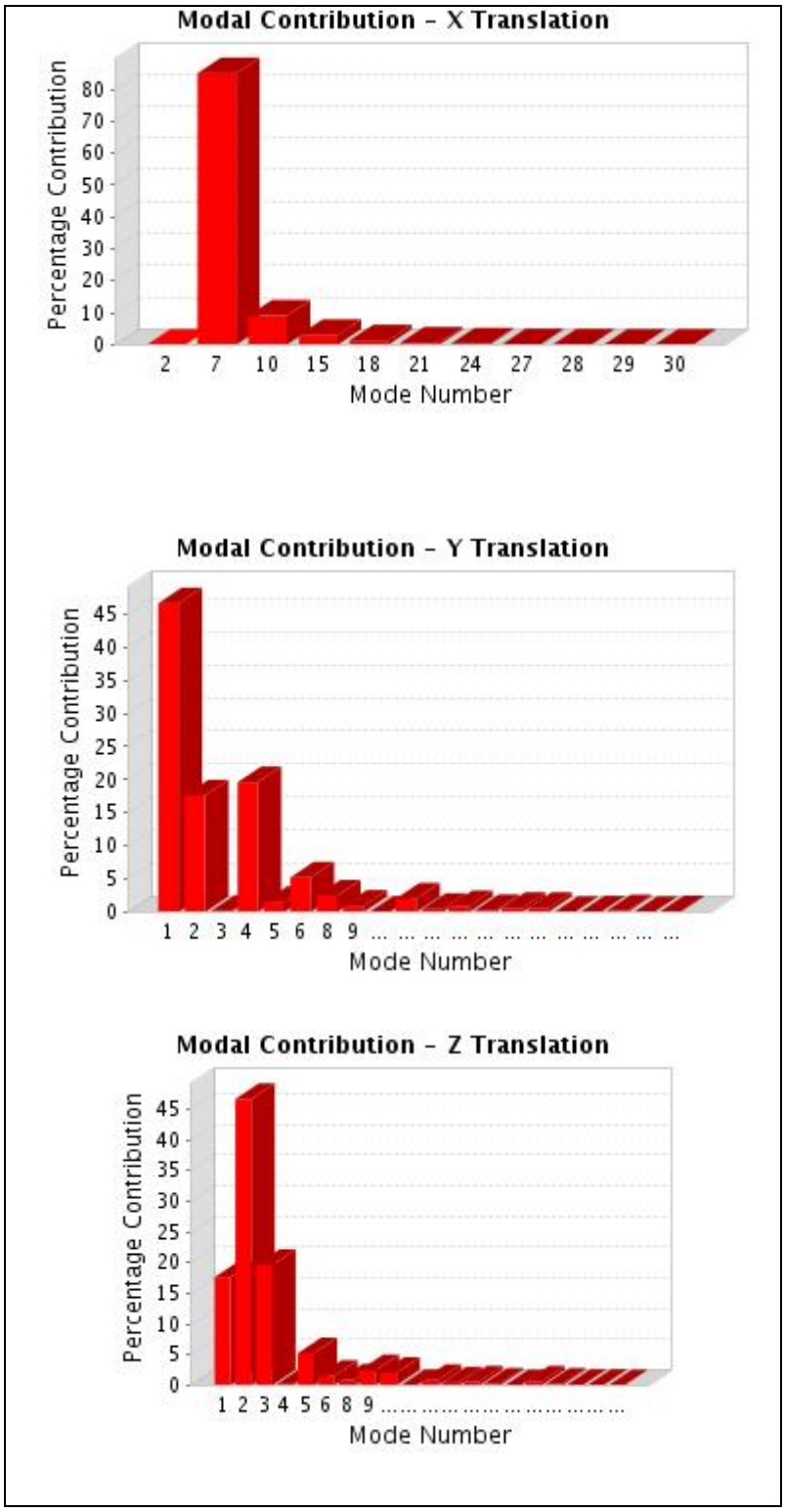

Figure C.1. Plots of Modal Contribution and Mode Numbers in 3 Translation directions with ref [22]